OPTIMAL RULE-BASED ENERGY MANAGEMENT AND VOLTAGE CONTROL USING BATTERY ENERGY STORAGE AND SMART POWER CONVERTERS

A THESIS

submitted by

RAMPELLI MANOJKUMAR

for the award of the degree

of

DOCTOR OF PHILOSOPHY

DEPARTMENT OF ELECTRONICS AND ELECTRICAL ENGINEERING

INDIAN INSTITUTE OF TECHNOLOGY GUWAHATI, GUWAHATI, INDIA

JAN 2023

To my daughter Darshini

THESIS CERTIFICATE

This is to certify that the thesis entitled **"OPTIMAL RULE-BASED ENERGY MANAGEMENT AND VOLTAGE CONTROL USING BATTERY ENERGY STORAGE AND SMART POWER CONVERTERS"** submitted by **RAMPELLI MANOJKUMAR** to the Indian Institute of Technology Guwahati, Guwahati, India for the award of the degree of Doctor of Philosophy is a bonafide record of the research work done by him under my supervision. The contents of this thesis, in full or in parts, have not been submitted to any other Institute or University for the award of any degree or diploma.

Place: Guwahati
Date: 20.01.2023

Dr. Chandan Kumar
Main Supervisor
Associate Professor
Department of Electronics and Electrical Engineering
IIT-Guwahati, 781039

Place: Guwahati
Date: 20.01.2023

Dr. Sanjib Ganguly
Co-Supervisor
Associate Professor
Department of Electronics and Electrical Engineering
IIT-Guwahati, 781039

DECLARATION

I certify that:

1. The work contained in this thesis is original and has been done by me under the guidance of my supervisor.
2. The work has not been submitted to any other Institute for any degree or diploma.
3. I have followed the guidelines provided by the Institute in preparing the thesis.
4. I have conformed to the norms and guidelines given in the Ethical Code of Conduct of the Institute.
5. Whenever I have used materials (data, theoretical analysis, figures, and text) from other sources, I have given due credit to them by citing them in the text of the thesis and giving their details in the references.

Place: Guwahati
Date: 20.01.2023

Rampelli Manojkumar

ACKNOWLEDGEMENTS

I would like to express my heartfelt gratitude to the people who have helped me during the journey of this research work.

I am extremely thankful to my supervisors, Dr. Chandan Kumar and Dr. Sanjib Ganguly for their continuous encouragement, guidance and support during my research work. I express my sincere gratitude for their commitment and interest towards the research which helped me in getting timely advices throughout the journey of this research work.

I express my gratitude to the ASEAN-India collaborative research project entitled "Design, control and management of distributed generation in microgrid", and research grant "ECR/2017/001564" under Science & Engineering Research Board (SERB) for providing technical and financial support during this tenure of research work.

I would like to acknowledge the financial, academic, and technical support offered by the Indian Institute of Technology Guwahati during the course of my doctoral studies. I am thankful to the Heads of the Department during the course of my study. I am very much grateful to Dr. Sisir Kumar Nayak, Dr. Praveen Tripathy, and Dr. Ravindranath Adda, for assessing my research work and providing thoughtful suggestions as members of Doctoral Committee. I am also thankful to Dr. H B Gooi, Dr. Saad Mekhilef, Dr. João P. S. Catalão for their technical advices on various issues of my research work.

I would like to express gratitude to the services offered by Mr. Paban Bujor Barua, staff of power and control Lab II, Mr. Mukut Baruah, and Mr. Dasarath Das, office staff of Electronics and Electrical Engineering department.

I am grateful to have Hrishikesan V M, Dwijasish Das, Sourav Kumar Ghosh, Arunima Dutta and Shubh Laxmi as our core research group members who have helped me in clarifying few issues related to research work and motivated me personally during the stay at campus. I am also thankful to the Smart Energy Conversion Lab members of Devendra Kumar, Somnath Meikap, Lakshmi Kanth, Anandh N, Sahil, Shwet Prasoon, Mayank, and Atul for their help during the research work. I would also like to thank

all my other friends from Power and Control Lab II for their good company during the time spent in IIT Guwahati.

I am thankful to my friends Samarjeet Das, Dino Moni Singha, Abhishek Paikray, Pramit Nandi, Pratanu, Sumitha, Somjith, Shubham Sahoo, Shiv, Debabratha, Sibasis, Biswajit, Driti and Momi, for giving some beautiful moments during my life in IIT Guwahati.

I am always be grateful for my parents Srinivas and Lalitha for their love, support, and encouragement at every stage of my life towards achieving my dreams. I thank my brothers Madhu, Mahender, and other family members for their support during my difficult times. Most importantly, I am very much thankful to my wife Prashanthi for always showing her unbounded love towards me at all the times.

Rampelli Manojkumar

ABSTRACT

KEYWORDS: Battery energy storage systems; energy management; renewable energy sources; smart power converters; voltage control

Energy management and voltage control are essentially required for the optimal management of energy flow when there is more than one energy source available for power supply (e.g. renewable energy sources (RESs), diesel generator (DG), etc.) and for improving the voltage profile, respectively. The battery energy storage and smart power converters are extensively used to implement the energy management and voltage control applications in low voltage (LV) distribution systems. Moreover, the optimal rule-based energy management approaches are considered as simple yet effective strategies used to implement energy management and voltage control applications. Out of the various energy management applications, the peak shaving is an important application which benefits both grid operators and end-users. Therefore, in this thesis firstly an optimal rule-based peak shaving method is proposed using battery energy storage system (BESS) which minimizes the peak grid demand in LV distribution system considering load and RES power profiles as inputs. However, the energy price is not considered as input while formulating the peak shaving control strategy. The demand response (DR) application becomes important when the energy price profile along with load and renewable energy sources (RESs) power profiles is considered as input. Therefore, further an optimal rule-based DR method is developed using BESS which minimizes the energy consumption cost of the system over a day.

These proposed rule-based peak shaving and DR methods are developed considering the aggregated load and RES at LV ac bus. However, in case if the loads and RESs are considered to be connected at various buses in the distribution system, the voltage control application becomes important for satisfactory operation of consumer equipment while maintaining the load bus voltages within the limits of grid codes. Therefore, an optimal rule-based voltage control method is proposed to know the optimal set points of LV ac bus voltage which minimizes the voltage deviation in LV distribution system over a day. Further, in order to show the impact of optimal control of BESS along with the LV ac bus voltage control and RESs converters reactive power control, an isolated DG supplied LV distribution system is considered. In such a system, the fuel consumption of DG not only depends on the LV ac bus demand but also on its rated power. The rated power of DG can be reduced through the peak shaving application. Accordingly, the proposed optimal rule-based peak shaving control is modified for the application in DG supplied distribution system while minimizing the LV ac bus demand using LV ac bus voltage and reactive power control of RES converters.

All these proposed energy management and voltage control methods are tested in MATLAB. The improved performance of the system with the proposed methods is observed through various performance indicators such as percentage peak shaving, energy consumption cost, average voltage deviation, fuel consumption of DG, etc.

TABLE OF CONTENTS

LIST OF TABLES

LIST OF FIGURES

ABBREVIATIONS

DERs	Distributed energy resources
RESs	Renewable energy sources
DR	Demand response
LV	Low voltage
BESS	Battery Energy Storage Systems
SoC	State of charge
GA	Genetic algorithm
DG	Diesel generator
PV	Photovoltaic
MG	Microgrid
DLC	Direct load control
I/C	Interruptible/curtailable
DB	Demand bidding
EDR	Emergency demand response
CM	Capacity market
ASM	Ancillary service market
ISO	Independent system operator
ToU	Time of use
RTP	Real time price
CPP	Critical peak pricing
CHPs	Combined heat power systems
APC	Active power curtailment
OLTC	On load tap changer
CVR	Conservation voltage reduction
SBTSPBOC	Switching between two set points based on current
DSTATCOM	Distribution Static synchronous compensator
UPQC	Unified power quality conditioner
DP	Dynamic programming

PSO	Particle swarm optimization
PHEVs	Plug-in hybrid electric vehicles
PCC	Point of common coupling
MPPT	Maximum power point tracking
EV	Electric vehicle

NOTATIONS

Parameters

t	Time
T_c	Control horizon
T	Prediction horizon
P_g	Grid power
P_{pv}, P_b, P_l	PV, battery and load powers
$P_{dl}(P_{fil})$	Demand (feed-in) limit of the day
t_d, t_{c1}, t_{c2}	Time slots of discharging mode, charging mode-1, and charging mode-2
$P_{b-cl}(P_{b-dl})$	Battery charging (discharging) power limit
SoC	SoC of the battery
$SoC_i(SoC_f)$	SoC at the start (end) of the day
$SoC_l(SoC_u)$	SoC lower (upper) limit
E^*_{b-d}	Dischargeable energy of the battery
E_{b-r}	Energy rating of the battery
C_g	Coefficient of grid energy to charge the battery
$P_{dl0}(P_{fil0})$	Operating demand (feed-in) limits
P_{dl1}, P_{dl2}	Initial demand limits
P_{fil1}, P_{fil2}	Initial feed-in limits
P_{b-c} (P_{b-d})	Charging (discharging) power of the battery
e	Tolerance of regula falsi method
m	Slope in regula falsi method
$P_{pv-c}(P_{g-c})$	Available PV (grid) power to charge the battery
t_0	Initial time
t_{pvmf}	Time when available PV power to charge battery is more than feed-in limit
i_b	Current flowing through the battery
$E_{b-c}(E_{b-d})$	Required energy for charging (to be discharged by) battery

	over a day
$e_c(e_d)$	Battery charging (discharging) efficiency
$E_{pv-c}(E_{g-c})$	Available PV (grid) energy to charge battery over a day
$P_{l-p}(P_{pv-i})$	Peak load (PV installed) power
Ah_{b-r}	Ampere-hour rating of the battery
ECC	Energy consumption cost
$TECC$	Energy consumption cost over a day
V_{wmax}	Worst maximum bus voltage
V_{wmin}	Worst minimum bus voltage
EP	Energy price
dp	Death penalty
$EP_{bl}, EP_{sbl}, EP_{sl}$	Energy buying price, sub-buying price and selling price limits of a day
$EP_b(EP_s)$	Energy buying (selling) price
$EP_{max-b}(EP_{min-b})$	Maximum (minimum) energy buying price
$P_{ac-d}(P_{dc-d})$	ac (dc) load power
$P_{acl-p}(P_{dcl-p})$	ac (dc) load peak power
P_{ex-d}	Load power that is not supplied by PV source
P_{ex-pv}	PV power that is more than load power
$P_{pv-c-b}(P_{g-c-b})$	PV (grid) power used to charge battery
$P_{pv-c1}(P_{pv-c2})$	Available PV power during charging mode-1 (charging mode-2)
$S_{pv-c}(S_{g-c})$	Cumulative sum of available PV (grid) power to charge battery
$t_l(t_e)$	Times when buying price is less than (equal to) sub-buying price limit
$t_{sl}(t_{se})$	Times when selling price is less than (equal to) selling price limit
E_{g-c-l}	Sum of available grid powers to charge battery for all the times of buying price less than sub-buying price limit
$E_{g-c-b-e}(t)$	Sum of grid powers already used to charge battery for all the times of buying price equal to sub-buying price limit
E_{pv-c-l}	Sum of available PV powers to charge battery for all the

	times of selling price less than selling price limit
$E_{pv-c-b-e}(t)$	Sum of PV powers already used to charge battery for all the times of selling price equal to selling price limit
$V_{lv}(V_l)$	LV ac (load) bus voltage
V_{ref}	Reference voltage
N_b	Number of load buses
P_{lv}	LV ac bus power
P_{loss}	Total line loss
n_l, n_r	Number of loads (RESs)
$P_{rc}(Q_{rc})$	Active (reactive) power supplied by RES converter
V_{min-g}	Minimum voltage limit given by grid code
V_{max-g}	Maximum voltage limit given by grid code
V_{rm}	Voltage rise margin
V_{dm}	Voltage drop margin
V_{avg-d}	Average voltage deviation
V_{sp1}	Voltage set point 1
V_{sp2}	Voltage set point 2
I_{d-lv}	Direct axis current of LV ac bus
V_{ld}	Voltage limit difference
V_{max-d}	Maximum voltage limit of the day
V_{min-d}	Minimum voltage limit of the day
V_{max}	Maximum bus voltage
V_{min}	Minimum bus voltage
I	Current flowing through line
R	Resistance of line
X	Inductance of line
n_{li}	Number of lines
pf_{rc-min}	Minimum Power factor of RES converters
$pf_{rc}(S_{rc-r})$	Power factor (kVA rating) of RES converter
$P_{dg-peak}$	Peak DG power over a day
$P_{dg}(P_{phs})$	DG (pumped hydro storage) power
P_{dgb}	DG bus powers
P_r	RES power

$E_{lvi-c}(E_{dg-c})$	Available LV ac bus injected (DG) energy to charge battery over a day
$P_{lvdl}(P_{lvfil})$	LV ac bus demand (feed-in) limit
C_{dg}	Coefficient of DG energy to charge the battery
V_{b-r}	Voltage rating of the battery
P_{dg-r}	Power rating of DG
FC_{dg}	Fuel consumption of DG
TFC_{dg}	Fuel consumption of DG over a day
SCR	Self consumption rate of the system
i	Index of loads
j	Index of RESs
k	Line index
o	Index of optimal value of the variables
t_{lvcm}	Time slots when available LV ac bus injected power to charge battery is more than LV ac bus feed-in limit
$P_{lvd}(P_{lvi})$	LV ac bus demand (injection) power
$E_r(E_{phs})$	Energy generated by RESs (exported to PHS) over a day
t_c	Charging mode time slots
$E_{lvi-c}(E_{dg-c})$	Available LV ac bus injected (DG) energy to charge battery over a day
$P_{lvi-c}(P_{dg-c})$	Available LV ac bus injected (DG) power to charge battery
$P_{lvi-c-b}(P_{dg-c-b})$	LV ac bus injected (DG) power used to charge battery
$P_{dgb-wcs}$	DG bus power in worst case scenario
$P_{lvdl0}(P_{dgbfil0})$	Operating LV ac bus demand (feed-in) limit
P_{lvdl1}, P_{lvdl2}	Initial LV ac bus demand limits

Indices

i	Index of loads
j	Index of RESs
k	Line index
o	Index of optimal value of the variables

CHAPTER 1

INTRODUCTION

There is a continuous increase in the energy demand due to the industrial growth in developing countries. The coal based power plants are the major conventional power producing options used to meet the required energy demand. The first coal based power plant was built in France in the year 1875 [1]. Later, the internal combustion engine was introduced by Daimler in 1886 which use oil and gas for power generation. This power generated using these fossil fuels at conventional power plants reaches consumers through various components of power systems i.e., transformers, transmission lines, and distribution lines. At the power plants, step up transformers are used to increase the voltage level of generated power. Further, the power is transmitted through transmission lines. Again, depending on the consumer voltage requirement, the step down transformers are used to transform the high voltage level to medium voltage level, and medium voltage level to low voltage (LV) level for utilization purposes. From these voltage levels, the energy is carried through different distribution lines to the consumers. Therefore, this transfer of energy from conventional power plants which are located far from the consumers results in higher energy losses. Moreover, the increase in pollution and depletion of the fossil fuels of coal, oil and natural gas are the other major disadvantages of conventional power generation methods. To tackle these challenges, the integration of distributed energy resources (DERs) is increasing in LV distribution systems [2].

The integration of DERs in the LV distribution systems provides the possibility for the consumers to produce energy [3]. However, it causes new challenges such as increased consumer expectations (e.g. improved reliability, satisfactory operation of loads, and energy consumption cost reduction), requirements for supporting bi-directional energy flow and communication infrastructure, increased system threats from environmental/cyber events, etc. It is important to deal with such challenges for ensuring economic and reliable operation of power distribution systems [4]. The energy management and voltage control play an important role in dealing with these challenges in LV distribution systems. The energy management approaches are developed for optimal management

of energy flow when there are more than one energy source available for power supply. The voltage control is used for maintaining the bus voltages within the required limits and for improving the voltage profile. In this scenario, the battery energy storage systems (BESSs) and smart power converters are extensively used to implement the energy management and voltage control applications in LV distribution systems. In literature, several energy management applications such as power balance, peak shaving, demand response (DR), and voltage control are implemented using different approaches such as dynamic programming (DP), meta-heuristic, and rule-based approaches.

This chapter is dedicated to the discussion of the available literature on energy management and voltage control in LV distribution systems in presence of DERs followed by the research gaps identified in the literature, and objectives of the thesis. Accordingly, the integration of DERs in LV distribution systems is discussed in Section 1.1. The energy management and voltage control for LV distribution systems is described in Section 1.2. The use of BESSs and smart power converters for implementing different energy management and voltage control applications is described in Section 1.3. The Section 1.4 presents the various approaches used for implementing energy management and voltage control applications. Further, the research gaps identified, objectives, and organization of the thesis are explained in Section 1.5, 1.6, and 1.7, respectively.

1.1 INTEGRATION OF DISTRIBUTED ENERGY RESOURCES IN LOW VOLTAGE DISTRIBUTION SYTEMS

The benefits and challenges of integration of renewable energy sources (RESs), diesel generators (DGs), and BESSs in the distribution systems are discussed as follows.

1.1.1 Renewable Energy Sources

The integration of RESs provides several benefits such as [5],

1. Environmental benefits such as reduction in pollution as well as green house gas emissions

2. Defers new power plants installations and transmission lines extensions

3. Power supply during emergency conditions

4. Energy access to the remote places

5. Social and economical growth with improved job opportunities

6. Possible line losses reduction when located near the load demand

7. Possible reduction in peak power requirements

Due to these benefits of RESs along with their reduced capital costs, and provision of incentives for their installations by local government utilities, there is continuous growth of their use in LV distribution systems. Moreover, there is a continuous decrease in the tariff of solar and wind energy as shown in Fig. 1.1 [6]. This has led to the increased use of solar photovoltaic (PV) and wind power sources in recent days.

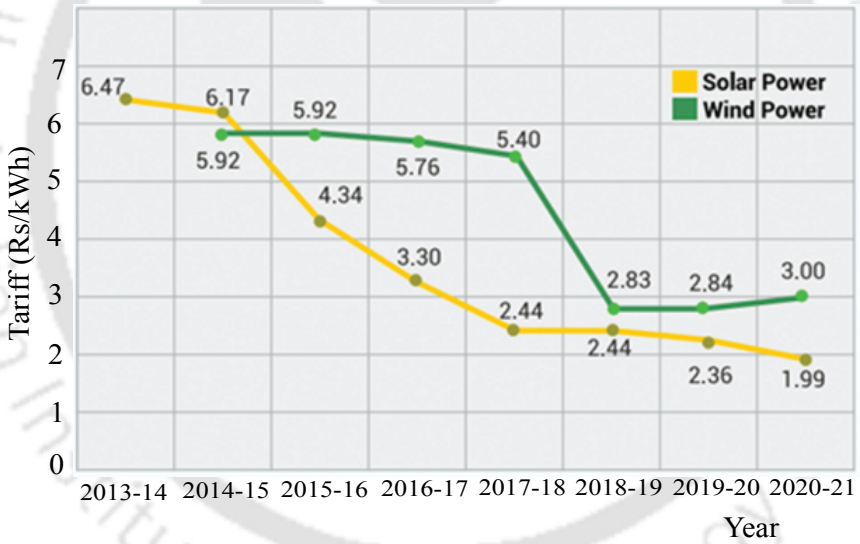

Fig. 1.1 Solar and wind energy tariff .

The installed capacity of power generation in India till October, 2022 is shown in Fig. 1.2 [7]. It indicates that the RESs installed capacity is 119.1 GW out of the total installed capacity of 408.71 GW i.e., the RESs installed capacity is nearly about 30% out of total installed capacity. The PV and wind power sources require power conversion systems in order to integrate them to the distribution systems [8]. The integration of PV source to the ac bus of the distribution system is shown in Fig. 1.3. The PV source is connected through the dc/dc and ac/ac converters to the ac bus. In general, the dc/dc converter is used for extracting maximum power from the PV source by implementing the maximum power point tracking (MPPT) algorithms.

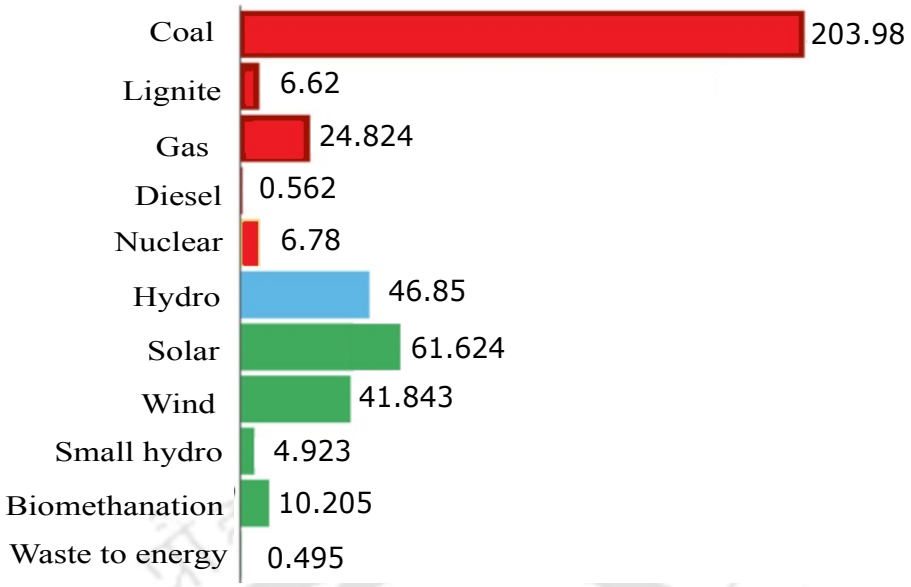

Fig. 1.2 Installed capacity in GW in India till October, 2022.

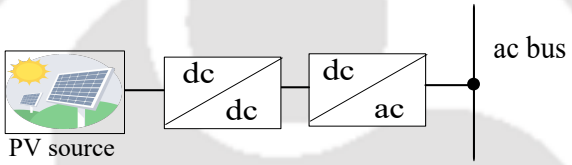

Fig. 1.3 Integration of PV source to the ac bus of the distribution system.

The integration of the wind power source to the ac bus of the distribution system is shown in Fig. 1.4. The wind power source is connected through the ac/dc and dc/ac

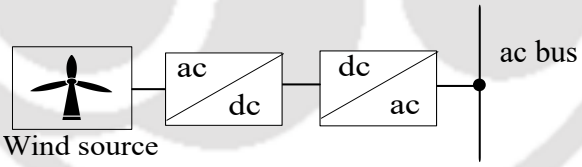

Fig. 1.4 Integration of wind power source to the ac bus of the distribution system .

converters to the ac bus. The ac/dc converter is used for extracting maximum power from the wind power source by implementing the MPPT tracking algorithms.

Even though there are several benefits associated with the integration of RESs in distribution systems, there exists certain technical challenges as given below [5], [9], [10].

1. Variation of power with respect to weather conditions (solar irradiation and wind availability)

2. Reliability issues

3. Power quality issues such as voltage variations, frequency variations, noise, harmonics, etc.

4. Stability issues

5. Cost of investment

6. Effects on conventional power plants such as increase in operation, maintenance, and fuel costs as well as decrease in the expected life of power plants

It is possible to solve the few of the above challenges using the other resources such as the DG and BESSs [11] as discussed in following sections.

1.1.2 Diesel Generator

A DG utilizes a diesel engine and electric generator to generate electrical energy. It is capable of providing steady power irrespective of weather conditions. It can inject both active and reactive power into the system [12]. The DGs are useful for supplying power when the RESs power is not sufficient to balance the required load demand. An example of PV and DG source connected to ac bus of the distribution system is shown in Fig. 1.5 [13]. In this case, the impact of variability of the PV power can be mitigated using DG.

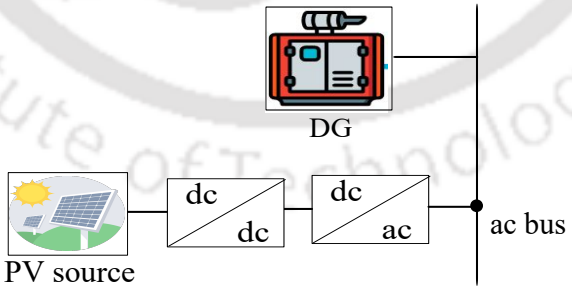

Fig. 1.5 DG and PV source connected to ac bus of the distribution system .

Moreover, DGs are used as a back-up source to provide power during the emergency conditions and power outages. The DGs are also used as main power supply to support the loads in isolated distribution systems [14]. In [15], the RESs and DG based hybrid power systems are discussed for improving the reliability of the system. Further, the DGs have low installation cost, and its operation is simple and reliable. However, the

high operating cost is the main disadvantage of DGs which depends on its fuel consumption. In DG based systems, the fuel consumption of DG depends not only on its power requirement but also on its rating [16]. Therefore, in order to avoid the high fuel consumption cost of DG, the use of energy storage systems along with the DGs is encouraged [17] in LV distribution systems as discussed in following section.

1.1.3 Battery Energy Storage System

A BESS is a combination of a power converter and the energy storage medium of the battery. The dc energy is stored in the battery. The converter is useful for maintaining the required charge/discharge powers. The BESS responds quickly to the frequency and voltage changes than the DGs and compensates the intermittency of RESs. It means that the BESSs can absorb and store the excess power available with the renewable sources and deliver power to the load as and when required [18]. Therefore, BESSs increase the reliability and provide more flexibility for the operation of distribution systems. An example of hybrid power system with the integration of the battery to the dc bus of the distribution system along with DG and RESs is shown in Fig. 1.6. The battery is connected through a dc/dc converter to the dc bus [8].

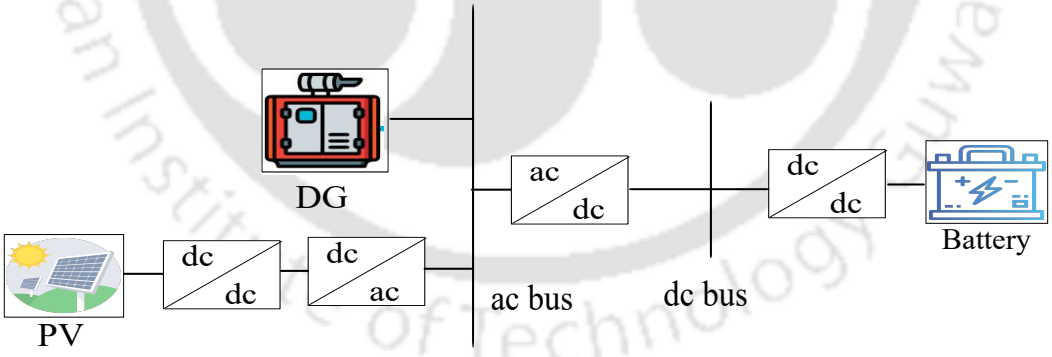

Fig. 1.6 Integration of the battery to the dc bus of the distribution system along with PV source and DG .

The use of these various DERs in LV distribution systems requires efficient control strategies/approaches for managing energy flow [19]. This requires the development of energy management methods which are discussed in following sections.

1.2 ENERGY MANAGEMENT AND VOLTAGE CONTROL FOR LOW VOLTAGE DISTRIBUTION SYSTEMS

The energy management is used to effectively coordinate energy sharing among the different energy sources while supplying required amount of load in the system. The voltage control methods are used for improving the voltage profile in distribution systems. In literature, there exists several energy management and voltage control approaches based on different applications, operating modes, control structure, optimization problem formulation, optimization methods, uncertainty modelling, etc. The application can be for residential, industrial or commercial loads [20]. The operating mode can be either grid-connected or islanded operation [21]. The control structure can be centralized, decentralized or hierarchical [22]. Further, the uncertainty can be modelled as deterministic or stochastic [23]. Similarly the optimization problem can be single objective or multi-objective [24]. The energy management approaches involve an objective function such as minimizing the energy loss, minimizing the energy consumption cost, minimizing the peak power, minimizing the voltage deviation, minimizing the fuel consumption, maximizing the lifetime of different components of the system (e.g., converters, batteries), maximizing the environmental benefits, etc [25]. These objectives have to be achieved while satisfying the various constraints of the system such as device ratings, bus voltage magnitudes constraints, thermal limits of the lines, etc.

Therefore, energy management and voltage control approaches involve different optimization problems with different objectives and constraints. These optimization problems are solved using optimization techniques. In this scenario, energy management and voltage control of the systems need the presence of flexible control devices for achieving these objectives. The BESSs and smart power converters are widely used for implementing the energy management applications. The use of these BESSs and smart power converters for different energy management and voltage control applications in LV distribution systems is discussed in following sections.

1.3 ENERGY MANAGEMENT AND VOLTAGE CONTROL USING BATTERY ENERGY STORAGE SYSTEMS AND SMART POWER CONVERTERS

1.3.1 Battery Energy Storage Systems

The BESSs are able to absorb and store the excess power available with the renewable sources as well as deliver power to the load as and when required. With these features, the BESSs can increase the reliability of power supply to the load and also increase the self consumption of the systems. They also provide the flexibility for the operation of distribution systems with their charge/discharge power control capability. Due to these advantages, it is possible to implement the energy management and voltage control applications using BESSs [26]. There are several real world implementations of BESSs which are used for different applications in various countries. The Hornsdale Power Reserve is the first largest BESS installed in South Australia in 2017 with an energy capacity of 100 MWh and power rating of 100 MW [27]. It is used for providing the energy arbitrage and contingency spinning reserve services. The Green Mountain Power project is the other grid scale BESS installed in Vermont in 2015 with a power rating of 4 MW and 20 MWh [28]. It is used for providing the back-up power and energy consumption cost savings. There are also several hybrid BESS installations in Braderup, Brilon, and Varel which are located in Germany to increase self consumption, provide power reserve, energy trading, reactive power, etc [26]. In India, the first grid-scale BESS is installed in Delhi in 2019 with a rating of 10 MW and 10 MWh to utilise for Tata power distribution network. The Tata power in collaboration with the company Nexcharge installed a BESS with a rating of 150 kW/528 kWh to improve the reliability, reduce the peak load [29].

The BESSs used for implementing the power balance, peak shaving, and DR applications are discussed in detail as follows.

Power Balance

The active power balance is the essential condition to be satisfied for normal operation of the power system [30]. Considering the variable nature of RESs and load demand,

it is important to maintain the power balance in the power systems [31]. The design and control of a hybrid ac/dc microgrid (MG) for power balance in both grid-connected mode and isolated mode has been studied in [21]. A system as shown in Fig. 1.7 is considered. In grid-connected mode, the grid ensures the power balance. The excess power produced by the hybrid MG is sent back to grid and the deficit power in the system is supplied by grid. Here, the storage system is not very important as grid ensures the balancing of power. However, in isolated mode, the energy storage becomes very important to ensure power balancing. There are four operating states in isolated mode. In state 1, the energy generated in both the MGs i.e. both ac and dc MGs meet their individual loads. Then, there is no exchange of power through main converter. In state 2, power generated in ac MG is not sufficient for its loads, but the power generated in dc MG is more than its load requirement. Then, the required power is transferred from dc bus to ac loads. In state 3, the dc load requirement is not supplied by dc MG, then it is supplied from ac MG. In state 4, the load demand is not met by both MGs, then automatic load shedding is applied.

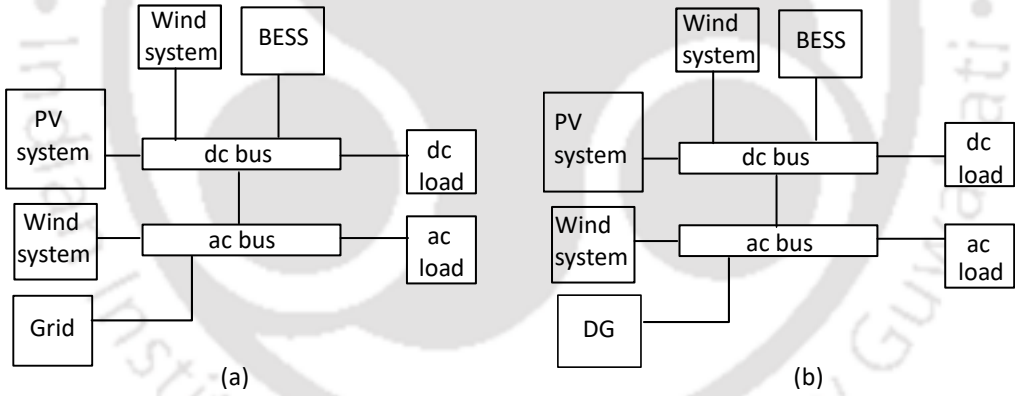

Fig. 1.7 Power balance. (a) Grid-connected mode. (b) Isolated mode .

Further, in literature BESS and super capacitor (SC) are considered for power balance application in isolated system consisting of wind power sources in [32]. In [33], [34], an isolated hybrid power system consisting of PV, wind and energy storage devices is considered where storage devices are used for ensuring power balance in the system.

The peak shaving is another important energy management application of BESSs which is discussed in following section.

Peak Shaving

The process of reducing the peak power is considered as peak shaving. It is possible to reduce the peak powers by discharging the energy storage during peak power hours. In literature the peak shaving application using energy storage is extensively discussed. In [35], the importance of peak shaving using energy storage devices for reducing the capital expenditure (by reducing the infrastructure cost) and operational expenditure (by reducing energy consumption cost) is presented. The energy storage options such as BESS and super capacitor for peak shaving application are discussed in detail. In [36], the application of energy storage devices for peak power reduction in a data center is presented and various peak shaving techniques are discussed. Further, the economic benefits associated with the peak shaving techniques are analyzed. In [37], the impacts of peak shaving techniques in a Google data center on energy consumption cost are discussed. Further, peak shaving application using energy storage is described. In [38], a peak shaving control strategy based on BESS is proposed for reducing the wind power curtailment and operation costs of the system. In [39], the application of peak shaving for energy loss reduction in a distribution system is presented. The energy storage devices are used for peak shaving and optimally placed for energy loss minimization.

In [40], an offline heuristic algorithm named MinPeak is developed to minimize the peak power consumption while scheduling the controllable appliances of the system. However, the application of the energy storage is not considered. In [41], an online computational approach is developed for minimizing the peak grid demand considering the electric vehicle (EV) charging. In [42], a heuristic algorithm is developed for minimizing the EV charging cost as well as the peak demand while controlling the charging powers of EV. However, the control of the battery power during discharging is not discussed in [41], [42]. In [43], an online algorithm is proposed to minimize the peak demand usage while determining the discharge quantity of the energy storage. However, the control of the battery power during charging is not considered.

The peak shaving control using power limits is widely used in industry due to its simplicity [37]. The maximum limit of power that is drawn from (injected into) the utility grid is known as the demand limit (feed-in limit). In [44], energy storage is employed for peak shaving using a demand limit while reducing the energy cost of the system. A system as shown in Fig. 1.8 is considered. The PV source and BESS are connected to

dc link through dc-dc converters. The bi-directional dc-ac converter is used to integrate PV-BESS to the grid.

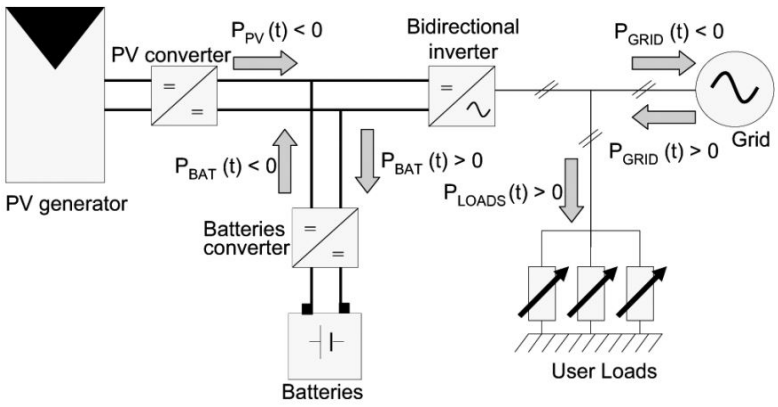

Fig. 1.8 Grid-connected PV storage system .

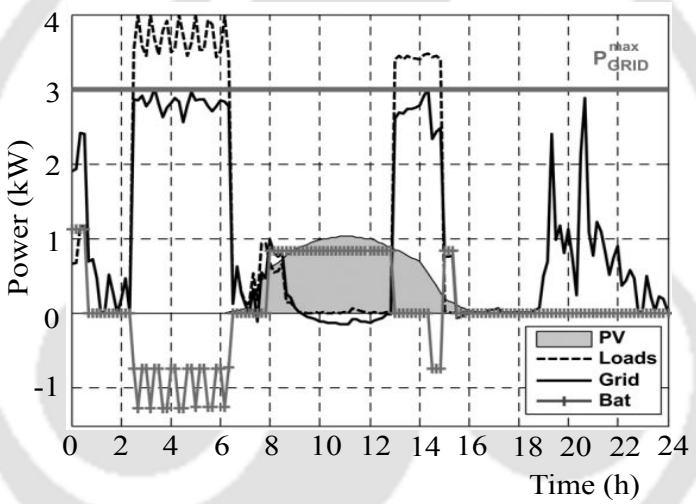

Fig. 1.9 Power flows in the grid-connected PV storage system .

The problem of optimal energy management is solved by considering the minimization of energy cost of the system as objective function. The peak power constraint is considered along with the power balance, the battery state of charge (SoC) and charge/discharge power constraints. The obtained power flows are shown in Fig. 1.9. The load demand above the demand limit is supplied by either PV or the battery to limit the peak grid power to the chosen grid maximum power limit of 3 kW. Battery is discharged during the peak load hours and charged when the load demand is less than the demand limit. Moreover, the flexible day-to-day management of the battery is maintained. Flexible day-to-day management with energy storage is the property of maintaining its SoC at the end of the day, the same as SoC of the start of the day.

In [45], a controller is designed for peak shaving which charges/discharges the storage system using a demand limit. In [46], storage systems are optimally sized for peak shaving and a peak shaving control strategy is proposed for minimizing peak load in distribution systems using demand limit. The improved distribution system performance and energy cost reductions due to peak shaving control are discussed. Similarly, in [47], [48], demand limit is considered for peak shaving with the battery controller. However, the feed-in limit is not considered. In [49], peak shaving using optimal schedules of BESS with a demand limit is considered. In [50], energy storage is used for peak shaving considering demand limit in order to enhance the reliability of supply. In [51], demand limit is considered to operate the appliances of the system economically. In [52], the peak shaving is done while minimizing the operating costs of the system. The demand limit is considered as a constraint. The trajectory of SoC of the battery, set points of voltage regulating devices, and reactive powers DERs are considered as control variables. The optimization problem is formulated as mixed-integer second-order cone program which is handled by CPLEX solver. However, the number of control variables are more as the trajectories are considered to be controlled (e.g. considering the SoC trajectory as the control variable leads to twenty four control variables over a day with hourly dispatch of the battery). Moreover, in [40]–[52], the feed-in limit is not considered.

The importance of peak feed-in limit for voltage control in distribution systems is presented in [53]. In [54], the feed-in limit is considered for peak shaving, but the demand limit is not considered. It is known that the voltage drop issues in the distribution network are due to the peak demand, and voltage rise issues are due to peak feed-in powers. Moreover, limiting peak powers leads to the reduction of energy losses in the system. Therefore, it is important to limit both peak demand and feed-in powers for a better voltage profile and increased energy efficiency of the distribution system.

Along with the power balance and peak shaving, the DR is another energy management application of BESSs which is discussed in following section.

Demand Response

The methods developed by energy utilities to influence the energy consumption patterns of consumers are termed as DR methods. The use of energy storage along with

RESs allows the consumers to change their load profile patterns and participate in DR programs. The DR programs are categorized into two types i.e. incentive based (IB) programs and price based (PB) programs. The incentive based programs are further classified into six types [55] as given in Table 1.1.

Table 1.1 Incentive Based Programs and their Functions

Incentive based program	Function
DLC	Control of loads directly by utility.
I/C	Offering discounts for reducing electricity consumption.
DB	Bidding by consumers for reducing load at a given price.
EDR	Offering financial incentives if system's reliability is in critical condition.
CM	Committing load reduction before the occurrence of critical condition.
ASM	Bidding a load reduction amount on the ancillary services market.

In direct load control (DLC) program, utility or system operator controls the consumer's equipment in case of local contingencies by offering incentive payment. In interruptible/curtailable (I/C) services, consumers receive a discount or credit for reducing load during contingencies. In demand bidding (DB) programs, large consumers are encouraged to provide their load reductions at a price at which they are interested to curtail, or to know how much load they would be interested to curtail at posted prices. In emergency demand response (EDR) program, consumers will be provided incentive payment for their load reduction during reliability-triggered events. In capacity market (CM) programs, consumers have to commit for providing specified load reductions during contingencies, if they don't provide penalty will be applied. In ancillary service markets (ASM), consumers are allowed to bid load curtailments in independent system operator (ISO) markets as operating reserves. If their load curtailments are needed, they will be paid spot market energy price by ISO.

The price based programs are further classified into three types [56] as given in Table 1.2. In time of use (ToU) program, based on the time of the day (peak, average and off-peak periods), different electricity rates are used. In real time price (RTP) program, the rates are dynamically changed throughout the day. Utility gives the forecasts of these rates to the consumers an hour or a day in advance. In critical peak pricing (CPP), consumers are charged with higher rates during the critical operating conditions

(contingencies), and so it is used in addition to ToU.

Table 1.2 Price Based Programs and their Functions

Price based program	Function
ToU	Changing electricity prices depending on time of the day like on-peak, average load and off-peak hours.
RTP	Changing electricity prices every hour of the day.
CPP	Charging higher prices during contingencies.

Use of energy storage along with PV sources allows the consumers to change their load profile patterns and participate in price based DR programs [57]. The importance of energy storage for DR under dynamic energy price market is presented in [58]. A smart MG including a smart home has been studied in [59] and energy consumption cost is reduced with the help of price based DR and DERs management. In accordance to DR decisions, DER management coordinates operations of micro combined heat power systems (CHPs) and the battery. A three level hierarchical optimization is proposed. The lowest level is DR which is performed by distributed agent in each home for reducing the energy consumption cost. In the next level, a centralized agent optimizes micro CHPs generation after getting load demand of each house with DR. In this strategy, generation of all micro CHPs is coordinated to minimize the cost of whole community. In the last level optimal control of the battery charging and discharging is done. The resulting energy consumption cost for different days with and without the DR is shown in Fig. 1.10. It indicates that the energy consumption cost is reduced with the application of DR method in all the days.

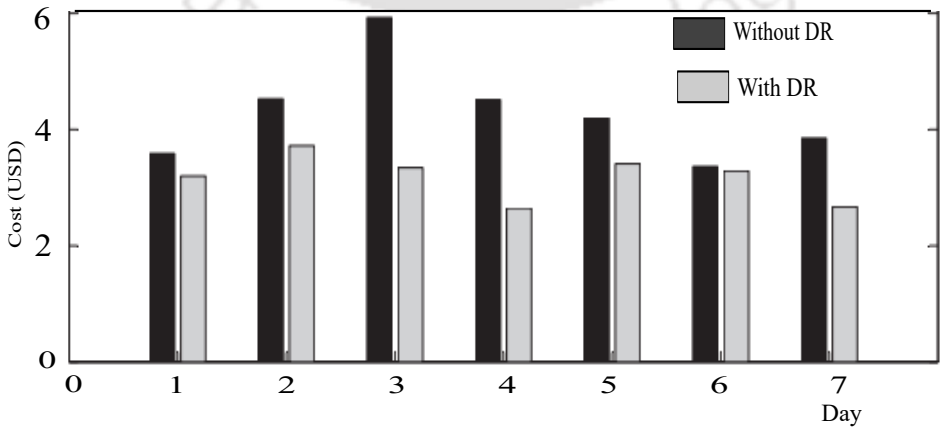

Fig. 1.10 Energy consumption cost without DR and with DR .

Further, the DR control using energy storage level thresholds, power limits and energy

price limits for economical operation of the system is discussed in the literature. In [60], energy storage level thresholds are considered for economical operation of the system. Both energy buying and selling prices are considered for implementing the control strategy and two thresholds are used for deciding schedules of energy storage. However, the presence of RESs along with the storage is not considered. Similarly, energy storage level thresholds are considered for economical operation of the system with RESs and ac/dc loads in [61]. However, the selling price of energy is not considered. In [62] and [63], power limits are considered for scheduling load appliances of the system in order to minimize the energy cost of the system. In [64], the power limit is considered to control the energy price of consumers.

In [65], the energy storage is used to reduce the operating cost of the system while considering both buying and selling prices of energy. An optimization model using energy storage is proposed in [66] for energy cost reduction of the system. In both [65], [66] the energy cost is reduced by charging the energy storage during low buying price hours and discharging it during high buying price hours. In [67], the effect of energy price limits for reducing the energy cost of the system using BESS is presented. However, the use of RESs with BESS is not considered. In [68], the energy price limit is considered as a price below which each appliance starts to operate for minimizing energy cost of the system. In [69], the buying price limit is considered to control the set-point temperature of the thermostat. In [70], buying price limit is considered while flexible day-to-day management is maintained. However, the price variation is considered for only two periods. In [71], a price limit is considered below which energy can not be sold. However, the buying price limit is not considered. The literature works based on consideration of system components, energy storage level thresholds, power limits, and energy price limits for energy consumption cost reduction are summarized in Table 1.3.

It is important to have both energy buying and selling price limits for DR control in PV storage systems. Because energy cost of the system is reduced if the battery is discharged when buying price is more than the buying price limit. It means that less or no power is drawn from grid when buying price is more than its limit. Similarly, if there is selling price involved, operating energy cost is reduced if PV source is used to charge the battery only when selling price is less than the selling price limit. It means that PV power is injected to grid when selling price is more than its limit. In this scenario it is important to have optimal energy buying and selling price limits for minimizing the

Table 1.3 Literature Works Based on Consideration of Various Parameters for Energy Consumption Cost Reduction

Work	RES	Energy storage	Energy storage threshold	Power limit	Energy buying price limit	Energy selling price limit
[60]	No	Yes	Yes	No	No	No
[61]	Yes	Yes	Yes	No	No	No
[62], [63]	No	No	No	Yes	No	No
[65], [66]	No	Yes	No	No	Yes	Yes
[67]	No	Yes	No	No	Yes	Yes
[68]	No	No	No	No	Yes	No
[69]	No	No	No	No	Yes	No
[70]	Yes	Yes	No	No	Yes	No
[71]	Yes	No	No	No	No	Yes

energy cost of the system.

Along with the above discussed applications, the BESSs are also used for increasing the self consumption of the system [72], [73], economic operation of grid-connected systems [74], [75], and economical operation of isolated systems [76], [77].

Further, the smart power converters are also widely used for implementing few energy management and voltage control applications as discussed in following section.

1.3.2 Smart Power Converters

The smart power converters are the devices capable of operating in grid-forming and grid-following modes [78]. In grid following mode, the power converters act as ac current sources providing active/reactive powers as per the given references. In grid forming mode, power converters operate as ac voltage sources while maintaining the terminal voltage and frequency as per given references [79]. A back-to-back converter which can act as smart power converter is shown in Fig. 1.11. For example, the ac/dc converter can be used to maintain the LV dc bus voltage and dc/ac converter can be used to maintain the LV ac bus voltage/frequency as per the given references by operating them in grid-forming mode.

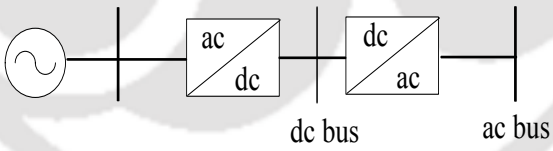

Fig. 1.11 Back-to-back converter which can be used as smart power converter .

Moreover, the dc/ac converters of PV and wind energy sources can also act as smart power converters. In literature, the smart power converters are mainly used for voltage control and energy demand reduction as discussed in following section.

Voltage Control

Voltage control is used to maintain the bus voltages of the system within the limits specified by the grid code. Various methods such as active power curtailment (APC), voltage regulation, and reactive power control are used for voltage control in distribution networks [80]. The APC leads to under-utilization of PV sources [81]. In [82], [83],

reactive power control is done for voltage control. The on load tap changers (OLTCs) are used for voltage regulation in distribution networks. However, their control action is slow due to the presence of mechanical switches and movable parts. Moreover, they cannot control the voltage continuously due to fixed number of taps. These OLTC transformers are typically used to achieve limited voltage regulation capability at higher substation voltage levels of 60/11 kV. In general, the conventional distribution transformers used at the voltage level of 11/0.4 kV do not have any voltage regulation capability for maintaining bus voltages within acceptable limits [84].

The smart power converters operating in grid following mode can be used for voltage control. In [85], different scenarios are considered to show the impact of PV inverters on voltage control in distribution network. The PV inverters are operated in grid following mode to control their active and reactive power references optimally as per the chosen objectives. The optimization problems are solved using gradient projection algorithm. The case of no voltage control is considered as Scenario 1. In Scenario 2, the PV inverters are optimally dispatched to regulate all the load bus voltages within the limits specified by grid code which are chosen as 0.95 p.u. and 1.05 p.u. [86]. In Scenario 3, the PV inverters are optimally dispatched to regulate all the load bus voltages within 0.97 p.u. and 1.03 p.u. for tight voltage regulation. In Scenario 4, the PV inverters are optimally dispatched for conservation voltage reduction (CVR) for energy savings purpose.

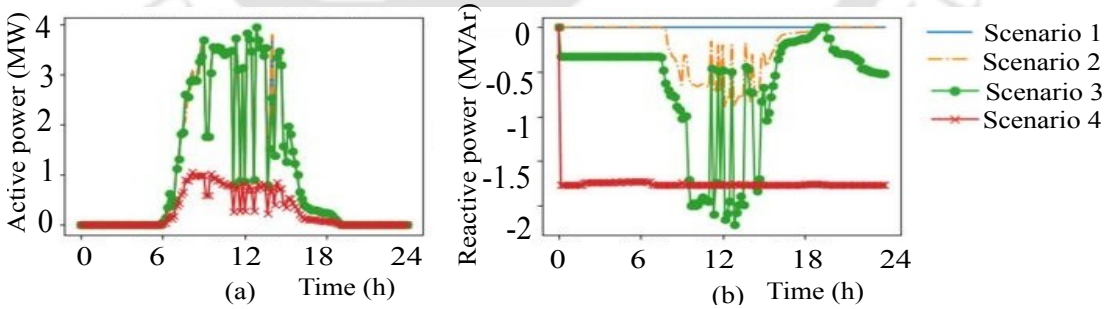

Fig. 1.12 (a) Active powers of PV inverters. (b) Reactive powers of PV inverters .

The optimal energy dispatch of PV inverters over a day is shown in Fig. 1.12. The Fig. 1.12(a) indicates that the active power is less in Scenario 4 as compared to other scenarios. This is because for the application of CVR, the reactive power supply is increased and maintained at higher possible value as shown in Fig. 1.12(b). The resulting load bus voltages are shown in 1.13.

The Fig. 1.13(a) indicates that for Scenario 1, there are voltage rise violations. For Scenario 2, the voltages are maintained within the limits. However, they are not close to 1 p.u. as they are regulated within 1.05 p.u. and 0.95 p.u. which are shown in Fig. 1.13(b). In Scenario 3, the voltages are maintained within the limits and they are not close to 1 p.u. due to tight voltage regulation as shown in Fig. 1.13(c). In Scenario 4, the voltages are maintained within the limits and towards the lower limit due to CVR application as shown in Fig. 1.13(d).

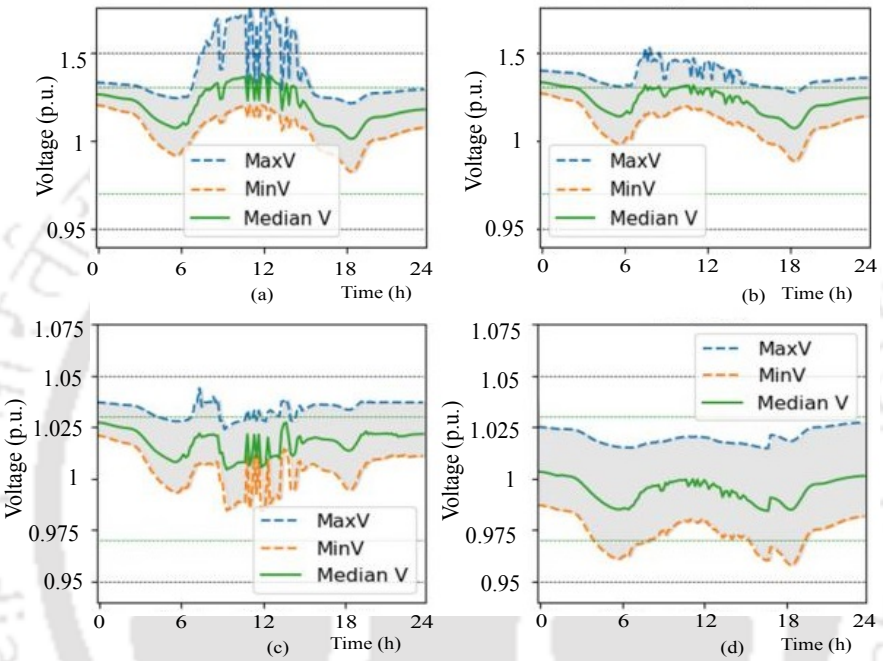

Fig. 1.13 Maximum, minimum, and median load bus voltages .

Moreover, the smart power converters operating in grid forming mode can be used for voltage control. In [87] full output voltage range based and set points based voltage control methods are studied. In a full output range based voltage control, the output voltage is infinitely adjustable within its range whereas in set points based voltage control the output voltage is chosen from the predefined set points. Therefore, set points based voltage control schemes are simple and has certain financial advantages as compared to full voltage range control methods. The set points based voltage control methods such as switching between two set points based on end-of-line voltage as well as switching between two set points based on current (SBTSPBOC) are discussed. Among all the methods discussed, the SBTSPBOC is shown as a practically feasible and better method of voltage control. In SBTSPBOC, the direct-axis transformer current is used to decide the set points of voltage. However, if the direct-axis transformer current is flowing in

one direction, it can not be said that the current at all other buses is also flowing in the same direction. In those cases, voltage control based on current does not work.

Along with the voltage control application, the smart power converters are also used for energy demand reduction in LV distribution systems as discussed in following section.

Energy Demand Reduction

The LV ac bus power depends on the power loss in the distribution lines as well as on load demand. The use of smart power converters for minimizing the power demand through the minimization of power loss and load demand is discussed in literature. The use of distribution static synchronous compensator (DSTATCOM) with an optimal location for minimizing power losses in distribution system is presented in [88]. The use of unified power quality conditioner (UPQC) and its optimal location for minimizing the power loss in distribution systems is studied in [89]. The reactive power control is possible with grid following mode using the renewable energy converters. In [82], reactive power control strategies for minimizing the losses in a wind farm system are presented. In [83], the reactive power control through PV inverters is employed to minimize the power losses while improving the voltage profile of distribution system. In [90], [91], the impact of voltage and reactive power control on reducing the power loss of the system is presented. In [92], [93], smart power converters are operated in grid forming mode to reduce the load demand through LV ac terminal voltage magnitude control. In [94], the impact of voltage and reactive power control using smart power converters is presented for reducing the power requirement of the system. literature works based on energy management applications and control devices are tabulated in Table 1.4.

The implementation of the above discussed energy management and voltage control applications using BESSs and smart power converters by different approaches is discussed in following section.

Table 1.4 Literature Works Based on Different Applications and Control Devices

Work	Control devices	Application
[21], [32]–[34]	BESS	Power balance
[35]–[39], [44]–[50]	BESS	Peak shaving
[58]–[61], [65]–[67]	BESS	DR
[72], [73]	BESS	Increasing self-consumption
[74], [75], [95]–[100]	BESS	Economical operation of grid-connected systems
[16], [76], [77], [101]–[103]	BESS	Economical operation of isolated systems
[81]–[83], [85], [87]	Smart power converters	Voltage control
[88]–[94]	Smart power converters	Energy demand reduction

1.4 APPROACHES OF ENERGY MANAGEMENT AND VOLTAGE CONTROL

The energy management and voltage control approaches such as DP, meta-heuristic, and rule-based approaches which are used for different applications in literature are discussed in this section.

1.4.1 Dynamic Programming Approaches

In DP approaches, a multistage problem is decomposed into a sequence of interrelated one-stage problems [104]. In [74], the PV storage system is considered and charge and discharge powers of the battery are scheduled using DP such that energy consumption cost is minimized. In [75], a DP approach is proposed for minimizing the operating cost of a hybrid system consisting of RESs, storage, and DG. In [95], the battery schedules are decided based on DP to maximize the benefits associated with the RESs energy and minimize the energy consumption cost. In [105], several residential systems consisting of PV source and energy storage are considered. An energy management system is proposed to improve the energy efficiency of the residential distribution network using adaptive DP approach. In [106], the DP is used for optimizing power split between the battery and SC.

Along with DP approaches, the meta-heuristic approaches are used for several energy

management and voltage control applications as discussed in following section.

1.4.2 Meta-heuristic Approaches

The heuristic approaches are the combination of rules that are useful for obtaining a solution which may or may not be the global optimal solution [107]. To avoid this possibility of obtaining non global optimal solutions meta-heuristic approaches are introduced. Meta-heuristic approaches are the combination of search methods which try to avoid local optimums and find the near global optimal solutions [108]. Heuristic approaches are problem dependent whereas meta-heuristic approaches are problem independent. Meta-heuristic approaches are global optimizers and very flexible. They use intelligence of biological evolution, artificial intelligence, etc. in order to obtain the solutions close to the global optimum [109]. In [96], particle swarm optimization (PSO) based energy management method is presented to minimize the operation, emission and reliability cost of the system while optimally controlling the DG and the battery powers. In [97], a system consisting of DERs such as RESs and energy storage devices is considered to implement the incentive based DR. The PSO is used to solve the multi objective optimization problem for minimizing the operating cost and emission cost of the system. The PSO algorithm was applied in [110] to a grid-connected MG consisting of wind power, storage device, hydro power and with the application of DR for changing load profile. In [111], an MG consisting of RESs, fuel cell, micro turbine and energy storage devices is considered. The PSO based energy management strategy is presented for minimizing the total energy and operating cost of the MG. The uncertainties of RESs and market prices are considered.

In [98], a smart energy management system is proposed. The genetic algorithm (GA) is used to optimally control the energy storage powers to minimize the operating cost of the system. In [99], the energy storage management is done to minimize the line losses, annual cost and emissions of the system using GA. In [112], an MG consisting of RESs, fuel cell and energy storage is considered and the net present worth is maximized using GA. In [113], the power generation cost is minimized and the useful life of energy storage is maximized using GA.

Further, the rule-based approaches are also used in literature for implementing different

energy management and voltage control applications as discussed in following section.

1.4.3 Rule-based Approaches

The rule-based algorithms attempt to execute instructions from a starting set of data (control inputs) and *if-then* statement rules [114]. These approaches are widely used in industry due to their simplicity and ease of application in real-time [115]. Moreover, the rule-based approach is the suggested approach by IEEE Std 2030.7 for microgrid control purpose due to their advantages like easy implementation, easy maintenance, clear meaning of the chosen rules, and low cost [116]–[118]. An example of rule-based control approach with its inputs and output is shown in Fig. 1.14. As per that, the required output is determined using the control inputs and rules of control algorithm for given base inputs (e.g. load, RES power, and energy price). The control inputs and rules are obtained using various methods i.e., heuristics, human expertise, mathematical models, forecasts knowledge, etc [119]. In general, the operating points of controllable components (e.g. active/reactive power references and voltage/frequency references for smart power converters) are chosen as output. The control inputs are specific to the particular application of rule-based control such as demand limit for peak shaving and maximum/minimum voltage limit for voltage control.

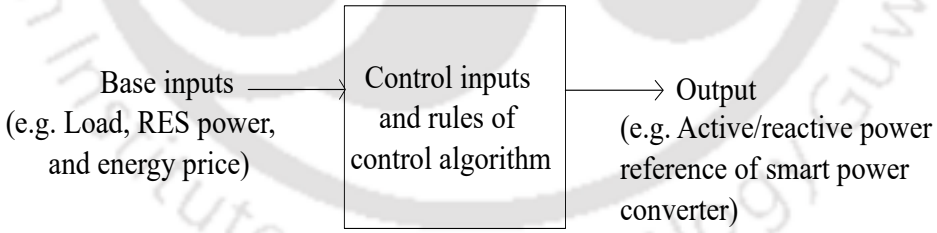

Fig. 1.14 Rule-based control approach with its inputs and output.

In literature, rule-based control strategies are used for several energy management applications. In [100], a smart residential energy system consisting of a fuel cell and a battery as an energy storage system is considered. A rule-based approach is proposed for optimal operation of battery to reduce the cost of the system. The ToU energy price and the battery efficiency are used to decide the charge/discharge modes of battery. The battery powers are decided based on residual energies at each time and battery capacity. In [120], a day-ahead rule-based scheduling method of micro storage system is proposed for economic benefits. The spot market energy prices are used as base inputs.

The minimum/maximum cutoffs of spot market energy prices and SoC of battery are used as control inputs to decide the battery power. A rule-based energy management approach is proposed in [121] to improve the fuel economy of hybrid vehicles. Based on the SoC and power limits, the output state of the system is decided. In [122], a rule-based control of BESS is used for smooth dispatch of RESs. The RESs power is considered as the base input. The SoC and power limits of battery are considered as control inputs. In [123], a rule-based control algorithm for efficient management of RESs power with energy storage is developed for minimizing energy costs. The ToU energy price, PV power, and load power are used as base inputs. The battery's remaining energy, available PV energy, and energy consumption over the next 24 hours are used as control inputs to decide the charge/discharge power. In [124], a rule-based MG scheduling algorithm is proposed in an isolated hybrid MG to reduce fuel consumption of DG. The net load is used as base input. The SoC constraints and DG power rating are used as control inputs to decide the battery schedules. A DR control strategy for the economic planning of MG is presented in [125] using fuzzy logic rules considering the time of operation, comfort level, temperature deviation, and connected loads as base inputs.

Further, in [126], a rule-based peak shaving control is proposed using energy storage. However, the feed-in limit and flexible day-to-day management of the battery are not considered. In [127], the rule-based voltage control and rule-based peak shaving control are proposed using BESS in presence of high penetration of PV energy. However, it is not optimized. In [128], a rule-based energy management approach is proposed for mitigating the impacts of PV sources such as voltage rise and reverse power flow issues in LV distribution systems using energy storage. However, it is not optimized.

The rule-based control is compared with DP while minimizing the operating cost of the hybrid MG in [75]. In [106], the rule-based control is compared with DP while optimizing power split between the battery and SC. Further, the rule-based approaches for DR are considered and compared with the optimization approaches in [129] and [130]. It is shown that even though rule-based approaches are simple, they do not provide optimal results. This is a limitation of rule-based approaches. However, to avoid this limitation it is possible to optimize the rule-based control approaches with proper selection of control inputs. To show this, a DP optimization based rule development strategy is proposed in [115] for improving the fuel economy of plug-in hybrid electric vehicles

(PHEVs). In [131], the control parameters used in rule-based control are optimized using GA for improving the fuel economy of PHEVs. In [132], an energy management method is proposed using rule-based approach coupled with PSO for improving the BESS life and reduce its stress. In [133], an optimal rule-based energy management approach is proposed for capacity planning of an isolated system consisting of RESs, energy storage, and DG.

The above discussed literature works based on energy management approaches and energy management applications are tabulated in Table 1.5.

Table 1.5 Literature Works Based on Different Approaches and Applications

Work	Energy management approach	Energy management application
[74], [75], [95]	DP	Economical operation of systems
[105]	DP	Minimizing the energy demand and voltage control
[97], [110]	Meta-heuristic	DR
[96], [98], [99], [111]–[113]	Meta-heuristic	Economical operation of systems
[75], [100], [120], [123], [124]	Rule-based	Economic operation of the systems
[126], [127]	Rule-based	Peak shaving
[127], [128]	Rule-based	Voltage control
[125], [129], [130]	Rule-based	DR
[115], [121], [131]	Rule-based	Improving fuel economy of HVs
[132]	Rule-based	Improving the life time of BESS
[133]	Rule-based	Capacity planning of isolated systems

Based on these literature works of different applications, control devices, and approaches, the identified research gaps and objectives of the thesis work are discussed in following sections.

1.5 RESEARCH GAPS/MOTIVATIONS

The research gaps identified in the literature works which are the motivations behind this thesis work are given as follows.

1. The peak shaving application provides several benefits to both grid operators and end-users. For grid operators, peak shaving is used to maintain balance between

the generation and demand, resulting in improved load factor and economical operation of generation. It also provides improved system efficiency and power reliability of the grid [134]. Similarly, peak shaving is helpful in reducing consumer's energy consumption cost by shifting peak demand from a high price period to a low price period [135]. Moreover, it offers improved power quality and reliability for end-users. Further, the voltage drop issues in the distribution network are mainly due to the peak demand, and voltage rise issues are due to peak feed-in powers. Therefore, limiting both peak demand and feed-in powers improves the voltage profile in the distribution network. The peak shaving methods considering both demand and feed-in limits together for minimizing the peak grid power over a day are not developed in the existing literature. Further, most of the literature works have proposed peak shaving methods considering fixed limits which are not optimal and flexible day-to-day management of the battery is not considered. Moreover, there are no literature works which have implemented peak shaving application through optimal rule-based approaches considering both demand and feed-in limits with flexible day-to-day management of battery.

2. Even though peak shaving has several benefits, it may not be useful for minimizing the energy consumption cost when time varying energy price profile is applied for energy consumption of the system. In this scenario, DR is an important energy management application which is used to reduce the energy consumption cost while utilizing the time varying energy price profile [136]. The DR methods considering both energy buying and selling price profiles together for minimizing the grid energy consumption cost over a day are not investigated in the existing literature. Moreover, there are no literature works which have implemented DR application through optimal rule-based approaches considering both energy buying and selling price limits with flexible day-to-day management of battery.

3. Along with peak shaving and DR, voltage control is another important application which is useful for maintaining the distribution system bus voltages within the limits of grid code [137]. High penetration of variable RESs and peak load demand conditions in the distribution systems cause voltage rise and voltage drop issues, respectively in the distribution systems. In this scenario, sensitive equipments do not work satisfactorily if the load bus voltages are not maintained within the specified limits of grid code. Therefore, voltage control is useful for satis-

factory operation of consumer equipment as well as for increasing RESs penetration and loading levels in the distribution grid [138]. The set points based voltage control method considering the maximum and minimum load bus voltages for minimizing the voltage deviation of the distribution system over a day is not presented in the existing literature. Moreover, there are no literature works which have implemented voltage control application through optimal rule-based approaches considering both maximum and minimum load bus voltages.

4. Further, in case of DG supplied islanded MGs, the reduction of fuel consumption of DG is an important energy management application. The fuel consumption of DG not only depends on the power drawn from DG but also on the rating of DG. In this scenario, the DG rating can be reduced by the peak shaving application. However, the impact of peak shaving on isolated DG supplied distribution systems is not discussed in the existing literature.

1.6 OBJECTIVES

Based on the literature and motivations, the objectives of the thesis work are given as follows:

1. To propose an optimal rule-based peak shaving method considering demand and feed-in limits together for minimizing the peak grid power over a day in a grid-connected PV-BESS system.

2. To propose an optimal rule-based DR method considering energy buying and selling price profiles for minimizing the energy consumption cost over a day in a grid-connected PV-BESS system.

3. To propose an optimal rule-based voltage control method considering the maximum and minimum load bus voltages for minimizing the voltage deviation over a day in a grid-connected PV-rich distribution system.

4. To modify the proposed optimal rule-based peak shaving method for minimizing the peak DG power over a day in an isolated DG-BESS-Wind-PV distribution system.

5. To test and validate the proposed optimal rule-based energy management methods and demonstrate their impact on various performance indicators of the system.

1.7 ORGANIZATION OF THE THESIS

The organization of the thesis is given as follows.

In **Chapter 1**, the role of energy management in modern power distribution systems is discussed. The importance of use of energy storage devices and smart power converters for different energy management applications is explained. The various energy management approaches used in literature are revealed. Further, the motivations and objectives of the thesis are presented.

In **Chapter 2**, the proposed optimal rule-based peak shaving method is discussed. Firstly the considered system is described. Then, operating modes of the battery, method of determination of control inputs for rule-based method and rules of the peak shaving control are explained. The determination method of optimal control inputs for the proposed control is presented. Further, the results and conclusions are revealed.

In **Chapter 3** the proposed optimal rule-based DR method is discussed. Firstly the considered system is described. Then, operating modes of the battery, method of determination of control inputs for rule-based DR and rules of the DR control are explained. The determination method of optimal control inputs for the proposed control is presented. Further, the results and conclusions are revealed.

In **Chapter 4** the proposed optimal rule-based voltage control method is discussed. Firstly the considered system is described. Then, method of determination of control inputs for rule-based method and rules of the voltage control are explained. The determination method of optimal control inputs for the proposed control is presented. Further, the results and conclusions are revealed.

In **Chapter 5** the modified peak shaving control for application in a DG supplied LV ac distribution system is discussed. Firstly the considered system is described. Then, overview of the proposed peak shaving control is presented. Accordingly, the process of minimizing the LV ac bus power, the modified rule-based peak shaving method, and the

determination of optimal control inputs for the proposed control are presented. Further, the results and conclusions are revealed.

In **Chapter 6**, the summary of the thesis work and the scope of the future work are presented.

CHAPTER 2

OPTIMAL RULE-BASED PEAK SHAVING WITH DEMAND AND FEED-IN LIMITS USING BATTERY ENERGY STORAGE SYSTEM

In Chapter 1, the importance of peak shaving in modern power distribution systems and the use of BESSs for peak shaving application are discussed. For grid operators, peak shaving is used to maintain the balance between the generation and demand, resulting in improved load factor and economical operation of generation. It also provides improved system efficiency and power reliability of the grid [134]. Similarly, peak shaving is helpful in reducing consumer's energy consumption cost by shifting peak demand from a high price period to a low price period [135]. Moreover, it offers improved power quality and reliability for end-users. It is possible to reduce the peak powers by discharging the energy storage during peak power hours. The peak shaving methods using power limits is widely used in industry due to its simplicity [37]. In the existing literature, the peak shaving methods are proposed mainly considering the demand limit.

Further, the voltage drop issues in the distribution network are due to the peak demand, and voltage rise issues are due to peak feed-in powers. The importance of feed-in limit for voltage control in distribution systems is presented in literature [53]. Moreover, limiting peak powers leads to the reduction of energy losses in the system. Therefore, it is important to limit both peak demand and feed-in powers for a better voltage profile and increased energy efficiency of the distribution system. The peak shaving method considering both demand and feed-in limits together for minimizing the peak grid power over a day is not developed in the existing literature. To fill this research gap, an optimal rule-based peak shaving method is proposed in this work considering both demand and feed-in limits in a grid-connected PV-BESS system.

Various approaches are used in literature to control the charge/discharge schedules of the battery such as GA, DP, rule-based algorithms, etc [124], [139], [140]. Out of

these, the rule-based methods are simple to implement and develop as compared to other methods. The rule-based approaches are compared with the optimization approaches in [129] and [130]. It is shown that rule-based approaches do not provide optimality even though they are simple. However, to avoid that limitation in the proposed method, the inputs required for proposed rule-based peak shaving method are determined optimally using GA. Therefore, in this chapter, an optimal rule-based peak shaving method is proposed. In summary, the contributions of this chapter are as follows:

1. A rule-based peak shaving method is proposed for peak shaving application which determines the charge and discharge schedules of the battery for limiting the grid demand and feed-in powers to the corresponding demand and feed-in limits of the day with the flexible day-to-day management of the battery.
2. The proposed rule-based peak shaving method is optimized by determining the optimal control inputs using GA which minimize the peak grid power of the day.

The remainder of the chapter is organized as follows: The chosen system is described in Section 2.1. Then, the overview of the proposed control is presented in Section 2.2. Later, the determination of operating modes of the battery and control inputs of the rule-based peak shaving method is discussed in Section 2.3. Further, the determination of battery schedules and optimal control inputs is explained in Section 2.4 and 2.5, respectively. The results and conclusions are presented in Section 2.6 and 2.7, respectively.

2.1 SYSTEM DESCRIPTION

A grid-connected system consisting of PV, BESS, and ac load is considered as shown in Fig. 2.1 [44]. The power balance equation at the point of common coupling (PCC), neglecting losses, is given as

$$P_g(t) + P_{pv}(t) + P_b(t) = P_l(t). \tag{2.1}$$

A discrete time model is assumed. The 't' represents the time interval $[(t-1)\times T_c, t\times T_c]$, where T_c is each time slot duration i.e., T_c = 1 hour. It means that all the defined powers are the average powers during the each hour of the day. The various components of the system are described as follows:

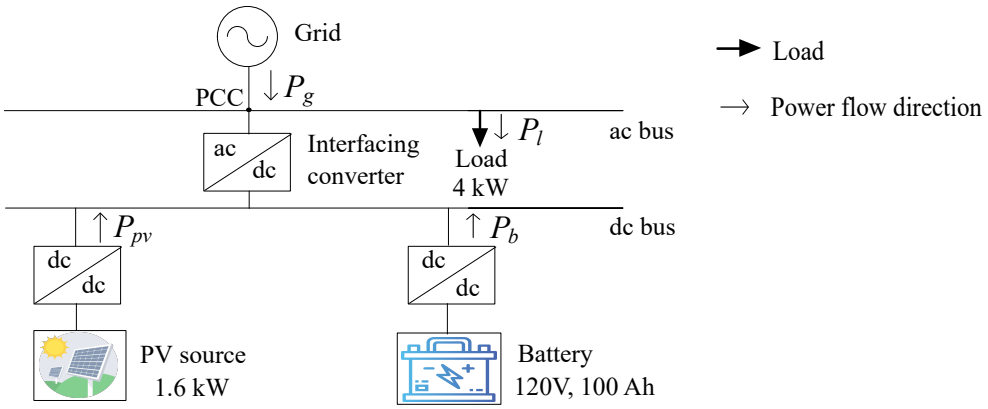

Fig. 2.1 Grid-connected PV-BESS system .

1. **Load**: The load is connected at the ac bus of the system. Two types of load power profiles, i.e., summer and winter profiles, are considered. Peak load occurs during 20:00 and 23:00 hours for summer with a peak load of 4 kW, whereas it occurs during 09:00 and 12:00 hours for winter with a peak load of 3.88 kW [141].

2. **Interfacing converter**: The ac and dc buses are connected by a bidirectional converter known as interfacing converter. The interfacing converter acts as a rectifier and inverter while transferring power from ac bus to dc bus and dc bus to ac bus, respectively. The interfacing converter controls the power balance and maintains constant dc-link voltage.

3. **Photovoltaic system**: The PV source is connected at the dc bus of the system through a dc-dc converter. This dc-dc converter helps the PV source to operate at maximum power point. It means that the dc-dc converter of the PV source operates in grid following mode and provides maximum power using MPPT algorithms. An installed PV power rating of 1.6 kW is considered.

4. **Battery energy storage system**: The battery is connected to the dc bus of the system through a dc-dc converter. This dc-dc converter is used to provide the required charge/discharge schedules of the battery. It means that the dc-dc converter of battery operates in grid following mode and provides required charge/discharge powers. A battery with a rating of 120 V, 100 Ah is chosen.

Now, the overview of the proposed peak shaving method in the chosen grid-connected PV-BESS system is discussed in following section.

2.2 OVERVIEW OF THE PROPOSED PEAK SHAVING METHOD

The overview of the proposed control is shown in Fig. 2.2. It includes various steps to realize the minimization of peak grid power which are discussed as follows:

1. The first step is the day-ahead forecasting of load and RES powers. The day-ahead forecasts of load and RES powers are required to determine the operating modes and control inputs of the rule-based peak shaving method. In recent years, several studies have been conducted for forecasting load and RESs power [142]. Data driven approaches for forecasting the RES and load power values have gained popularity due to the increased availability of monitoring data [143]. This monitoring data mainly includes weather forecast and historical energy usage data. Therefore, using the data driven approaches such as statistical and machine learning methods, the required day-ahead load and RESs power can be forecasted [144].

2. The second step is the determination of the operating modes of the battery and control inputs for rule-based peak shaving method. The operating modes of the battery and control inputs for rule-based peak shaving are determined using the load and PV power forecast curves of the day. The operating modes of the battery are chosen such that peak grid power is limited to the demand limit. The demand limit is defined as the load demand above which the grid is not used to supply the power to the system.

   The control inputs for rule-based peak shaving method are determined such that they depend on a control variable known as the dischargeable energy of the battery. The dischargeable energy of the battery is defined as the amount of energy that can be discharged from the battery over the forecast horizon without violating its power and SoC constraints. In this scenario, there exists a dischargeable energy of the battery which results in minimum peak power over a day. It means that the control inputs of rule-based peak shaving method are same for the whole day corresponding to the dischargeable energy of the battery of that particular day. This indicates that the control inputs have to be determined only once per day.

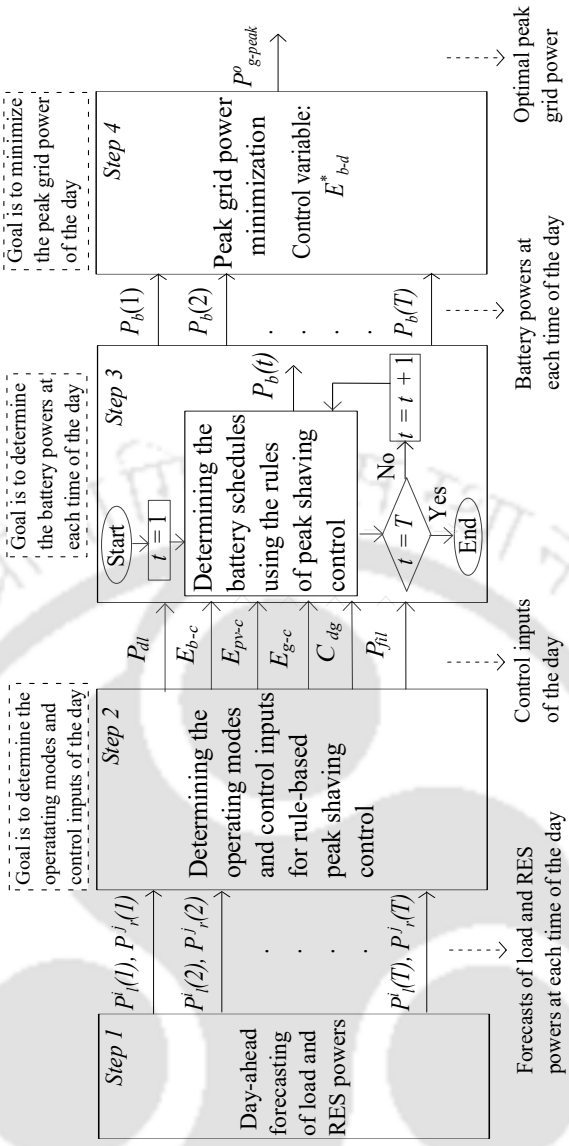

Fig. 2.2 Overview of the proposed peak shaving method.

3. The third step is the determination of the battery schedules using the rules of peak shaving method. The rules of the peak shaving method are formulated based on the control inputs which are obtained in Step 2 to decide the charge/discharge schedules of the battery over a day.

4. The fourth step is the determination of the optimal control inputs. The optimization problem is formulated to minimize the peak grid power while controlling the dischargeable energy of the battery. The control inputs corresponding to the optimal dischargeable energy of the battery are considered as the optimal control inputs of the day.

In this work, it is assumed that the forecasts required as per Step 1 are available and the entire analysis carried out based on these day-ahead forecasts. The steps 2-4 of the proposed method are discussed in detail in following sections.

2.3 DETERMINATION OF OPERATING MODES OF THE BATTERY AND CONTROL INPUTS

The method of determination of operating modes of the battery and control inputs for rule-based peak shaving method are discussed in this section.

2.3.1 Operating Modes of the Battery

With the considered battery along with the PV source, it is possible to limit $P_g(t)$ to P_{dl}. The operating modes of the battery for typical load demand and PV power profiles, are indicated in Fig. 2.3. There are three operating modes to limit $P_g(t)$ to P_{dl} using the battery in presence of the PV source. These are defined as follows:

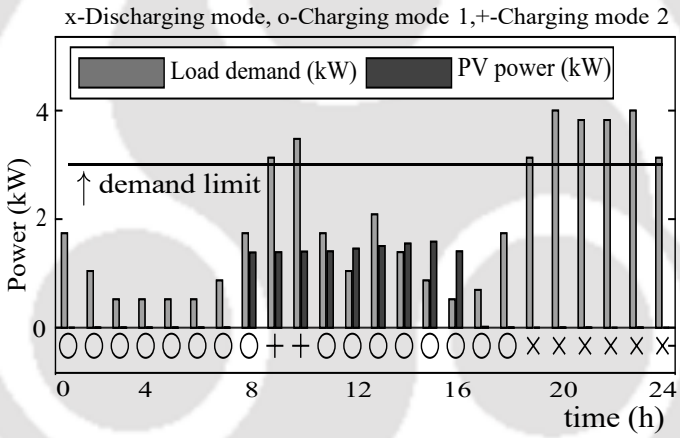

Fig. 2.3 Operating modes of the battery

1. **Discharging mode**: The discharging mode is during the time t_d, when the load demand is more than demand limit and the PV source is unable to supply the required power i.e., $P_l(t) > P_{dl} \&\& P_{pv}(t) \leq P_l(t) - P_{dl}$. The symbol '&&' indicates logical AND operator.

2. **Charging mode 1**: The charging mode 1 is during the time t_{c1}, when the load demand is less than demand limit i.e., $P_l(t) \leq P_{dl}$.

3. **Charging mode 2**: The charging mode 2 is during the time t_{c2}, when the load demand is more than demand limit and the PV source is able to supply the required power i.e., $P_l(t) > P_{dl} \&\& P_{pv}(t) > P_l(t) - P_{dl}$.

Now, the determination of control inputs for rule-based peak shaving method is explained as follows:

2.3.2 Control Inputs

The required inputs for the proposed rule-based peak shaving method are demand limit, required energy for charging the battery over a day, available PV energy to charge the battery over a day, available grid energy to charge the battery over a day, coefficient of grid energy to charge the battery, and feed-in limit. The sequential process of determination of these control inputs is given in flow chart of Fig. 2.4. Firstly, demand limit, Required energy for charging the battery over a day and available PV energy to charge the battery over a day are determined. Then, available grid energy to charge the battery over a day and coefficient of grid energy to charge the battery are determined if available PV energy to charge the battery is less than the required energy for charging the battery over a day. The feed-in limit is determined if available PV energy to charge the battery is more than the required energy for charging the battery over a day. The method of determination of these inputs is discussed as follows:

Demand limit

The demand limit is determined such that the energy to be discharged by battery over a day is equal to dischargeable energy of the battery over a day. The dischargeable energy of the battery over a day is chosen between 0 kWh and energy rating of battery (including both 0 kWh and E_{b-r}) i.e.,

$$0 \leq E^*_{b-d} \leq E_{b-r}. \tag{2.2}$$

Therefore,

$$E_{b-d} = E^*_{b-d}. \tag{2.3}$$

$$\sum (P_{b-d}(t) \times T_c) - E^*_{b-d} = 0, \forall t \in t_d. \tag{2.4}$$

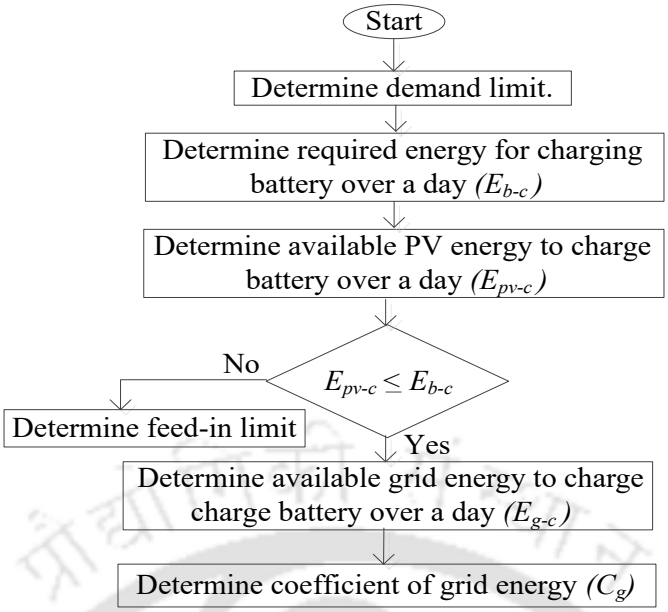

Fig. 2.4 The sequential process of determination of control inputs.

To limit grid power to demand limit, the required amount of power i.e., the difference between the demand and demand limit $(P_d(t) - P_{dl})$, is supplied either by the PV source or the battery to load when demand is more than the demand limit. However, the battery provides the amount of power which couldn't be supplied by the PV source. Therefore,

$$\begin{aligned} P_{b-d}(t) &= (P_d(t) - P_{dl}) - P_{pv}(t), \forall t \in t_d \\ &= 0, \text{ otherwise.} \end{aligned} \tag{2.5}$$

Substituting (2.5) in (2.4) gives,

$$\sum(((P_d(t) - P_{dl}) - P_{pv}(t)) \times T_c) - E^*_{b-d} = 0, \forall t \in t_d. \tag{2.6}$$

Equation (2.6) is in form of $f(P_{dl}) = 0$, where

$$f(P_{dl}) = \sum(((P_d(t) - P_{dl}) - P_{pv}(t)) \times T_c) - E^*_{b-d}, \forall t \in t_d. \tag{2.7}$$

In (2.7), demand limit is an independent variable. To solve for demand limit, root-finding algorithm of regula falsi method is used [145]. The regula falsi method is a combination of secant method and bisection search theorem. The regula falsi method is faster than bisection method, and root convergence is guaranteed. The applied regula falsi method to determine demand limit is shown as a flowchart in Fig. 2.5.

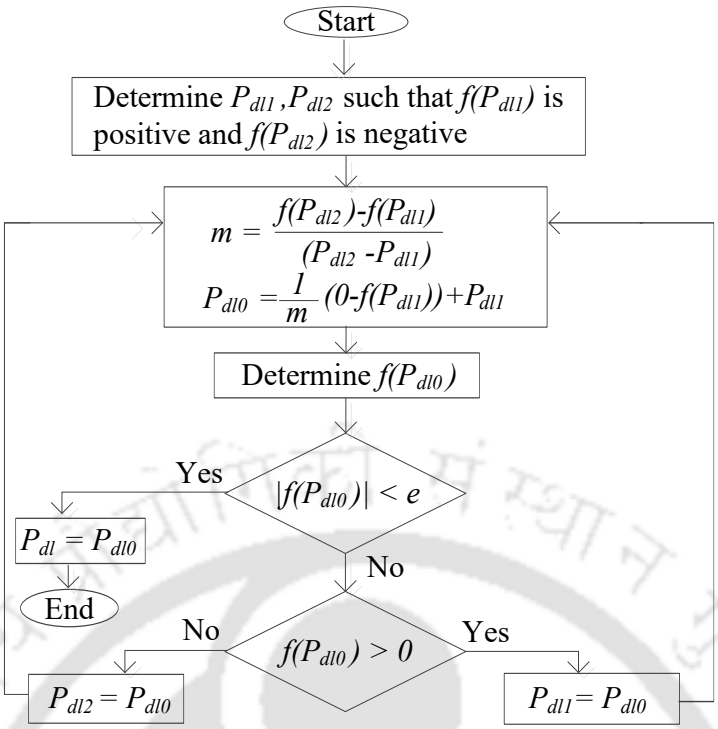

Fig. 2.5 Determination of demand limit using regula falsi method.

According to regula falsi method two initial demand limits (P_{dl1}, P_{dl2}) are chosen such that $f(P_{dl1})$ is positive and $f(P_{dl2})$ is negative. Then, P_{dl0} is determined as follows:

$$\begin{aligned} P_{dl0} &= \frac{1}{m}(0 - f(P_{dl1})) + P_{dl1}, \text{ where} \\ m &= \frac{f(P_{dl2}) - f(P_{dl1})}{(P_{dl2} - P_{dl1})}. \end{aligned} \tag{2.8}$$

Using (2.7), $f(P_{dl0})$ is determined. When $|f(P_{dl0})| < e$, P_{dl0} is considered as demand limit. When $|f(P_{dl0}| > e$, either P_{dl1} is replaced by P_{dl0} (if $f(P_{dl0}) > 0$) or P_{dl2} is replaced by P_{dl0} (if $f(P_{dl0}) < 0$). Then, the above process is continued till P_{dl0} becomes demand limit.

Required energy for charging the battery over a day

For flexible day-to-day management the battery has to be charged with same energy that is to be discharged by the battery. This condition maintains the SoC at the end of the day same as that of SoC of start of the day. Therefore, required energy for charging the battery is equal to energy to be discharged by the battery over a day as given follows.

$$E_{b-c} = E_{b-d} = E^*_{b-d}. \tag{2.9}$$

Available PV energy to charge the battery over a day

From (5.22), the battery is to be charged by the amount of energy E_{b-c}, either by the PV source or grid. Firstly, available PV energy to charge the battery over a day (without injecting into grid) is calculated. If it is not sufficient, then available grid energy to charge the battery is determined. During charging mode 1, the complete PV power is available for charging battery. During charging mode 2, the PV power which is in excess of the difference between demand and demand limit is available for charging battery. Accordingly, the available PV power for charging battery is given as

$$\begin{aligned} P_{pv-c} &= P_{pv}(t), \forall t \in t_{c1} \\ &= P_{pv}(t) - (P_d(t) - P_{dl}), \forall t \in t_{c2} \\ &= 0, \text{ otherwise.} \end{aligned} \tag{2.10}$$

Then, available PV energy for charging the battery over a day is the sum of available PV powers to charge the battery as given in (2.11).

$$E_{pv-c} = \sum_{t=1}^{T} P_{pv-c}(t) \times T_c. \tag{2.11}$$

Available grid energy to charge the battery over a day

When available PV energy to charge the battery is less than the required energy for charging the battery over a day, it means that available PV energy is not sufficient to charge the battery with the required amount of energy. Then, deficit amount of energy is drawn from grid provided that its demand is not more than the demand limit. It means that grid is not used to charge the battery during charging mode 2. During charging mode 1, the available power from grid to charge the battery ($P_{g-c}(t)$) for limiting grid power to demand limit is $P_{dl} - P_d(t)$ i.e.,

$$\begin{aligned} P_{g-c}(t) &= P_{dl} - P_d(t), \forall t \in t_{c1} \\ &= 0, \text{ otherwise.} \end{aligned} \tag{2.12}$$

Then, available grid energy for charging the battery over a day is the sum of available grid powers for charging the battery as given in (2.13),

$$E_{g-c} = \sum_{t=1}^{T} P_{g-c}(t) \times T_c. \tag{2.13}$$

Coefficient of grid energy to charge the battery

When available PV energy to charge the battery is less than the required energy for charging the battery over a day, the deficit amount of energy for completely charging the battery i.e., $E_{b-c} - E_{pv-c}$ has to be supplied by grid. However, only a fraction of grid energy is required to charge the battery while utilizing the total available PV energy for charging the battery. In this case if $C_g E_{g-c}$ is considered as the required grid energy to charge the battery, it is equal to the deficit amount of energy for completely charging the battery as given in (2.14),

$$\begin{aligned} C_g E_{g-c} &= E_{b-c} - E_{pv-c} \\ C_g &= \frac{E_{b-c} - E_{pv-c}}{E_{g-c}}. \end{aligned} \tag{2.14}$$

Feed-in limit

When available PV energy to charge the battery is more than the required energy for charging the battery over a day, the complete available PV energy is not required to charge the battery with the required amount of energy. Therefore, a limit of PV power feed-in limit is determined such that the PV source is not used to charge the battery when available PV power to charge battery is less than the feed-in limit. It means that the battery is completely charged with the difference of available PV power to charge battery and feed-in limit when available PV power to charge battery is more than the feed-in limit i.e.,

$$\sum (P_{pv-c}(t) - P_{fil}) \times T_c = E_{b-c}, \forall t \in t_c \&\& t_{pvmf}. \tag{2.15}$$

In (2.15), t_{pvmf} is the time when $P_{pv-c}(t) > P_{fil}$. Moreover, $P_{pv-c}(t) = P_{pv}(t)$ when $t_c = t_{c1}$ and $P_{pv-c}(t) = P_{pv}(t) - (P_d(t) - P_{dl})$ when $t_c = t_{c2}$.

$$\sum (P_{pv-c}(t) - P_{fil}) \times T_c - E_{b-c} = 0, \forall t \in t_c \&\& t_{pvmf}. \tag{2.16}$$

Equation (2.16) is in form of $f(P_{fil}) = 0$, where

$$f(P_{fil}) = \sum (P_{pv-c}(t) - P_{fil}) \times T_c - E_{b-c}, \forall t \in t_c \&\& t_{pvmf}. \tag{2.17}$$

In (2.16), feed-in limit is an independent variable. Therefore, to solve for feed-in limit, the root finding algorithm of regula falsi method is used. The determination of feed-in limit using regula falsi method is similar to the determination of demand limit which is shown as a flowchart in Fig. 2.6.

Firstly, two initial feed-in limits (P_{fil1}, P_{fil2}) are chosen such that $f(P_{fil1})$ is positive and $f(P_{fil2})$ is negative. Then, P_{fil0} is determined as follows:

$$\begin{aligned} P_{fil0} &= \frac{1}{m}(0 - f(P_{fil1})) + P_{fil1}, \text{ where} \\ m &= \frac{f(P_{fil2}) - f(P_{fil1})}{(P_{fil2} - P_{fil1})}. \end{aligned} \tag{2.18}$$

Using (2.17), $f(P_{fil0})$ is determined. When $|f(P_{fil0})| < e$, P_{fil0} is considered as feed-in limit. When $|f(P_{fil0}| > e$, either P_{fil1} is replaced by P_{fil0} (if $f(P_{fil0}) > 0$) or P_{fil2} is replaced by P_{fil0} (if $f(P_{fil0}) < 0$). Then, the above process is continued till P_{fil0} becomes feed-in limit.

Now, the determination of battery schedules using the rules of proposed peak shaving method is explained in following section.

2.4 DETERMINATION OF THE BATTERY SCHEDULES USING THE RULES OF PEAK SHAVING METHOD

Considering the above determined inputs, rules for peak shaving method are formulated to know the charge/discharge schedules of the battery. The formulated rules during discharging and charging modes are shown as a flowchart in Fig. 2.7 and explained as follows:

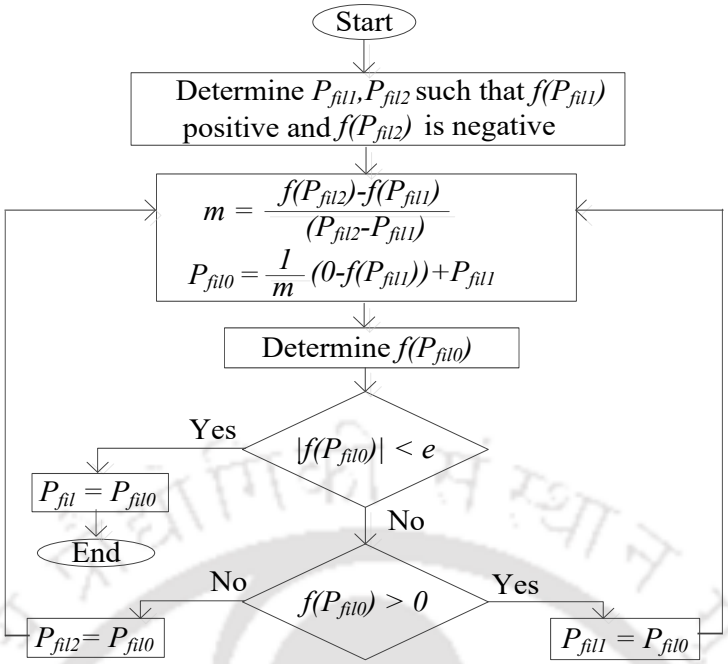

Fig. 2.6 Determination of feed-in limit using regula falsi method.

2.4.1 Discharging Mode

The discharging mode of the battery is during the time when $P_l(t) > P_{dl} \&\& P_{pv}(t) \leq (P_l(t) - P_{dl})$. In this mode, there is only one rule for deciding battery power as given follows.

Rule 1: In this mode, $P_l(t) > P_{dl}$. Therefore, the battery is used to supply the load power which is not supplied by the PV source. It means that the battery discharges by the amount $(P_l(t) - P_{dl}) - P_{pv}(t)$ as per (2.5) to limit the grid power to the demand limit.

2.4.2 Charging Mode 1

The charging mode 1 of the battery is during the time when $P_l(t) \leq P_{dl}$. In this mode, there are three rules which decide the battery power as given follows.

Rule 2: If $E_{pv-c} \leq E_{b-c}$, the PV source and grid are used to charge the battery by the amount $P_{pv}(t) + C_g(P_{dl} - P_l(t))$ as per (2.10), (2.12) and (2.14).

Rule 3: If $E_{pv-c} > E_{b-c} \&\& P_{pv}(t) > P_{fil}$, the PV source is used to charge the battery by the amount $P_{pv}(t) - P_{fil}$ as per (2.10) and (2.15).

Rule 4: If $E_{pv-c} > E_{b-c} \&\& P_{pv}(t) \leq P_{fil}$, the PV source is not used to charge the battery.

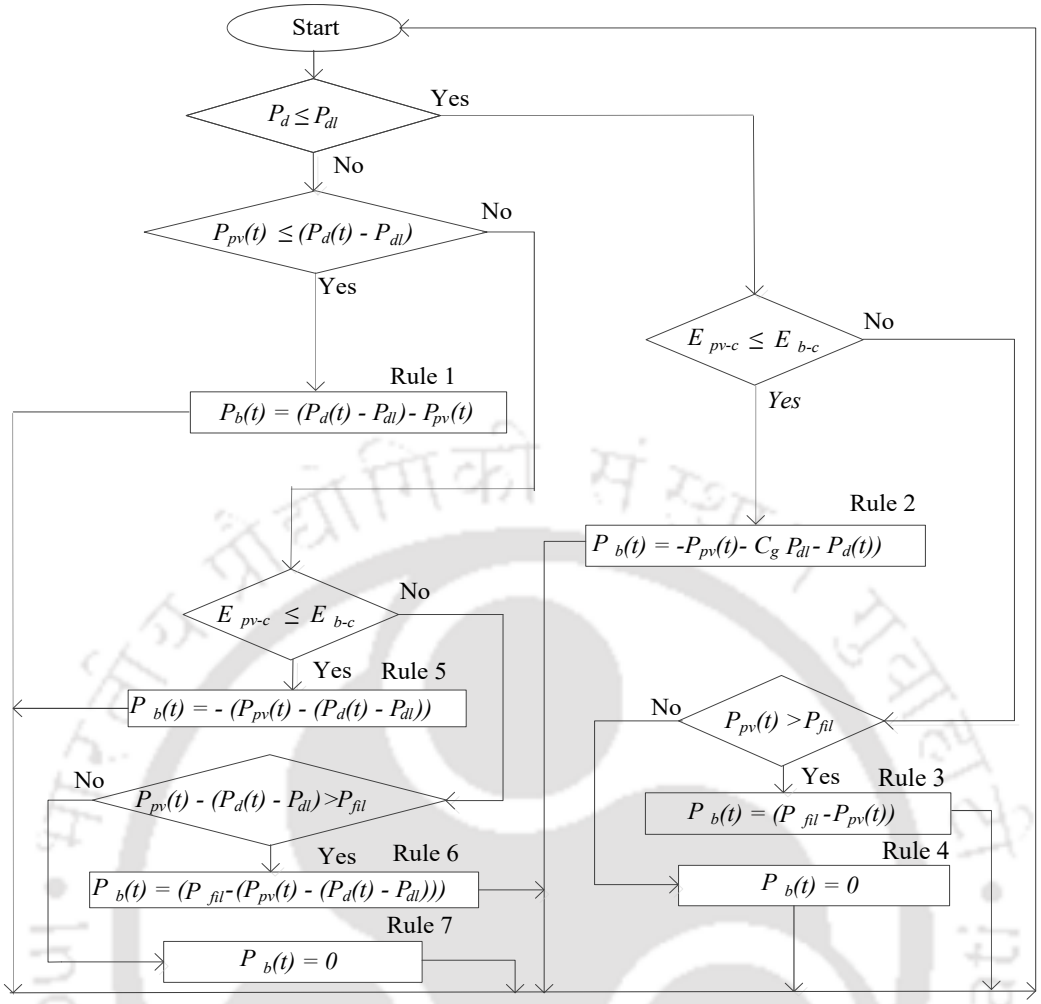

Fig. 2.7 The proposed rule-based peak shaving method.

2.4.3 Charging Mode 2

The charging mode 2 of the battery is during the time when $P_l(t) > P_{dl} \&\& P_{pv}(t) > (P_l(t) - P_{dl})$. In this mode, there are three rules which decide the battery power as given follows.

Rule 5: If $E_{pv-c} \leq E_{b-c}$, the PV source is used to charge the battery by the amount $P_{pv}(t) - (P_l(t) - P_{dl})$ as per (2.10).

Rule 6: If $E_{pv-c} > E_{b-c} \&\& (P_{pv}(t) - (P_l(t) - P_{dl})) > P_{fil}$, the PV source is used to charge the battery by the amount $(P_{pv}(t) - (P_l(t) - P_{dl})) - P_{fil}$ as per (2.10) and (2.15).

Rule 7: If $E_{pv-c} > E_{b-c} \&\& (P_{pv}(t) - (P_l(t) - P_{dl})) \leq P_{fil}$, the PV source is not used to charge the battery.

The SoC of the battery during discharging and charging modes is calculated using

coulomb-counting method as follows [146]:

$$SoC(t) = 1 - \frac{\sum_{t_0}^{t} i_b \times T_c}{Ah_{b-r}}. \tag{2.19}$$

Now, the determination of optimal control inputs for optimizing the proposed rule-based peak shaving method is discussed.

2.5 DETERMINATION OF OPTIMAL CONTROL INPUTS

The optimization problem formulation for determining the optimal control inputs and its solution method are discussed in this section.

2.5.1 Optimization Problem Formulation

The considered objective function and constraints are given from (2.20)-(2.25), respectively,

$$\text{minimize} \quad f = \text{maximum}(P_g(t)). \tag{2.20}$$

subjected to

1. Power balance constraint

$$P_g(t) + P_{pv}(t) + P_b(t) = P_l(t). \tag{2.21}$$

2. Battery SoC Constraints

$$SoC_l \leq SoC(t) \leq SoC_u, SoC_f = SoC_i. \tag{2.22}$$

3. Battery charge/discharge power constraints

$$P_{b-c}(t) \leq P_{b-cl}, P_{b-d}(t) \leq P_{b-dl}. \tag{2.23}$$

4. Battery energy capacity constraint

$$E^*_{b-d} \leq E_{b-r}. \tag{2.24}$$

5. Constraint of available energy to charge the battery

$$E_{g-c} + E_{pv-c} \geq E_{b-c}. \tag{2.25}$$

Equation (2.21) gives the power balance constraint. Equation (2.22) indicates the constraints of SoC limits of the battery and the flexible day-to-day operation of the battery. The SoC of the battery is calculated using coulomb counting method [147], [148]. Equation (2.23) indicates the constraints of charge/discharge powers of the battery, respectively. Equation (2.24) indicates that dischargeable energy of battery should be less than the battery energy capacity. Equation (2.25) shows that the sum of available grid and PV energies to charge the battery should be more than or equal to the required energy for charging the battery.

2.5.2 Solving the Optimization Problem

The formulated problem is an off-line optimization problem with a non-linear fitness function, which is solved using GA solver in MATLAB. Because GA is a popular method for solving optimization problems with nonlinear fitness function [149]. The GA is based on biological genetics where successive generations receive features from their parents through crossover in a random manner [149]. It has been successfully applied to solve real-life complex problems of various fields such as economics, engineering and management [150]. It maintains the diversity in population to avoid the solutions to stuck in local optima. In GA, it is important to choose parameters such as population size, rate of mutation and crossover carefully to avoid the possible risk of non-convergence. If they are chosen inappropriately it will be difficult for the algorithm to converge or it will produce meaningless results [151]. The default values are chosen for various parameters of GA, except for population size. The population size is an important parameter to choose. Because if it is small, the convergence might not be achieved. Therefore, population size is chosen based on the number of control variables. There is only one control variable in this optimization problem i.e., the dischargeable energy of the battery. Further, in GA it is possible for different runs to provide different optimal values. Therefore, to avoid any sub-optimal solutions and guarantee global optimum solution the population size is tuned such that multiple simulation runs converge precisely to the same value and chosen as 20.

The method of solving optimization problem using GA is shown as a flowchart in Fig. 2.8. According to that firstly population initialization is done. The individuals i.e., solutions which are currently involved in the search process are together known as pop-

ulation. Then, fitness function is calculated. The death penalty method is used for handling constraints. This is a simple method of handling the constraints [152]. The death penalty is applied considering that the optimization constraints should not be violated. Accordingly the unfeasible solutions from the population are discarded if any of the constraint is violated. It means that the death penalty is chosen as given follows [153].

$$\begin{aligned} dp &= inf, \text{ when there is any constraint violation} \\ &= 0, \text{ otherwise.} \end{aligned} \tag{2.26}$$

The calculation of fitness function is repeated through selection, crossover and mutation till the stop criteria is reached. The selection process randomly selects the solutions from population based on fitness function value. After the selection process, the population consists of better solutions. Then, crossover is done to create new better solutions from selected solutions. After crossover, the mutation is performed in order to avoid the algorithm to be trapped in a local minimum and maintains diversity in the population. The stop criteria of GA uses certain options to decide when to stop such as maximum number of generations (iterations), function tolerance, etc. If any one of these options is satisfied, the GA stops doing iterations and provides optimal set points as output. In this chapter, the maximum number of iterations are chosen by default which is 100 times the number of control variables. Once the stop criteria is reached the algorithm provides the optimal dischargeable energy of the battery (${E^{*o}}_{b-d}$). Once the ${E^{*o}}_{b-d}$ is determined, the inputs corresponding to ${E^{*o}}_{b-d}$ are considered as the optimal control inputs required for the proposed rule-based control i.e., P^o_{dl}, E^o_{b-c}, E^o_{pv-c}, E^o_{g-c}, C^o_g, and P^o_{fil}.

Now, the simulation results of the proposed optimal rule-based peak shaving method are discussed in following section.

2.6 SIMULATION RESULTS

The proposed method is tested on the considered system in MATLAB on a 64-bit operating system PC with a processor of Intel(R) Core(TM) i5-6500 CPU @ 3.2 GHz. The chosen system parameters are given in Table 2.1 [44], [154].

The rule-based methods discussed in literature [42], [100], [127], [128], [133] have

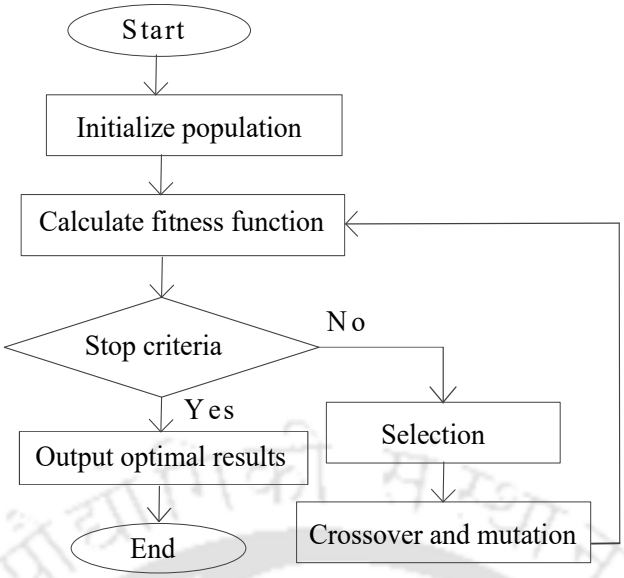

Fig. 2.8 GA for determining optimal dischargeable energy of the battery.

Table 2.1 System Parameters

Parameter	Value	Parameter	Value
P_{l-p}	4 kW	SoC_l/SoC_u	0.2/0.9
P_{pv-i}	1.6 kW	SoC_i	0.5
E_{b-r}	12 kWh	P_{b-cl}	3 kW
Ah_{b-r}	100 Ah	P_{b-dl}	3 kW

validated their algorithms for various possible scenarios as per their proposed method. As per the proposed method in this chapter, there exists only two different scenarios based on the available PV energy on a given day i.e., 1) The available PV energy over a day is less than or equal to the required energy for charging the battery and 2) The available PV energy over a day is more than the required energy for charging the battery. Therefore, the proposed method is validated for following cases which include both the possible scenarios.

Case 1: Winter load profile with more PV energy availability

Case 2: Winter load profile with less PV energy availability

Case 3: Summer load profile with more PV energy availability

Case 4: Summer load profile with less PV energy availability

2.6.1 Case 1

In this case, load power profile of winter with more PV energy availability over a day is considered.

Optimal control inputs of the day

The best fitness values are obtained for multiple runs of GA as shown in Fig. 2.9. It shows that the minimum value for all the runs is equal to 1.72 kW which is the optimal peak grid power. The optimal dischargeable energy of the battery is found to be 5.46 kWh. The optimal control inputs i.e., optimal demand limit, energy required for charging battery, available PV energy to charge battery, and feed-in limit (P^o_{dl}, E^o_{b-c}, E^o_{pv-c} and P^o_{fil}) are 1.72 kW, 5.46 kWh, 5.69 kWh and 0.05 kW, respectively. The available PV energy to charge the battery is more than the required energy for charging the battery ($E^o_{pv-c} > E^o_{b-c}$). It means that there is no need of grid energy to charge battery. Therefore, available grid energy to charge battery and coefficient of grid energy to charge battery (E^o_{g-c} and C^o_g) are not applicable (NA) in this case as given in Table 2.2.

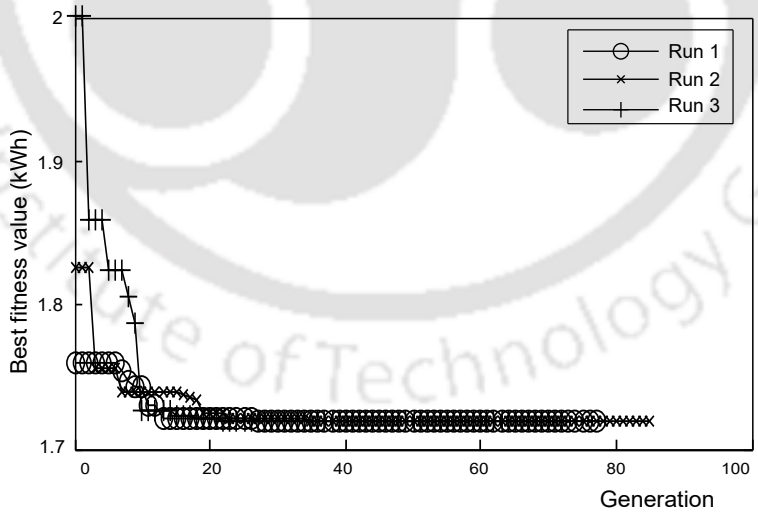

Fig. 2.9 Best fitness values obtained using GA for multiple simulation runs in Case 1.

Battery schedules and grid powers over the day

The load and PV power profiles of this case are shown in Fig. 2.10(a). For the determined P^o_{dl}, the discharging mode is during t = 4, 5, 6, 7, 8, 9, 10, 11, 12, 19, 20, 21,

Table 2.2 Optimal Control Inputs of Rule-based Peak Shaving Method

Input Parameter	Case 1	Case 2	Case 3	Case 4
P^o_{dl} (kW)	1.72	2.44	2.85	2.85
E^o_{b-c} (kWh)	5.46	6.53	4.79	5.48
E^o_{pv-c} (kWh)	5.69	0.02	12.19	0.066
E^o_{g-c} (kWh)	NA	20.66	NA	28.067
C^o_g	NA	0.31	NA	0.19
P^o_{fil} (kW)	0.05	NA	0.82	NA

22 hours, charging mode 1 is during t = 1, 2, 3, 14, 15, 16, 17, 18, 23, 24 hours and charging mode 2 is during t = 13 hour. Resulting optimal charge/discharge schedules of the battery for these modes are shown in Fig. 2.10(b). This indicates that the battery power is maintained between the maximum charging and discharging power limits of the battery (0 kW and 3 kW). It is observed that the battery is charged only by the PV source. The SoC for these battery schedules is shown in Fig. 2.10(c). This indicates that the SoC of the battery is maintained between the maximum and minimum SoC limits of the battery (20% and 90%). Moreover, $SoC_f = SoC_i = 50\%$, which is desired for flexible day-to-day management of the battery. The resulting grid demand is shown in Fig. 2.10(d). This indicates that grid demand is limited to P^o_{dl} of 1.72 kW and there is no feed-in power into the grid.

2.6.2 Case 2

In this case, load demand profile of winter with less PV energy availability over a day is considered.

Optimal control inputs of the day

The optimal control inputs i.e., optimal demand limit, energy required for charging battery, available PV energy to charge battery, available grid energy to charge battery, and coefficient of grid energy to charge battery (P^o_{dl}, E^o_{b-c}, E^o_{pv-c}, E^o_{g-c}, and C^o_g) are 2.44 kW, 6.53 kWh, 0.02 kWh, 20.66 kWh and 0.31, respectively. The available PV energy to charge the battery is less than the required energy for charging the battery ($E_{pv-c} \leq E_{b-c}$). It means that the complete available PV energy is used to charge

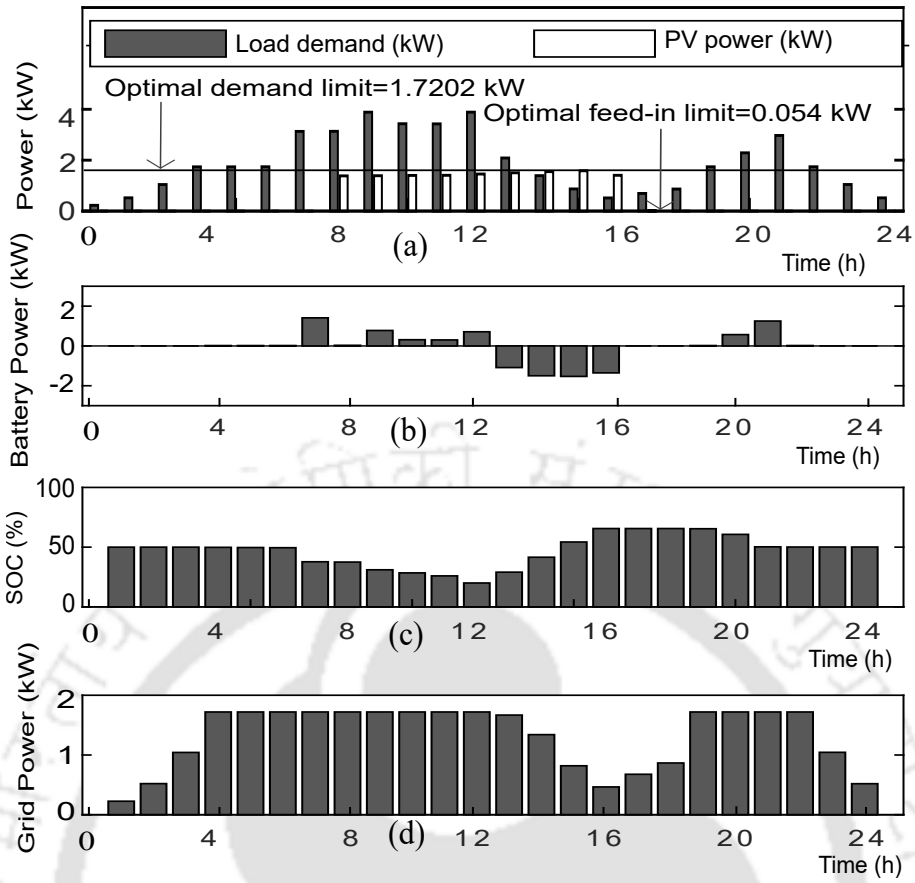

Fig. 2.10 Case 1. (a) Load and PV power profiles. (b) Charge/discharge schedules of the battery. (c) SoC of the battery. (d) Grid power.

battery. Therefore, feed-in limit (P^o_{fil}) is NA in this case as given in Table 2.2.

Battery schedules and grid powers over the day

The load and PV power profiles of this case are shown in Fig. 2.11(a). For the determined P^o_{dl}, the discharging mode is during t = 7, 8, 9, 10, 11, 12 and 21 hours, charging mode 1 is during t = 1, 2, 3, 4, 5, 6, 13, 14, 15, 16, 17, 18, 19, 20, 22, 23 and 24 hours. There is no charging mode 2 in this case due to less availability of PV power over a day. Resulting optimal charge/discharge schedules of the battery for these modes are shown in Fig. 2.11(b). This indicates that the battery power is maintained between the maximum charging and discharging power limits of the battery. It is observed that the battery is charged by both the PV source and grid. The SoC for these battery schedules is shown in Fig. 2.11(c). This indicates that the SoC of the battery is maintained between the maximum and minimum SoC limits of the battery. Moreover, $SoC_f = SoC_i = 50\%$, which is desired for flexible day-to-day management of the battery. The resulting grid demand is shown in Fig. 2.11(d). This indicates that grid demand is limited to P^o_{dl} of

2.44 kW and there is no feed-in power into the grid.

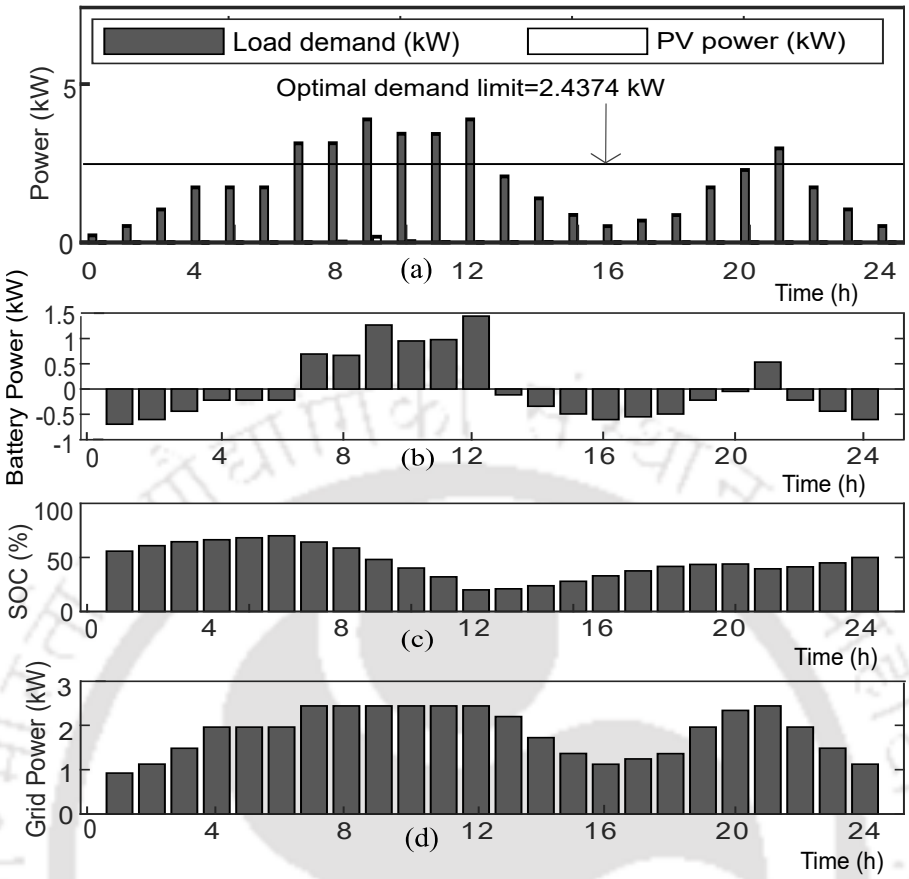

Fig. 2.11 Case 2. (a) Load and PV power profiles. (b) Charge/discharge schedules of the battery. (c) SoC of the battery. (d) Grid power.

2.6.3 Case 3

In this case, load demand profile of summer with more PV energy availability over a day is considered.

Optimal control inputs of the day

The determined optimal demand limit, energy required for charging battery, available PV energy to charge battery, and feed-in limit (P^o_{dl}, E^o_{b-c}, E^o_{pv-c}, and P^o_{fil}) are 2.85 kW, 4.79 kWh, 12.19 kWh and 0.83 kW, respectively. The available PV energy to charge the battery is more than the required energy for charging the battery ($E^o_{pv-c} > E^o_{b-c}$). It means that there is no need of grid energy to charge battery. Therefore, available grid energy to charge battery and coefficient of grid energy to charge battery (E^o_{g-c} and C^o_g) are NA in this case as given in Table 2.2.

Battery schedules and grid powers over the day

The load and PV power profiles of this case are shown in Fig. 2.12(a). For the determined P^o_{dl}, the discharging mode is during t = 19, 20, 21, 22, 23 and 24 hours, charging mode 1 is during t = 1, 2, 3, 4, 5, 6, 7, 8, 11, 12, 13, 14, 15, 16, 17 and 18 hours, charging mode 2 is during t = 9 and 10 hours. Resulting optimal charge/discharge schedules of the battery for these modes are shown in Fig. 2.12(b). This indicates that the battery power is maintained between the maximum charging and discharging power limits of the battery. It is observed that only by the PV source is used to charge the battery. The SoC for these battery schedules is shown in Fig. 2.12(c). This indicates that the SoC of the battery is maintained between the maximum and minimum SoC limits of the battery. Moreover, $SoC_f = SoC_i = 50\%$, which is desired for flexible day-to-day management of the battery. The resulting grid demand is shown in Fig. 2.12(d). This indicates that grid demand is limited to P^o_{dl} of 2.85 kW and the feed-in power is limited to P^o_{fil} of 0.8249 kW.

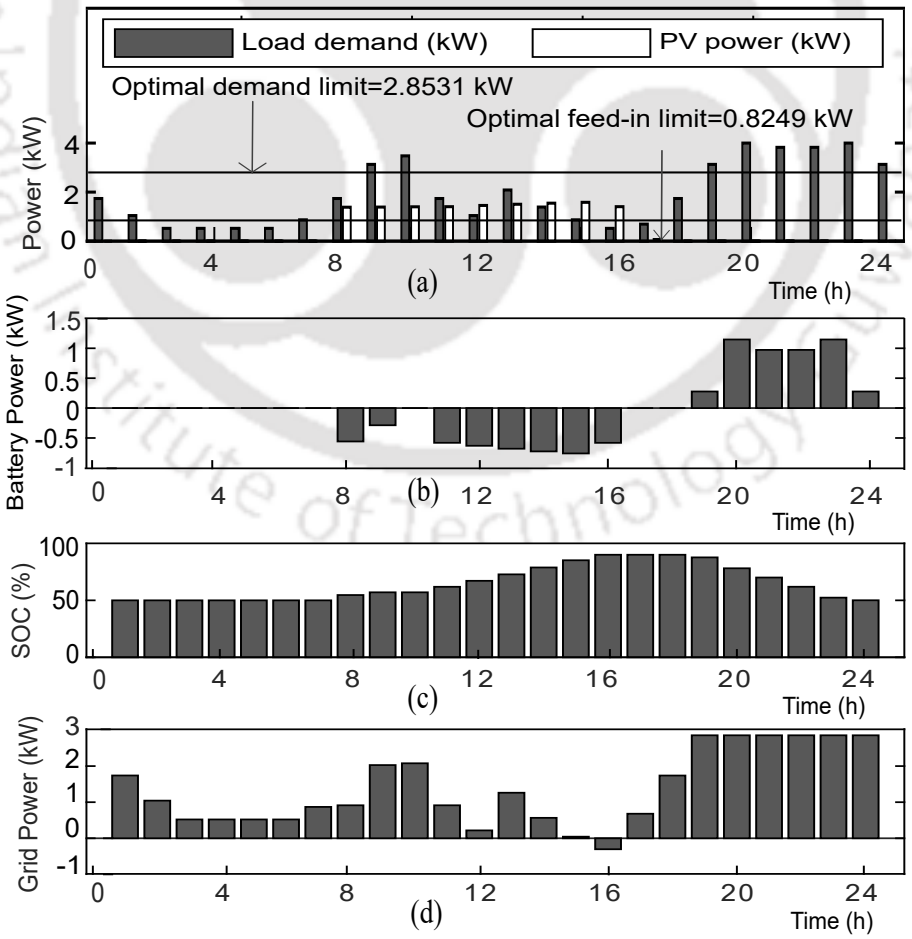

Fig. 2.12 Case 3. (a) Load and PV power profiles. (b) Charge/discharge schedules of the battery. (c) SoC of the battery. (d) Grid power.

2.6.4 Case 4

In this case, load demand profile of summer with less PV energy availability is considered.

Optimal control inputs of the day

The determined optimal demand limit, energy required for charging battery, available PV energy to charge battery, available grid energy to charge battery, and coefficient of grid energy to charge battery (P^o_{dl}, E^o_{b-c}, E^o_{pv-c}, E^o_{g-c} and C^o_g) are 2.85 kW, 5.48 kWh, 0.066 kWh, 28.07 kWh and 0.19, respectively. The available PV energy to charge the battery is less than the required energy for charging the battery ($E_{pv-c} \leq E_{b-c}$). It means that the complete available PV energy is used to charge battery. Therefore, feed-in limit (P^o_{fil}) is NA in this case as given in Table 2.2.

Battery schedules and grid powers over the day

The load and PV power profiles of this case are shown in Fig. 2.13(a). For the determined P^o_{dl}, the discharging mode is during t = 9, 10, 19, 20, 21, 22, 23, 24 hours, charging mode 1 is during t = 1, 2, 3, 4, 5, 6, 7, 8, 11, 12, 13, 14, 15, 16, 17, 18 hours. There is no charging mode 2 in this case due to less availability of PV energy. Resulting optimal charge/discharge schedules of the battery for these modes are shown in Fig. 2.13(b). This indicates that the battery power is maintained between the maximum charging and discharging power limits of the battery. It is observed that both the PV source and grid are used to charge the battery. The SoC for these battery schedules is shown in Fig. 2.13(c). This indicates that the SoC of the battery is maintained between the maximum and minimum SoC limits of the battery. Moreover, $SoC_f = SoC_i = 50\%$, which is desired for flexible day-to-day management of the battery. The resulting grid demand is shown in Fig. 2.13(d). This indicates that grid demand is limited to P^o_{dl} of 2.85 kW and there is no feed-in power into the grid.

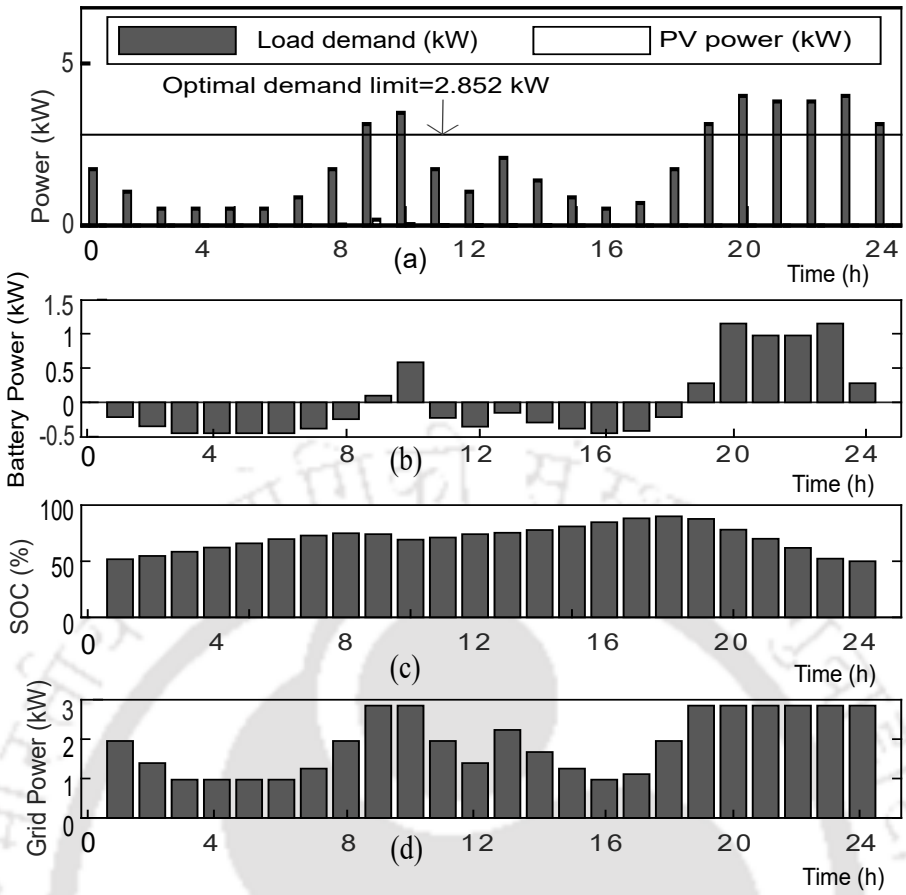

Fig. 2.13 Case 4. (a) Load and PV power profiles. (b) Charge/discharge schedules of the battery. (c) SoC of the battery. (d) Grid power.

2.6.5 Performance Indicators

The performance indicators such as percentage peak shaving, energy consumption cost over the day, and voltage profile are considered to show the impact of proposed method as discussed follows.

Percentage peak shaving

The percentage peak shaving is the ratio of the peak grid power with the proposed method and the peak load power of the day. The PPS achieved for the above discussed cases is shown in Table 2.3. It indicates that peak shaving of 55.66%, 37.18%, 28.6725%, and 28.7% is achieved in Case 1-4, respectively with respect to peak load power of the day.

Table 2.3 Percentage Peak Shaving

Parameter	Case 1	Case 2	Case 3	Case 4
P_{g-peak} (kW)	1.72	2.44	2.85	2.85
Percentage peak shaving (%)	55.66	37.18	28.67	28.7

Energy consumption cost over the day

The energy consumption cost of the system over the day is considered as other performance indicator. The time-of-use price of the energy is considered [155]. The peak time is when load power is more than 75% of the peak load. The off-peak time is when load demand is less than 25% of the peak load. The energy price during peak and off-peak hours is 5.39 INR and 4.15 INR, respectively. The energy price for the remaining time is 4.39 INR [156]. The energy consumption cost over the day is calculated using (2.27),

$$TECC = \sum_{t=1}^{T} P_{g-d}(t) \times T_c \times EP(t). \tag{2.27}$$

The $P_{g-d}(t) = P_g$ if $P_g > 0$ and $P_{g-d}(t) = 0$ if $P_g \leq 0$. The $TECC$ without BESS for Case 1 to 4 are 162.3459 INR/day, 217.2627 INR/day, 179.2068 INR/day, and 228.1274 INR/day, respectively. The $TECC$ with BESS using the proposed control for Case 1 to 4 are 149.5737 INR/day, 209.7624 INR/day, 166.5379 INR/day, and 221.8238 INR/day, respectively. This indicates that the energy costs are less with the proposed method as compared to the case of without BESS.

Voltage profile

To show the impact of the proposed peak shaving method on voltage profile, a two bus system as shown in Fig. 2.14 is considered.

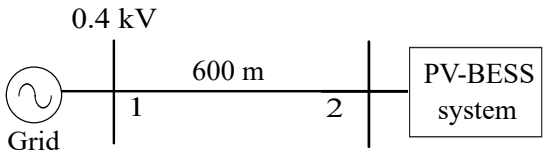

Fig. 2.14 Considered PV-BESS system connected in LV ac distribution network.

The system represents the considered PV-BESS system connected in a LV ac distribution network. The bus 1 and 2 are considered as slack bus and load bus, respectively. The resistance and reactance of line are 3.69 Ω/km and 0.094 Ω/km, respectively [157]. The voltage of the load bus over a day is determined using backward forward sweep power flow method [158].

The worst maximum bus voltage (V_{wmax}) i.e., the maximum bus voltage over a day without BESS for Case 1 to 4 are 1.01 p.u., 1 p.u., 1.01 p.u., and 1 p.u., respectively. The V_{wmax} with BESS using the proposed control for Case 1 to 4 are 1 p.u., 1 p.u., 1.004 p.u., and 1 p.u., respectively. The V_{wmax} values are less with the proposed method as compared to the case without BESS. The worst minimum bus voltage (V_{wmin})i.e., the minimum bus voltage over a day without BESS for Case 1 to 4 are 0.955 p.u., 0.94 p.u., 0.94 p.u., and 0.94 p.u., respectively. The V_{wmin} with BESS using the proposed control for Case 1 to 4 are 0.975 p.u., 0.965 p.u., 0.96 p.u., and 0.96 p.u., respectively. The V_{wmin} values are more with the proposed method as compared to the case without BESS. This shows that both voltage drop and voltage rise are less due to the consideration of demand and feed-in limits in the proposed peak shaving method, respectively. These obtained $TECC$, V_{wmax} and V_{wmin} values for four cases are shown in Table 2.4. It indicates that the energy consumption cost over the day is reduced using the proposed method as compared to the case of without BESS. Moreover, the voltage profile is improved using the proposed method as compared to the case of without BESS.

2.7 CONCLUSIONS

In this chapter, an optimal rule-based peak shaving method is proposed. The proposed method is tested for various possible cases of load and PV power profiles. The obtained results show that the grid demand and feed-in powers are limited to the respective demand and feed-in limits of the day, respectively. Moreover, the state of charge at the end of the day is maintained equal to the state of charge at the start of the day for flexible day-to-day-management of the battery. It is observed that the peak shaving in the range of 28.67%-55.66% is achieved using the proposed method with respect to the peak load demand. Moreover, the energy consumption cost is reduced in the range of 2.77%-7.87% over the day with respect to the case of without BESS. Moreover, the improved voltage profile with the proposed method is observed.

Table 2.4 Energy Cost, Maximum and Minimum Bus Voltages

Parameter	Case 1		Case 2		Case 3		Case 4	
	without BESS	Proposed	without BESS	Proposed	without BESS	Proposed	without BESS	Proposed
$TECC$ (INR/day)	162.35	149.57	217.26	209.76	179.2	166.54	228.13	221.82
V_{max} (p.u.)	1.01	1	1	1	1.01	1.004	1	1
V_{min} (p.u.)	0.955	0.975	0.94	0.965	0.94	0.96	0.94	0.96

CHAPTER 3

OPTIMAL RULE-BASED DEMAND RESPONSE WITH ENERGY BUYING AND SELLING PRICE LIMITS USING ENERGY STORAGE

In Chapter 2, the optimal rule-based peak shaving method is proposed for minimizing the peak grid power in a PV-BESS system. The proposed method determines the charge/discharge schedules of the battery considering the day-ahead forecasts of the load and PV powers as inputs. However, the charge/discharge efficiencies and charge/discharge power limits of battery are not considered while formulating the proposed rule-based peak shaving method. Moreover, the energy price is not considered as input while formulating the rule-based peak shaving method. It means that even though peak shaving has several benefits, it may not be useful for minimizing the energy consumption cost when time varying energy price profile is applied for energy consumption of the system. In this scenario, DR application becomes important which is used to reduce the energy consumption cost while utilizing the time varying energy price profile. Therefore, in this work, a DR method is proposed to minimize the energy consumption cost using the day-ahead energy price profile along with the load and PV power profiles as inputs. Moreover, the charge/discharge efficiencies and charge/discharge power limits of battery are not considered while formulating the DR method.

The DR is an important characteristic of residential customers for realizing smart grids. The price based DR is an energy management method used by residential customers to reduce their energy consumption cost while utilizing the time varying energy price profile [136]. Use of BESS along with the PV sources allows the customers to change their load profile patterns and participate in price based DR programs [57]. It is important to have energy price limits for DR control in PV-BESS storage systems. Because energy consumption cost of the system is reduced if battery is discharged when buying price is more than the buying price limit. It means that less or no power is drawn from the grid when buying price is more than its limit. Similarly if there is selling price involved,

operating energy consumption cost is reduced if the PV source is used to charge battery only when selling price is less than the selling price limit. It means that PV power is injected to the grid when selling price is more than its limit. In the existing literature of DR application based on energy price limits, following research gaps are identified.

1. The DR method considering both energy buying and selling price profiles together is not investigated.
2. Further, the DR application using energy price limits when both RESs and energy storage devices are present in the system is not explained.

Therefore, the objective of this chapter is to formulate a DR method considering both buying and selling price profiles for a residential PV storage system.

Moreover, as discussed in previous chapters, the rule-based control with the optimal control inputs is considered as a simple yet optimal approach used for controlling battery charge/discharge schedules. Therefore, in this chapter, an optimal rule-based DR method is proposed considering both buying and selling price profiles for a residential PV storage system. In summary, the contributions of this chapter are given as follows:

1. A rule-based DR method is proposed to determine the charge/discharge schedules of the battery which limit the energy buying and selling prices to the corresponding buying and selling price limits of the day with the flexible day-to-day management of the battery.
2. The proposed rule-based DR method is optimized by determining the optimal control inputs using GA which minimize the energy consumption cost over a day.

The remainder of the chapter is organized as follows: The chosen system is described in Section 3.1. Then, the overview of the proposed control is presented in Section 3.2. Later, the determination of operating modes of the battery and control inputs of the rule-based DR method is discussed in Section 3.3. Further, the determination of battery schedules and optimal control inputs is explained in Section 3.4 and 3.5, respectively. The results and conclusions are presented in Section 3.6 and 3.7, respectively.

3.1 SYSTEM DESCRIPTION

A grid-connected system consisting of ac/dc loads, PV-BESS is considered as shown in Fig. 3.1 [58]. The grid is a power source that is capable of delivering/absorbing power. The power balance equation at the PCC, neglecting losses, is given as

$$P_g(t) + P_{pv}(t) + P_b(t) = P_l(t). \tag{3.1}$$

A discrete time model is assumed. The 't' represents the time interval $[(t-1)\times T_c, t\times T_c]$, where T_c is each time slot duration i.e., T_c = 1 hour. It means that all the defined powers are the average powers during the each hour of the day.

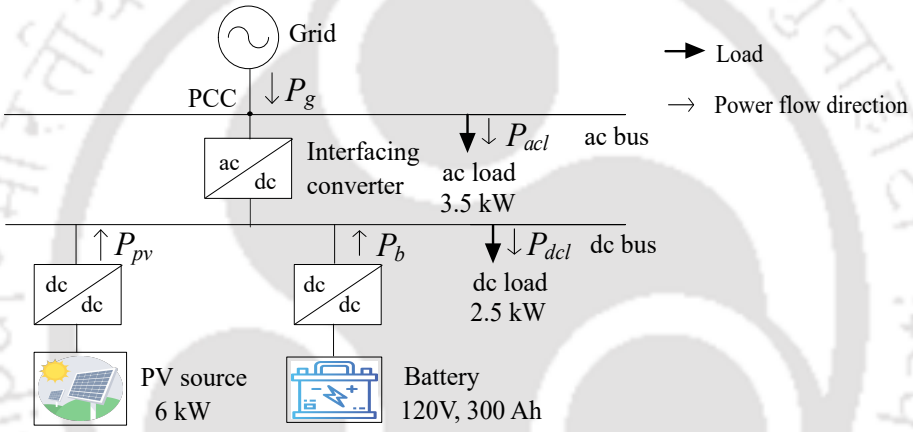

Fig. 3.1 Grid-connected PV-BESS system .

1. **Load**: The ac/dc loads are connected at the ac/dc buses of the system. The Peak ac and dc load powers of 3.5 kW and 2.5 kW, respectively are considered. The load power is the sum of ac and dc load powers as given in (3.2)

$$P_l(t) = P_{acl}(t) + P_{dcl}(t). \tag{3.2}$$

2. **Interfacing Converter**: The ac and dc buses are connected by interfacing converter. The interfacing converter acts as a rectifier and inverter while transferring power from ac bus to dc bus and dc bus to ac bus, respectively. It controls the power balance and maintains constant dc-link voltage.

3. **Photovoltaic system**: The PV source is connected at the dc bus of the system through a dc-dc converter. This dc-dc converter helps the PV source to operate at maximum power point as explained in Section 2.1 of Chapter 2. An installed PV

power rating of 6 kW is considered.

4. **Battery energy storage system**: The battery is connected to the dc bus of the system through a dc-dc converter. This dc-dc converter is used to provide the required charge/discharge schedules of the battery as explained in Section 2.1 of Chapter 2. A battery with a rating of 120 V, 300 Ah is chosen.

In Chapter 2, the battery charge/discharge efficiencies are neglected while formulating the proposed peak shaving method. However, in this work the DR method is proposed by considering the charge/discharge efficiencies of the battery. Therefore, the battery power considering the charge/discharge efficiencies is given as

$$\begin{aligned} P_b(t) &= P_{b-c}(t)/e_c, \text{ while charging} \\ &= P_{b-d}(t) \times e_d, \text{ while discharging.} \end{aligned} \tag{3.3}$$

Now, the overview of the proposed DR method in the chosen grid-connected PV-BESS system is discussed in following section.

3.2 OVERVIEW OF PROPOSED DEMAND RESPONSE METHOD

The overview of the proposed control is shown in Fig. 3.2. It includes various steps to realize the minimization of energy consumption cost over a day which are discussed as follows:

1. The first step is the day-ahead forecasting of load, RES powers, and energy prices. The day-ahead forecasts of load, RES powers, and energy buying and selling prices are required to determine the operating modes and control inputs of the rule-based DR method. These day-ahead forecasts of load, RESs power and energy price profiles can be obtained using the available methods present in literature [144], [159].

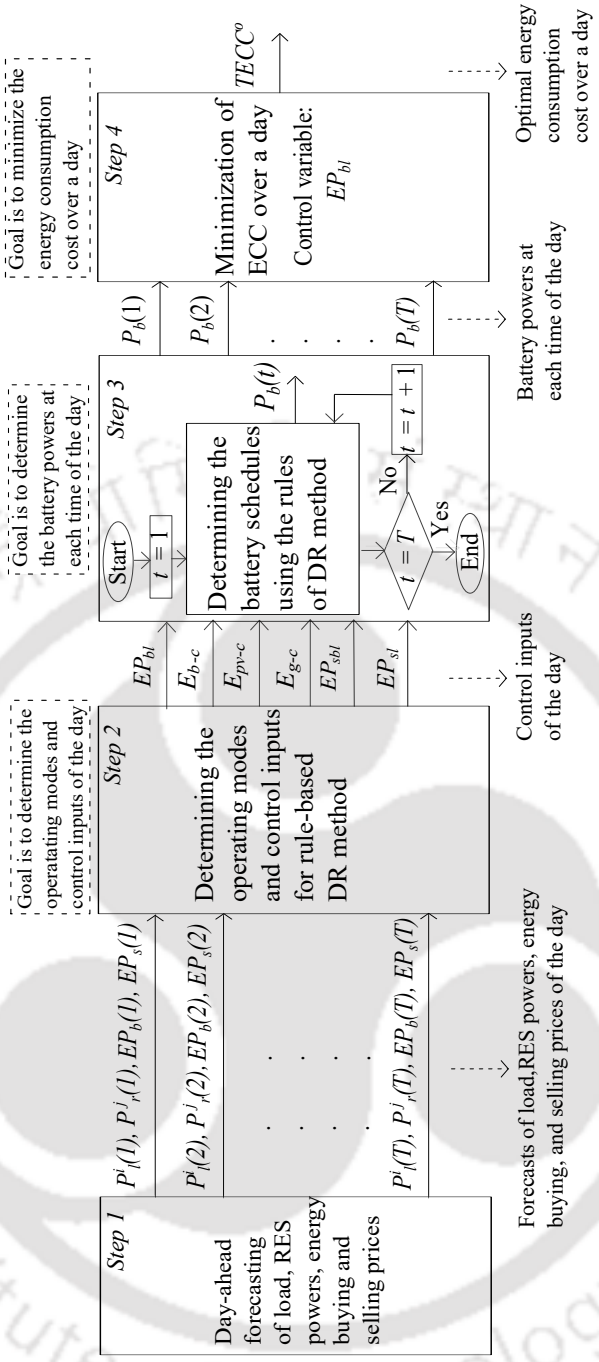

Fig. 3.2 Overview of the proposed DR method.

2. The second step is the determination of the operating modes of the battery and control inputs for rule-based DR method. The operating modes of the battery and control inputs for rule-based DR method are determined using the load, PV power, energy buying and selling price forecast curves of the day. The operating modes of the battery are chosen such that energy buying price is limited to the buying price limit. The buying price limit is defined as the buying price above which there is no power drawn from the grid.

   The control inputs for rule-based DR method are determined such that they depend on energy buying price limit. It means that the control inputs of rule-based DR

are same for the whole day corresponding to the energy buying price limit of that particular day. This indicates that the control inputs have to be determined only once per day.

3. The third step is the determination of the battery schedules using the rules of DR method. The rules of the DR method are formulated based on the control inputs which are obtained in Step 2 to decide the charge/discharge schedules of the battery over a day.

4. The fourth step is the determination of the optimal control inputs. The optimization problem is formulated to minimize the energy consumption cost over a day while controlling the energy buying price limit of the day. The control inputs corresponding to the optimal energy buying price limit are considered as the optimal control inputs of the day.

In this work, it is assumed that the forecasts required as per Step 1 are available and the entire analysis carried out based on these day-ahead forecasts. The steps 2-4 of the proposed method are discussed in detail in following sections.

3.3 DETERMINATION OF OPERATING MODES OF THE BATTERY AND CONTROL INPUTS

The method of determination of operating modes of the battery and control inputs for rule-based DR method are discussed in this section.

3.3.1 Operating Modes of the Battery

It is possible to limit buying price to a limit price known as buying price limit with the use of the battery along with the PV source. The operating modes to limit buying price to its limit are shown in Fig. 3.3 and discussed as follows.

1. **Discharging mode:** The battery is discharged when buying price is more than buying price limit and PV power is less than the load power ($EP_b(t) > EP_{bl}$ && $P_{pv}(t) \leq P_l(t)$). It means that the grid power is not drawn when $EP_b(t) > EP_{bl}$

which reduces energy consumption cost of the system. The symbol '&&' is logical AND operator.

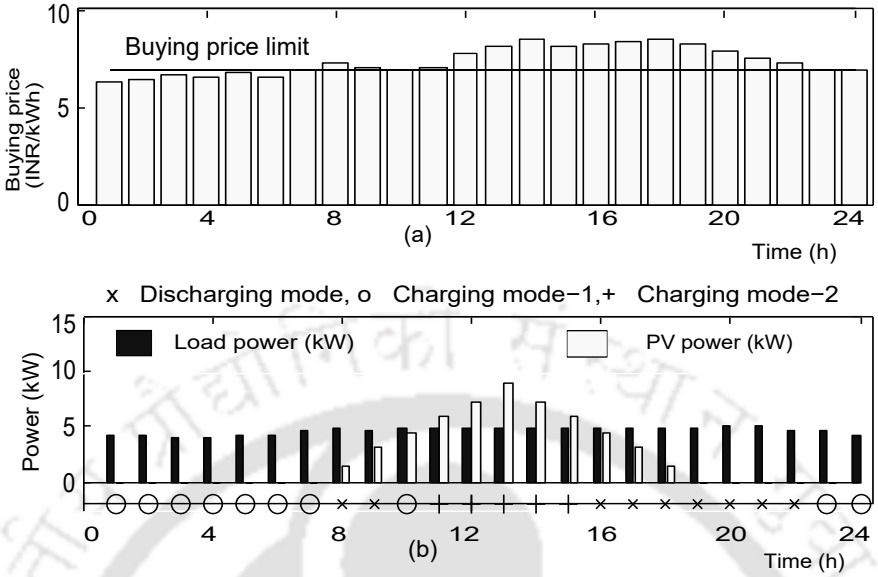

Fig. 3.3 Operating modes of the battery. (a) Energy buying price . (b) Load and PV powers

2. **Charging mode 1:** The battery is charged when buying price is less than buying price limit ($EP_b(t) \leq EP_{bl}$). In this mode both the grid and the PV source are used to charge the battery.
3. **Charging mode 2:** The battery is charged when buying price is more than buying price limit and PV power is more than the load power ($EP_b(t) > EP_{bl} \&\& P_{pv}(t) > P_l(t)$). In this mode the grid power is not used to charge the battery as $EP_b(t) > EP_{bl}$. This reduces energy consumption cost of the system. Therefore, only the PV source is used to charge the battery.

Now, the determination of control inputs for rule-based DR method is explained as follows:

3.3.2 Control Inputs

The sequential process of determination of the control inputs is given in flow chart of Fig. 3.4. Initially, buying price limit, energy required for charging the battery and PV energy available for charging the battery are determined. Then, selling price limit is determined if PV energy available for charging the battery is more than the energy

required for charging the battery. Otherwise, the grid energy available for charging the battery and sub-buying price limit are determined. The determination of these inputs is discussed as follows:

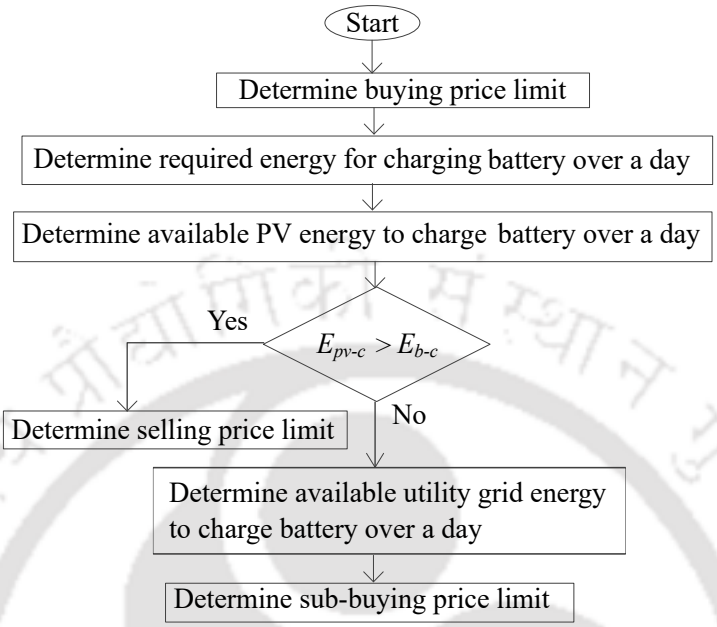

Fig. 3.4 The sequential process of determination of control inputs.

Buying price limit

Buying price limit is chosen as a control variable which lies between the maximum and minimum of predicted buying prices of the day.

$$EP_{min-b} \leq EP_{bl} \leq EP_{max-b}. \tag{3.4}$$

The EP_b^{max} and EP_b^{min} are the maximum and minimum values of the available day-ahead buying price profile of the day, respectively.

Required energy for charging the battery over a day

To limit $EP_b(t)$ to EP_{bl}, the required load power when $EP_b(t) > EP_{bl}$ is supplied either by the PV source or the battery. The power to be discharged from the battery is equal to the load power that is not supplied by the PV source. Considering discharging power

limit and efficiency, the battery discharging power is given as

$$\begin{aligned} P_{b-d}(t) &= P_{ex-d}(t)/e_d, \forall t \in t_d \&\& P_{ex-d}(t) \leq P_{b-dl} \\ &= P_{b-dl}, \forall t \in t_d \&\& P_{ex-d}(t) > P_{b-dl} \\ &= 0, \text{ otherwise.} \end{aligned} \tag{3.5}$$

In (3.5), the P_{ex-d} is the load power that is not supplied by the PV source. This is given as follows:

$$P_{ex-d}(t) = (P_l(t) - P_{pv}(t)). \tag{3.6}$$

Then, energy to be discharged from the battery is the sum of the powers to be discharged from the battery over a day, and given as

$$E_{b-d} = \sum_{t=1}^{T} P_{b-d}(t) \times T_c. \tag{3.7}$$

For flexible day-to-day management, the required energy for charging the battery over a day must be equal to the energy to be discharged from the battery over a day i.e.,

$$E_{b-c} = E_{b-d}. \tag{3.8}$$

Available PV energy to charge the battery over a day

The battery is to be charged by E_{b-c} over a day, either by the PV source or grid. Firstly, for increasing the self consumption, the available PV energy to charge the battery (without injecting into the grid) is calculated. If it is not sufficient, then the available grid energy to charge the battery is determined. The $P_{pv-c}(t)$ is considered as sum of $P_{pv-c1}(t)$ and $P_{pv-c2}(t)$. Considering the charging power limit of the battery, the $P_{pv-c1}(t)$ is given as follows:

$$\begin{aligned} P_{pv-c1}(t) &= P_{pv}(t), P_{pv}(t) \leq P_{b-cl} \\ &= P_{b-cl}, P_{pv}(t) > P_{b-cl}. \end{aligned} \tag{3.9}$$

The $P_{pv-c2}(t)$ is given in (3.10),

$$\begin{aligned} P_{pv-c2}(t) &= P_{ex-pv}(t), P_{ex-pv}(t) \leq P_{b-cl} \\ &= P_{b-cl}, P_{ex-pv}(t) > P_{b-cl}. \end{aligned} \tag{3.10}$$

In (3.10), the term P_{ex-pv} is the PV power that is more than the load power given as

$$P_{ex-pv}(t) = P_{pv}(t) - P_l(t). \tag{3.11}$$

Now, the available PV energy to charge the battery is the sum of the available PV powers to charge the battery over a day as given in (5.24).

$$E_{pv-c} = \sum_{t=1}^{T} P_{pv-c}(t) \times T_c. \tag{3.12}$$

Selling price limit

When the available PV energy to charge the battery is more than the energy required for charging the battery over a day, it is economical if the battery is charged with PV power during the time of selling price less than the selling price limit. Therefore, selling price limit is a selling price value below which the PV source is used to charge the battery. It means that the available PV power is either used to supply load or injected to the grid when selling price is more than its limit in order to reduce the energy consumption cost of the system. The determination of this limit is given as flowchart in Fig. 3.5.

Firstly the time slots of charging modes i.e., t_{c1} and t_{c2} are determined. Then, selling prices during t_{c1} and t_{c2} are determined and considered as vectors [$\boldsymbol{EP_{s1}}$] and [$\boldsymbol{EP_{s2}}$]. Now, a selling price vector ($\boldsymbol{EP_{svc}}$) is defined as [$\boldsymbol{EP_{s1}}$ $\boldsymbol{EP_{s2}}$]. Then, $\boldsymbol{EP_{svc}}$ is sorted and considered as sorted selling price vector ($\boldsymbol{EP_{svc-s}}$). Then, cumulative sum of the available PV power to charge the battery corresponding to each element of $\boldsymbol{EP_{svc-s}}$ is computed as

$$\begin{aligned} S_{pv-c}(t) &= S_{pv-c}(t-1) + P_{pv-c}(t), \forall t \in t_c \\ &= 0, \text{ otherwise} \end{aligned} \tag{3.13}$$

where t_c includes both t_{c1} and t_{c2}. This process is repeated if $S_{pv-c}(t)$ is less than the

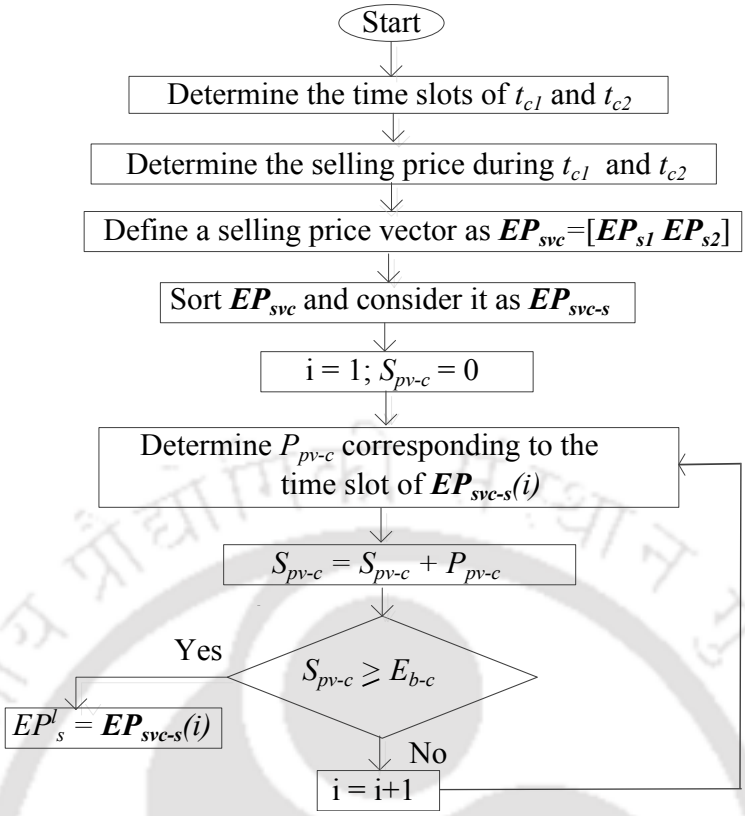

Fig. 3.5 Determination of selling price limit.

required energy for charging the battery i.e, E_{b-c}. If $S_{pv-c}(t)$ is more than or equal to E_{b-c}, the corresponding element of $\boldsymbol{EP_{svc-s}}$ is considered as selling price limit. This signifies that the PV source is used to charge the battery only during the time slots when selling price is less than selling price limit.

Available grid energy to charge the battery over a day

When the available PV energy to charge the battery is less than the required energy to charge the battery, deficit amount of energy is drawn from the grid. However, the grid is not used to charge the battery during t_d and t_{c2} i.e., when buying price is more than its limit. Considering the charging power limit of the battery, the available grid power to charge the battery is given in (3.14),

$$\begin{aligned} P_{g-c}(t) &= P_{b-cl} - P_{pv-c1}(t), \forall t \in t_{c1} \\ &= 0, \text{ otherwise.} \end{aligned} \tag{3.14}$$

Equation (3.14) indicates that the grid is used to charge the battery only during t_{c1}. Then, the available grid energy to charge the battery is sum of the available grid powers

to charge the battery given as

$$E_{g-c} = \sum_{t=1}^{T} P_{g-c}(t) \times T_c. \tag{3.15}$$

Sub-buying price limit

When $E_{pv-c} \leq E_{b-c}$, the grid is also used to charge the battery along with the PV source. In this case, only the amount of energy $E_{pv-c} - E_{b-c}$ is to be provided by the grid to completely charge the battery (not all the available grid energy to charge the battery which limit energy buying price to the energy buying price limit). Therefore, it is economical to use grid to charge the battery only when buying price is less than its sub-buying price limit. Therefore, the sub-buying price limit is a buying price value above which grid is not used to charge the battery. The method of determination of the sub-buying price limit is similar to the determination of selling price limit. This is given in flowchart of Fig. 3.6.

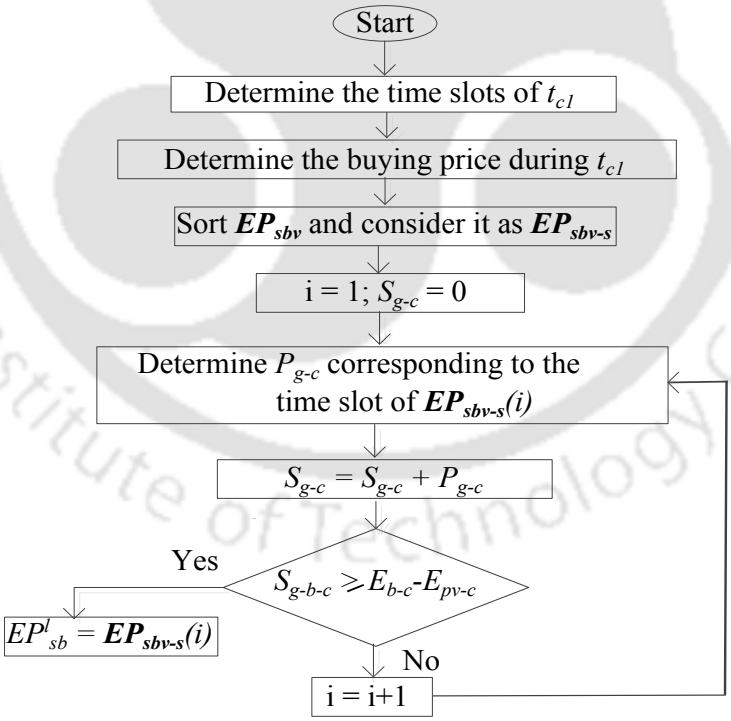

Fig. 3.6 Determination of sub-buying price limit.

Firstly, the time slots of charging mode 1 are determined (because the grid energy is available to charge the battery only during t_{c1} for limiting the energy buying price to the energy buying price limit). The buying prices during t_{c1} are determined and considered as the sub-buying price vector $\boldsymbol{EP}_{sbv}$. Then, $\boldsymbol{EP}_{sbv}$ is sorted and considered as the

sorted sub-buying price vector ($\boldsymbol{EP_{sbv-s}}$). Then, cumulative sum of the available grid power to charge the battery corresponding to each element of $\boldsymbol{EP_{sbv-s}}$ is computed as

$$\begin{aligned} S_{g-c}(t) &= S_{g-c}(t-1) + P_{g-c}(t) \times T_c, \forall t \in t_{c1} \\ &= 0, \text{ otherwise.} \end{aligned} \tag{3.16}$$

This process is repeated if $S_{g-c}(t)$ is less than required grid energy for charging the battery i.e, $E_{b-c} - E_{pv-c}$. If $S_{g-c}(t)$ is more than or equal to $E_{b-c} - E_{pv-c}$, the corresponding element of $\boldsymbol{EP_{sbv-s}}$ is considered as EP_{sbl}. This signifies that the grid is used to charge the battery only during the time slots when buying price is less than the sub-buying price limit.

Now, the determination of battery schedules using the rules of proposed DR method is explained in following section.

3.4 DETERMINATION OF THE BATTERY SCHEDULES USING THE RULES OF DEMAND RESPONSE METHOD

Considering the above proposed control inputs, the rules for DR are formulated to know the day-ahead schedules of the battery. These rules are formulated such that day-to-day management is flexible while considering buying price limit, selling price limit and sub-buying price limit as given follows.

3.4.1 Discharging Mode

The discharging mode of the battery is during the time when $EP_b(t) > EP_{bl}$ && $P_{pv}(t) \leq P_l(t)$. In this mode, there is only one rule for deciding battery power as given follows.

Rule 1

In this mode $EP_b(t) > EP_{bl}$. The battery is used to supply the load power which is not supplied by the PV source. It means that the battery discharges by $P_{b-d}(t)$ as per (3.5).

3.4.2 Charging Mode 1

The charging mode 1 of the battery is during the time when $EP_b(t) \leq EP_{bl}$. In this mode, there are two rules which decide the battery power as given follows.

Rule 2

When $E_{pv-c} \leq E_{b-c}$, the grid is used to charge the battery along with the PV source. It means that the battery is charged by $P_{pv-c-b}(t) + P_{g-c-b}(t)$. Here the complete available PV power is used to charge the battery i.e., $P_{pv-c-b}(t) = P_{pv-c1}(t)$. However, the amount of the grid power used to charge the battery depends on the values of buying price and sub buying price limit which is discussed as follows:

Before discussing the various possibilities, two important terms are defined. 1) The sum of the available grid powers to charge the battery for all the times of buying price less than sub-buying price limit (i.e., $\forall$ t $\in t_l$) as E_{g-c-l}. 2) The sum of the grid powers already used to charge the battery for all the times of buying price equal to sub-buying price limit (i.e., $\forall$ t $\in t_e \&\& t_e < t$) as $E_{g-c-b-e}(t)$.

1. If $EP_b(t) < EP_{sbl}$: In this case, complete available grid power is used to charge the battery as per (5.25). Therefore, $P_{g-c-b}(t) = P_{g-c}(t)$.
2. If $EP_b(t) = EP_{sbl}$: Here, the number of time slots of t_e can be more than one. During these slots a total of $(E_{b-c} - E_{pv-c} - E_{g-c-l})$ is supplied by the grid for charging the battery. Therefore, $P_{g-c-b}(t)$ depends on $E_{g-c-b-e}(t)$ and $S_{g-c}(t)$ which is discussed as follows:
   (a) If $(E_{g-c-b-e}(t) < E_{b-c} - E_{pv-c} - E_{g-c-l})$ && $(S_{g-c}(t) \leq E_{b-c} - E_{pv-c})$, It means that the battery is not yet charged with the required amount of energy during t_e. Moreover, $S_{g-c}(t)$ is less than the required amount of the grid energy to charge the battery. Therefore, the complete available grid power is used to charge the battery i.e., $P_{g-c-b}(t) = P_{g-c}(t)$.
   (b) If $(E_{g-b-c-e}(t) < E_{b-c} - E_{pv-c} - E_{g-c-l})$ && $(S_{g-c}(t) > E_{b-c} - E_{pv-c})$, It means that the battery is not yet charged with the required amount of energy during t_e. However, $S_{g-c}(t)$ is more than the required amount of the grid energy to charge the battery. In this scenario, it is not possible to charge the battery with the complete available grid power. Because it leads to the SoC violation

of flexible day-to-day management. Therefore, $P_{g-c-b}(t) = (S_{g-c}(t) - (E_{b-c} - E_{pv-c}))/T_c$ such that the flexible day-to-day management is maintained.

(c) If $E_{g-b-c-e}(t) \geq E_{b-c} - E_{pv-c} - E_{g-c-l}$, It means that the battery is already charged with the required amount of energy during t_e. Therefore, the grid is not used to charge the battery i.e., $P_{g-c-b}(t) = 0$.

3. If $EP_b(t) > EP_{sbl}$: The grid is not used to charge the battery as per the definition of sub-buying price limit. Therefore, $P_{g-c-b}(t) = 0$.

Rule 3

When $E_{pv-c} > E_{b-c}$, only the PV source is used to charge the battery. The amount of PV power used to charge the battery depends on selling price and selling price limit.

Before discussing the various possibilities, two important terms are defined with variables. 1) The sum of the available PV powers to charge the battery for all the times of selling price less than selling price limit (i.e., $\forall$ t $\in t_{sl}$) as E_{pv-c-l}. 2) The sum of PV powers already used to charge the battery for all the times of selling price equal to selling price limit (i.e., $\forall$ t $\in t_{se} \&\& t_{se} < t$) as $E_{pv-c-b-e}(t)$.

1. If $EP_s(t) < EP_{sl}$: In this case the complete available PV power is used to charge the battery as per (3.9). Therefore, $P_{pv-c-b}(t) = P_{pv-c1}(t)$.
2. If $EP_s(t) = EP_{sl}$: Here, the number of time slots of t_{se} can be more than one. During these slots a total of $(E_{b-c} - E_{pv-c-l})$ is supplied by the PV source for charging the battery. Therefore, $P_{pv-c-b}(t)$ depends on $E_{pv-c-b-e}(t)$ and $S_{pv-c}(t)$ which is discussed as follows:
   (a) If ($E_{pv-c-b-e}(t) < E_{b-c} - E_{pv-c-l}$ && $S_{pv-c}(t) \leq$E$_{b-c}$), it means that the battery is not yet charged with the required amount of energy during t_e. Moreover, $S_{pv-c}(t)$ is less than the required energy for charging the battery. Therefore, complete available PV power is used to charge the battery i.e., $P_{pv-c-b}(t) = P_{pv-c1}(t)$.
   (b) If ($E_{pv-c-b-e}(t) < E_{b-c} - E_{pv-c-l}$) && $S_{pv-c}(t) > E_{b-c}$, it means that the battery is not yet charged with the required amount of energy during t_e. However,

$S_{pv-c}(t)$ is more than the required energy for charging the battery. In this scenario, it is not possible to charge the battery with the complete available PV power as it leads to the SoC violation of flexible day-to-day management of the battery (the final SoC of the day can not be maintained equal to the initial SoC of the day). Therefore, $P_{pv-c-b}(t) = (S_{pv-c}(t) - E_{b-c})/T_c$ such that the flexible day-to-day management of the battery is maintained.

(c) If $E_{pv-c-b-e}(t) \geq E_{b-c} - E_{pv-c-l}$, it means that the battery is already charged with the required amount of energy during t_e. The PV source is not used to charge the battery any more. Therefore, $P_{pv-c-b}(t) = 0$.

3. If $EP_s(t) > EP_{sl}$: The PV source is not used to charge the battery as per the definition of selling price limit. Therefore, $P_{pv-c-b}(t) = 0$.

3.4.3 Charging Mode 2

The charging mode 2 of the battery is during the time when $EP_b(t) > EP_{bl}$ && $P_{pv}(t) > P_l(t)$. In this mode, there are two rules which decide the battery power as given follows.

Rule 4

If $E_{pv-c} \leq E_{b-c}$, only the PV source is used to charge the battery as $EP_b(t) > EP_{bl}$. The PV source charges the battery by the amount $P_{pv-c2}(t)$ as per (3.10).

Rule 5

If $E_{pv-c} > E_{b-c}$, only the PV source is used to charge the battery. The $P_{pv-c-b}(t)$ depends on the values of $EP_s(t)$ and EP_{sl} as mentioned in Rule 3.

1. If $EP_s(t) < EP_{sl}$: Here the complete available PV power is used to charge the battery as per (3.9). Therefore, $P_{pv-c-b}(t) = P_{pv-c2}(t)$.
2. If $EP_s(t) = EP_{sl}$: Here, $P_{pv-c-b}(t)$ depends on $E_{pv-c-b-e}(t)$ and $S_{pv-c}(t)$ which is given as follows:
   (a) If ($E_{pv-c-b-e}(t) < E_{b-c} - E_{pv-c-l}$ && $S_{pv-c}(t) \leq$E$_{b-c}$), the complete available PV power is used to charge the battery. Therefore, $P_{pv-c-b}(t) = P_{pv-c2}(t)$.

(b) If $(E_{pv-c-b-e}(t) < E_{b-c} - E_{pv-c-l}$ && $S_{pv-c}(t) > E_{b-c})$, it is not possible to charge the battery with the complete available PV power as it leads to the SoC violation of flexible day-to-day management. Therefore, $P_{pv-c-b}(t) = (S_{pv-c}(t) - E_{b-c})/T_c$ such that the flexible day-to-day management is maintained over a day.

(c) If $E_{pv-c-b-e}(t) \geq E_{b-c} - E_{pv-c-l}$, the PV source is not used to charge the battery. Therefore, $P_{pv-c-b}(t) = 0$.

3. $EP_s(t) > EP_{sl}$: The PV source is not used to charge the battery. Therefore, $P_{pv-c-b}(t) = 0$.

The SoC of the battery during discharging and charging modes is calculated using coulomb-counting method. This process of determination of battery charge/discharge schedules using the proposed rules for DR method is shown as flowchart in Fig. 3.7.

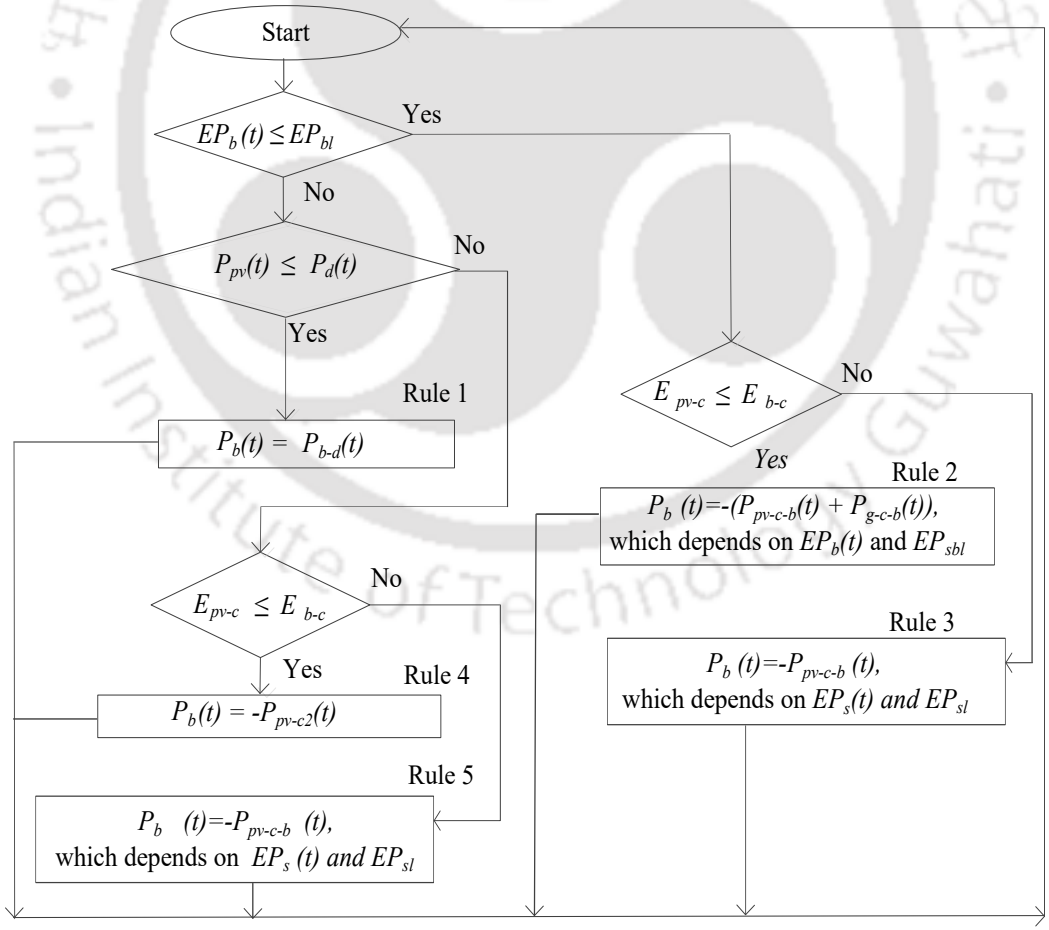

Fig. 3.7 Proposed rule-based DR method.

Now, the determination of optimal control inputs for optimizing the proposed rule-based DR method is discussed.

3.5 DETERMINATION OF OPTIMAL CONTROL INPUTS

The optimization problem formulation for determining the optimal control inputs and its solution method are discussed in this section.

3.5.1 Optimization Problem Formulation

The considered objective function and constraints are given from (3.17)-(3.21), respectively

$$\text{minimize} \quad f = \sum_{t=1}^{T} ECC(t) \tag{3.17}$$

subjected to

1. Power balance constraint

$$P_g(t) + P_{pv}(t) + P_b(t) = P_l(t). \tag{3.18}$$

2. Battery SoC Constraints

$$SoC_l \leq SoC(t) \leq SoC_u, SoC_f = SoC_i. \tag{3.19}$$

3. Battery charge/discharge power constraints

$$P_{b-c}(t) \leq P_{b-cl}, P_{b-d}(t) \leq P_{b-dl}. \tag{3.20}$$

4. Battery energy capacity constraint

$$E_{g-c} + E_{pv-c} \geq E_{b-c}. \tag{3.21}$$

Equation (3.17) aims to minimize energy consumption cost of the system over a day. The *ECC* is calculated using (3.22) i.e.,

$$ECC(t) = E_{g-d}(t) \times EP_b(t) - E_{g-i}(t) \times EP_s(t). \tag{3.22}$$

Equation (3.18) gives the power balance constraint. Equation (3.19) indicates the constraints of SoC limits of the battery and the flexible day-to-day operation of the battery. The SoC of the battery is calculated using coulomb counting method [147], [148]. Equation (3.20) indicates the constraints of charge/discharge powers of the battery, respectively. Equation (3.21) shows that the sum of the available grid and PV energies to

charge the battery should be more than or equal to the required energy for charging the battery.

3.5.2 Solving the Optimization Problem

The formulated problem is an off-line optimization problem with a non-linear fitness function, which is solved using GA solver in MATLAB. The method of solving the optimization problem using GA is explained in detail in Section 2.5 of Chapter 2. The default values are chosen for various parameters of GA, except for population size. The population size is an important parameter to choose. Because if it is small, the convergence might not be achieved. Therefore, population size is chosen based on the number of control variables. There is only one control variable in this optimization problem i.e., the energy buying price limit of the day. As it is possible for different GA runs to provide different optimal values, to avoid any sub-optimal solutions and guarantee global optimum solution the population size is tuned such that multiple simulation runs converge precisely to the same value and chosen as 10. The control inputs corresponding to EP^{o}_{bl} are the optimal control inputs for the proposed method i.e., E^{o}_{b-c}, E^{o}_{pv-c}, E^{o}_{g-c}, EP^{o}_{sbl} and EP^{o}_{sl}.

Now, the simulation results of the proposed optimal rule-based DR method are discussed in following section.

3.6 SIMULATION RESULTS

The proposed method is tested on the considered system in MATLAB on a 64-bit operating system PC with a processor of Intel(R) Core(TM) i5-6500 CPU @ 3.2 GHz. The chosen system parameters are given in Table 3.1 [58]. The day-ahead forecasts of ac/dc load power profiles are shown in Fig. 3.8.

The rule-based methods discussed in literature [42], [100], [127], [128], [133] have validated their algorithms for various possible scenarios as per their proposed method. As per the proposed method in this chapter, there exists only two different scenarios based on the available PV energy on a given day i.e., 1) The available PV energy over a day is less than or equal to the required energy for charging the battery and 2) The

available PV energy over a day is more than the required energy for charging the battery. Therefore, the proposed method is validated for following cases which include both the possible scenarios.

Case 1: More PV energy availability over a day

Case 2: Less PV energy availability over a day

Table 3.1 System Parameters

Parameter	Value	Parameter	Value
P_{acl-p}/P_{dcl-p}	3.5/2.5 kW	SoC_l/SoC_u	0.2/0.9
P_{pv-i}	6 kW	SoC_i	0.5
E_{b-r}	36 kWh	P_{b-cl}	6 kW
Ah_{b-r}	300 Ah	P_{b-dl}	6 kW
e_c	0.95	e_d	0.95

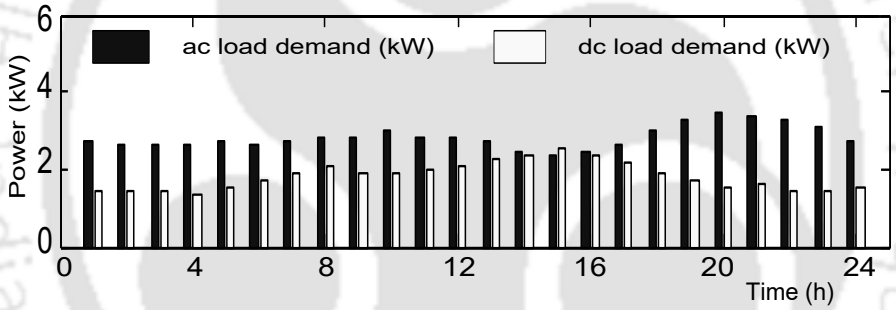

Fig. 3.8 ac and dc load profiles .

3.6.1 Case 1

In this case more PV energy availability over a day is considered. The optimal control inputs are determined with the help of the available day-ahead forecasts of energy price, load, PV power profiles and the proposed rules as discussed follows.

Optimal control inputs

The results of GA i.e., best fitness values for multiple runs are shown in Fig. 3.9. It is observed that all the runs provide same optimal result. It means that the minimum of best fitness values is same in all the runs which is equal to 542.74 INR. Therefore, optimal energy consumption cost of system is 542.74 INR. The corresponding energy

buying price limit is the optimal energy buying price limit which is equal to 8.235 INR. For this, the corresponding optimal control inputs are given in Table 3.2. It shows that the optimal available PV energy to charge the battery is more than the required energy for charging the battery ($E^o_{pv-c} > E^o_{b-c}$). It means that the grid energy is not required to charge the battery. Therefore, the available grid energy to charge battery and energy sub-buying price limit (E^o_{g-c} and EP^o_{sbl}) are not applicable (NA).

Battery schedules and grid powers over the day

The day-ahead forecasted buying and selling price profiles along with the determined optimal buying and selling price limits are shown in Fig. 3.10(a). The day-ahead forecasted load and PV power profiles are shown in Fig. 3.10(b). For these inputs, the discharging mode is during t = 14, 17 and 18 hours and remaining hours are of charging mode 1. There is no charging mode 2 according to the proposed operating modes of the battery. It is observed that the PV source is not used to charge the battery when $EP_s(t) > EP^o_{sl}$ i.e., during t = 8, 12-22 hours as shown in Fig. 3.10(c). Fig. 3.10(d) shows that the battery is operated at SoC values of above 50% over the day and within its upper/lower limits. Moreover, $SoC_f = SoC_i = 50\%$, which is desired for flexible day-to-day management. This justifies the proposed rule-based DR method.

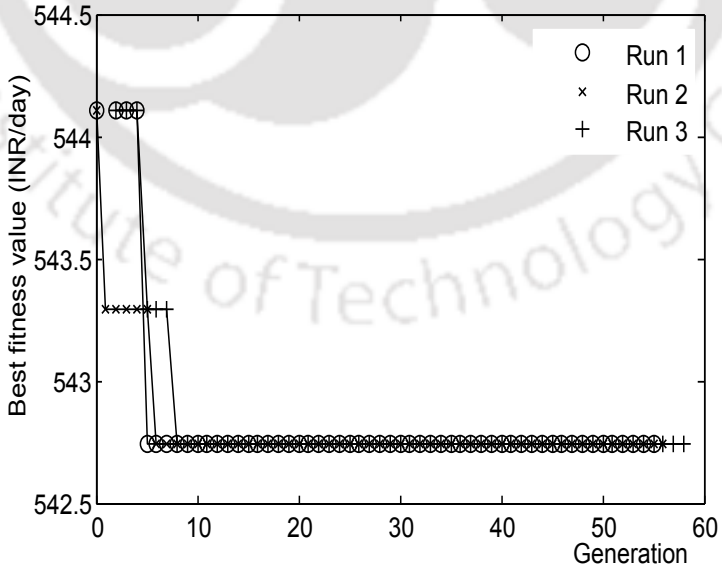

Fig. 3.9 Best fitness values obtained using GA during Case 1

The grid power is determined using (3.18) and shown in Fig. 3.10(e). It indicates that when $EP_b(t) > EP^l_{bl}$ i.e., during t = 14, 17 and 18 hours, there is no grid power demand.

Table 3.2 Optimal Control Inputs

Input parameter	Case 1 Availability	Case 2 Availability
EP^o_{bl} (INR)	8.23	8.29
E^o_{b-c} (kWh)	7.13	14.55
E^o_{pv-c} (kWh)	27.6	3
E^o_{g-c} (kWh)	NA	123
EP^o_{sbl} (INR)	NA	6.43
EP^o_{sl} (INR)	6.43	NA

Similarly, there can be power injected to grid only when $EP_s(t) > EP^o_{sl}$ i.e., during t = 8, 12-22 hours. However, the grid power injection is observed only during t = 13 hour as the available PV power is more than the load power during that hour. The grid power profile indicates that buying price and selling price are limited to their corresponding optimal limits of the day to minimize the energy consumption cost of the system. This justifies the proposed rule-based DR method.

3.6.2 Case 2

In this case less PV energy availability over a day is considered. The determined optimal control inputs are discussed as follows:

Optimal control inputs

In this case the minimum of best fitness values is determined to be 779.03 INR using GA. Then, the optimal energy buying price limit is found to be equal to 8.29 INR. For this, the corresponding optimal control inputs are given in Table 3.2. It indicates that the optimal available PV energy to charge the battery is less than the required energy for charging the battery ($E^o_{pv-c} < E^o_{b-c}$). It means that the complete available PV energy is used to charge the battery. Therefore, the energy selling price limit (EP^o_{sl}) is NA.

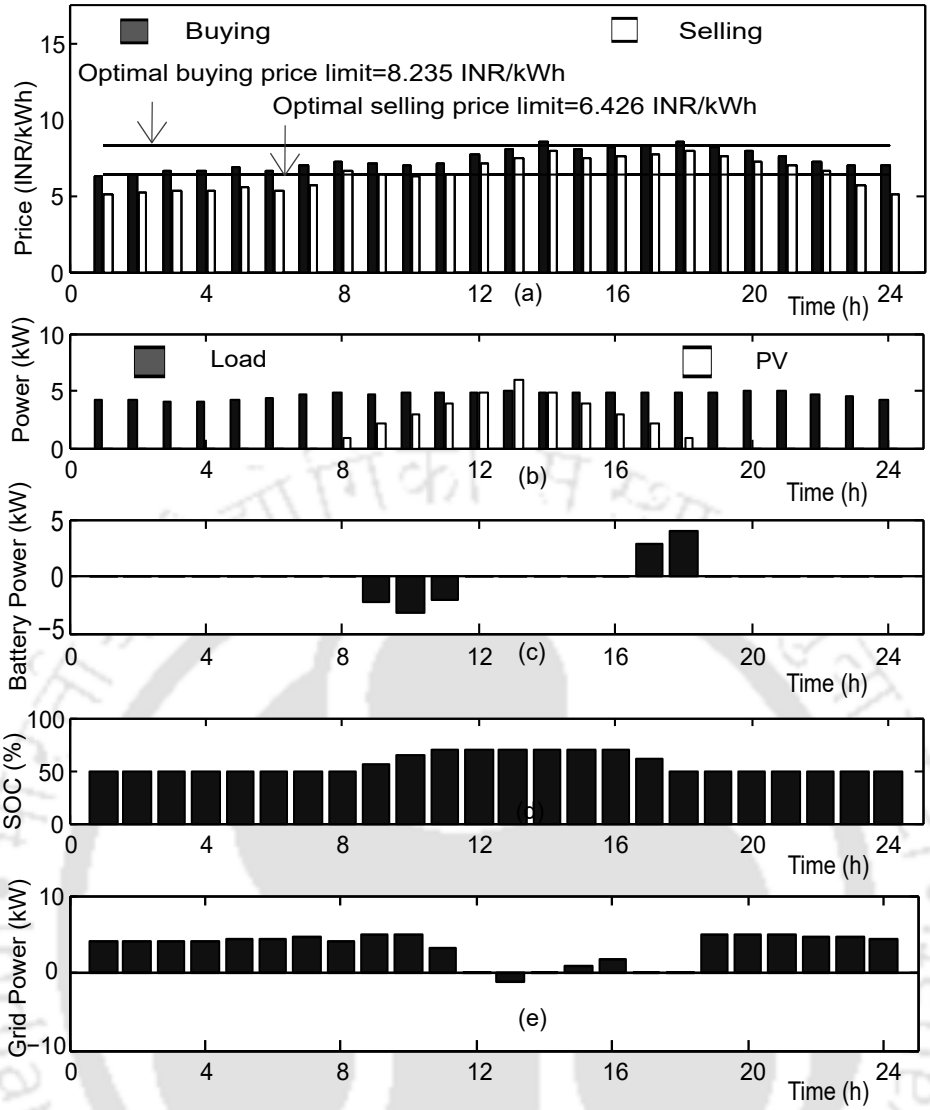

Fig. 3.10 Case 1. (a) Energy price . (b) Load and PV power profiles . (c) Charge/discharge schedules of the battery. (d) SoC of the battery. (e) Grid power.

Battery schedules and grid powers over the day

The day-ahead forecasts of energy prices along with the optimal buying and sub-buying price limits are shown in Fig. 3.11(a). The day-ahead forecasts of load and PV powers are shown in Fig. 3.11(b). For these inputs discharging mode is during t = 14, 17 and 18 hours and remaining hours are of charging mode 1. There is no charging mode 2 according to the proposed operating modes of the battery. The battery modes of hours are same as that of the case of more PV energy availability even though there is less PV energy available for charging the battery. Because, in this case, the grid is also used to charge the battery along with the PV source. The complete available PV energy is used to charge the battery as shown in Fig. 3.11(c). The grid is used to charge the battery only when $EP_b(t) \leq EP^o_{sbl}$ i.e., during t = 1, 2 hours. Fig. 3.11(d) shows that the battery

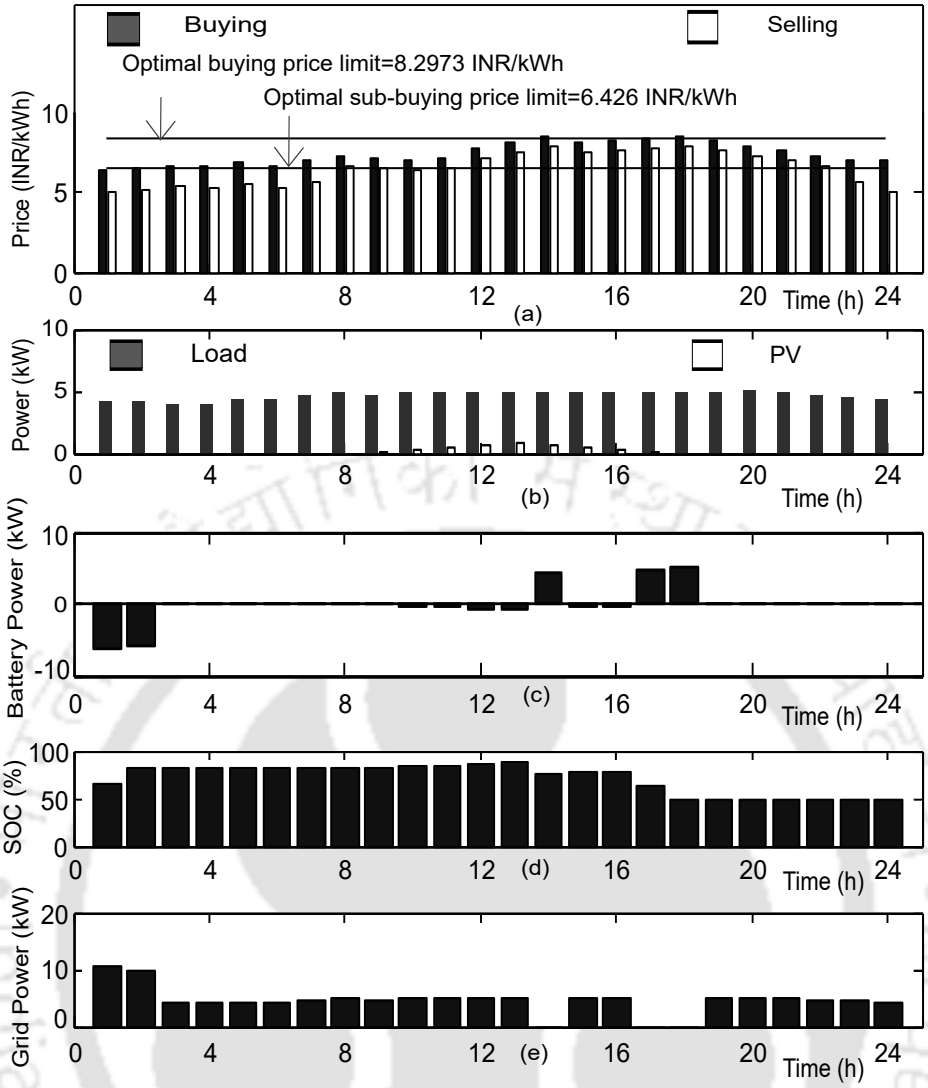

Fig. 3.11 Case 2. (a) Energy price . (b) Load and PV power profiles . (c) Charge/discharge schedules of the battery. (d) SoC of the battery. (e) Grid power.

is operated at SoC values of above 50% over the day and within its upper/lower limits. Moreover, $SoC_f = SoC_i = 50\%$, which is desired for flexible day-to-day management. This justifies the proposed rule-based DR method.

The grid power is determined using (3.18) and shown in Fig. 3.11(e). It indicates that when $EP_b(t) > EP^o_{bl}$ i.e., during t = 14, 17 and 18 hours, there is no grid demand. It means that the buying price is limited to the optimal buying price limit of the day to minimize energy consumption cost of the system. Since less PV energy is available, there is no power injected to the grid. This justifies the proposed rule-based DR method.

3.6.3 Energy Consumption Cost Analysis

The energy consumption cost of the system for base case i.e., without PV-BESS is calculated as 823.51 INR/day. The energy consumption costs calculated for Case 1 and 2 with the proposed method are shown in Table 3.3 and discussed as follows:

1. **Case 1**: In this case the energy consumption cost without BESS (with only the PV source) is calculated as 547.28 INR/day. It means that cost savings of 33.54% are obtained with only the PV source as compared to base case. However, using PV-BESS with the proposed method results in an energy consumption cost of 542.745 INR/day. It means that cost savings of 34.09% are obtained with the proposed method using PV-BESS as compared to base case. This shows that the energy consumption cost savings with BESS are not significant as compared to the case of without BESS. Because, in this case with more PV energy availability over the day, the energy consumption cost is reduced even without BESS as the energy selling price is considered.
2. **Case 2**: In this case the energy consumption cost without BESS is calculated as 794.10 INR/day. It means that cost savings of 3.57% are obtained with only the PV source as compared to base case. However, using PV-BESS with the proposed method results in an energy consumption cost of 779.02 INR/day. It means that cost savings of 5.4% are obtained with the proposed method using PV-BESS as compared to base case. This shows that the energy consumption cost savings with BESS are significant as compared to the case of without BESS. Because, in this case with less PV energy availability over the day, the energy consumption cost is not reduced even with the consideration of energy selling price.

3.7 CONCLUSIONS

In this chapter, an optimal rule-based demand response method is proposed considering both energy buying and selling price profiles. The proposed method is tested for the two possible cases: i) more PV energy availability over a day and ii) less PV energy availability over a day. The obtained results show that the energy buying and selling prices are limited to the respective energy buying and selling price limits of the day,

respectively. Moreover, the state of charge at the end of the day is maintained equal to the state of charge at the start of the day for flexible day-to-day-management of the battery. It is observed that the energy consumption cost savings of 34.09% and 5.4% are obtained on the day of more PV energy and less PV energy availability over a day, respectively as compared to the case when there is no battery energy storage system.

Table 3.3 Energy Consumption Cost and Cost Savings

Parameter	Base case	Case 1		Case 2	
		without BESS	Proposed DR with PV-BESS	without BESS	Proposed DR with PV-BESS
energy consumption cost (INR/day)	823.51	547.28	542.745	794.10	779.03
Cost Savings (%)	0	33.54	34.09	3.57	5.4

CHAPTER 4

OPTIMAL RULE-BASED VOLTAGE CONTROL WITH MAXIMUM AND MINIMUM BUS VOLTAGE LIMITS USING SMART POWER CONVERTER

In Chapter 2 and 3, the proposed optimal rule-based peak shaving and DR methods are discussed considering the aggregated load and RES powers in LV distribution system. The LV ac bus voltage is maintained at 1.0 p.u., irrespective of load and RES power variation over the day. However, in case if the loads and RESs are considered to be connected at various buses in the distribution system, the voltage control application becomes important. Because, a high PV penetration at the LV residential distribution network results in an increase of voltage throughout the feeder [160]. Moreover, increased loading levels in the distribution network results in a decrease of voltage throughout the feeder. In this scenario, sensitive equipment does not work satisfactorily [161]. Therefore, voltage control is necessary for the voltage rise/drop mitigation and for satisfactory operation of consumer equipment.

The smart power converters can be used for voltage control in modern LV distribution systems. In [87], full output voltage range based and set points based voltage control methods are studied using smart power converter. In a full output range based voltage control, the output voltage is infinitely adjustable within its range whereas in set points based voltage control, the output voltage is chosen from the predefined set points. Therefore, set points based voltage control schemes are simple and have certain financial advantages as compared to full voltage range control methods [87]. Suppose, if LV ac bus voltage is controlled through a set points based voltage control method, the frequent operation of controller for maintaining the reference voltage will be avoided. This is due to the fact that the reference voltages changes only among few set points unlike the full output voltage range based control over a day. With this, the frequent delays (transient times) which occurs when controllers are changing their output from one reference value to another reference value are reduced. Moreover, the real-time problems

associated with the tracking of set point references for controllers are reduced [162], [163]. However,it is important to choose the set points appropriately. The set points based voltage control methods such as switching between two set points based on end-of-line voltage as well as SBTSPBOC are discussed in [87]. Among all the methods discussed, the SBTSPBOC is shown as a practically feasible and better method of voltage control. In SBTSPBOC, the direct-axis LV ac bus current is used to decide the set points of voltage. However, if the direct-axis LV ac bus current is flowing in one direction, it can not be said that the current at all other buses is also flowing in the same direction. In those cases, voltage control based on current does not work. To avoid this limitation, an optimal rule-based voltage control method based on maximum and minimum bus voltages is proposed in this chapter. The set points are chosen based on the maximum and minimum load bus voltages to improve the voltage profile in the distribution systems. Accordingly, the contributions of this chapter are given as follows

1. A rule-based voltage control method is proposed to determine the LV ac bus voltages to be maintained by smart power converter such that the voltage rise and drop issues are mitigated in the distribution system over a day.
2. The proposed rule-based voltage control method is optimized by determining the optimal control inputs using GA for minimizing the voltage deviation over a day.

The remainder of the chapter is organized as follows: The chosen system is described in Section 4.1. Then, the overview of the proposed control is presented in Section 4.2. Later, the determination of operating modes of the smart power converter and control inputs of the rule-based voltage control method is discussed in Section 4.3. Further, the determination of LV ac bus voltage and optimal control inputs is explained in Section 4.4 and 4.5, respectively. The developed performance indicators to know the impact of voltage control method are discussed in Section 4.6. The results and conclusions are presented in Section 4.7 and 4.8, respectively.

4.1 SYSTEM DESCRIPTION

A modified CIGRE benchmark LV residential distribution network consisting of loads and PV sources at different buses is considered as shown in Fig. 4.1 [157], [164]. The power balance equation at the LV ac bus is given as

$$P_{lv}(t) = \sum_{i=1}^{n_l} P_l^i(t) + P_{loss}(t) - \sum_{j=1}^{n_r} P_{rc}^j(t). \tag{4.1}$$

A discrete time model is assumed. The 't' represents the time interval $[(t-1)\times T_c, t\times T_c]$, where T_c is each time slot duration, i.e., T_c = 1 hour. It means that all the defined powers are the average powers during the each hour of the day. The various components of the system are described as follows:

1. **Back-to-back converter**: The residential distribution network is connected to grid through a back-to-back converter. It is operated in grid forming mode to maintain the required LV ac bus voltage magnitude.
2. **Loads**: The loads L1-L5 with rated peak load of 30 kW, 40 kW, 50 kW, 20 kW and 45 kW, respectively are considered. The summer load power profile is considered where peak load occurs during 20:00 and 23:00 hours. The load power profile when the peak load power is equal to the rated peak load power is shown in Fig. 4.2(a) [141].
3. **Photovoltaic sources**: The PV sources PV1-PV5 are considered to be present with loads L1-L5, respectively. Each PV source is connected through dc-dc and dc-ac converters to the load terminal. This dc-dc converter helps the PV source to operate at maximum power point using MPPT algorithms. Further, the dc-ac converter operates in grid following mode to provide required active/reactive powers to the system. In this study, they are operated at unity power factor.

   It is considered that the installed PV power is equal to the rated peak power of the load at which it is connected. The PV penetration level of 100% is considered at each load of the distribution network. where PV penetration level (λ) is defined as the ratio of the installed PV power (P_{pv-i}) to the peak load demand of the building (P_{d-p}) [165] i.e.,

$$\lambda = \frac{P_{pv-i}}{P_{d-p}}. \tag{4.2}$$

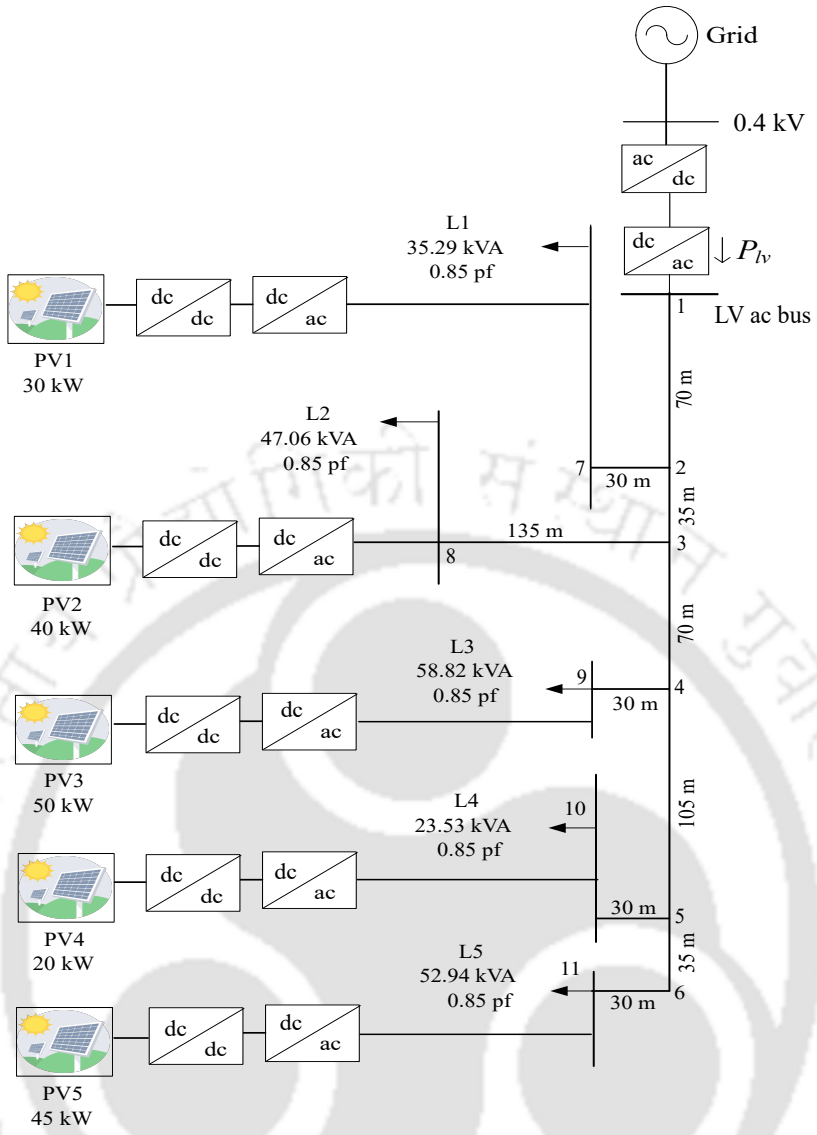

Fig. 4.1 Modified CIGRE benchmark residential distribution network .

The PV power profiles when the peak PV power is equal to the installed PV power is shown in Fig. 4.2(b) [166].

Now, the overview of the proposed voltage control method in the chosen grid-connected LV ac residential distribution system is discussed in following section.

4.2 OVERVIEW OF THE PROPOSED VOLTAGE CONTROL METHOD

The overview of the proposed control is shown in Fig. 4.3. It includes various steps to realize the minimization of voltage deviation over a day which are discussed as follows:

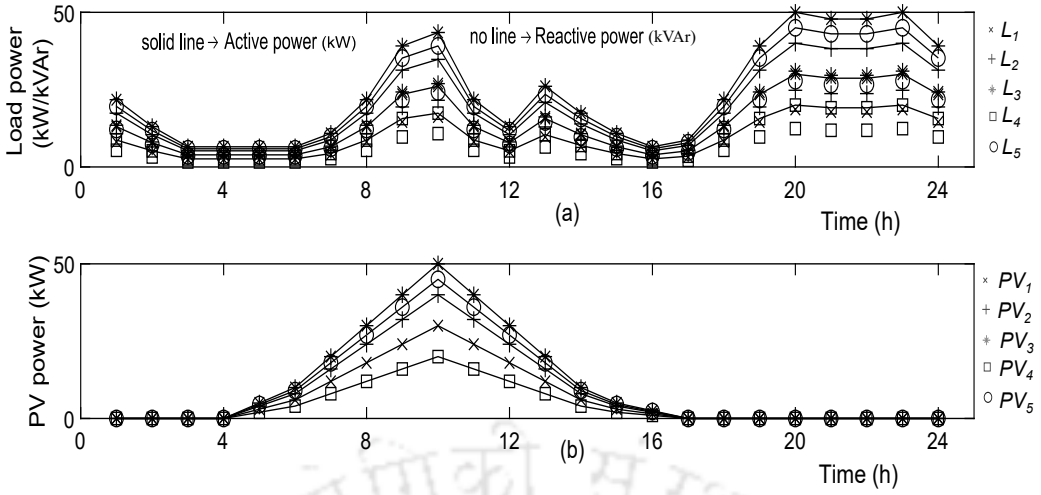

Fig. 4.2 Power profiles. (a) Load power profiles . (b) PV power profiles .

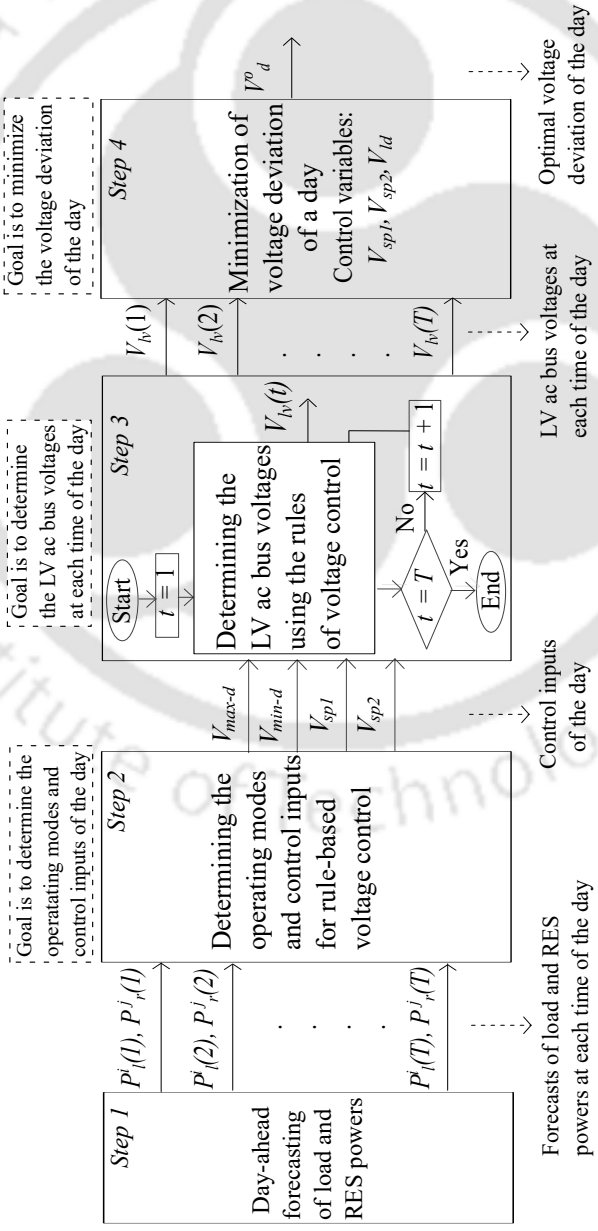

Fig. 4.3 Overview of the proposed voltage control method.

1. The first step is the day-ahead forecasting of load and RES powers. The day-ahead forecasts of load and RES powers are required to determine the operating modes and control inputs of the rule-based voltage control method. In recent years, several studies have been conducted for forecasting the load and RES power [142]. Data driven approaches for forecasting the RES and load power values have gained popularity due to the increased availability of monitoring data [143]. This monitoring data mainly includes weather forecast and historical energy usage data. Therefore, using the data driven approaches such as statistical and machine learning methods, the required day-ahead load and RES power can be forecasted [144]. In this work, it is assumed that these forecasts are available and the entire analysis carried out in this work is based on these day-ahead forecasts.

2. The second step is the determination of the operating modes of the back-to-back converter and control inputs for rule-based voltage control method. The operating modes of the back-to-back converter and control inputs for rule-based voltage control are determined using the load and PV power forecast curves of the day. The operating modes are chosen to mitigate the voltage rise and voltage drop in the distribution network.

   The control inputs for rule-based voltage control are considered as maximum, minimum voltage limits of the day, and voltage set points. These control inputs are same for the whole day which have to be determined only once per day.

3. The third step is the determination of the LV ac bus voltages using the rules of voltage control method. The rules of the voltage control method are formulated based on the control inputs which are obtained in Step 2 to decide the LV ac bus voltages over a day.

4. The fourth step is the determination of the optimal control inputs. The optimization problem is formulated to minimize the voltage deviation over a day while controlling the voltage set points and limit difference of the day. The control inputs corresponding to the optimal voltage set points and limit difference are considered as the optimal control inputs of the day.

These steps of the proposed method are discussed in detail in following sections.

4.3 DETERMINATION OF OPERATING MODES OF THE BACK-TO-BACK CONVERTER AND CONTROL INPUTS

The method of determination of operating modes of the back-to-back converter and control inputs for rule-based voltage control is discussed in this section.

4.3.1 Operating Modes of the Back-to-back Converter

The operating modes to mitigate the voltage rise and voltage drop are considered as follows:

1. **Voltage rise mitigation mode:** This mode is during the time when maximum bus voltage is more than the maximum bus voltage limit of the day i.e., $V_{max}(t) > V_{max-d}$.
2. **Voltage drop mitigation mode:** This mode is during the time when minimum bus voltage is less than the minimum bus voltage limit of the day i.e., $V_{min}(t) < V_{min-d}$.

Now, the determination of control inputs for rule-based voltage control method is explained as follows:

4.3.2 Control Inputs

The control inputs of maximum voltage limit of the day, minimum voltage limit of the day, voltage set point 1, voltage set point 2 are considered as discussed follows.

Maximum voltage limit of the day

The maximum voltage limit of the day is considered as the voltage value above which the LV ac bus voltage is changed to mitigate the voltage rise in the distribution system. Therefore, it is considered as the difference between the maximum voltage limit specified by the grid and a control variable known as the limit difference.

$$V_{max-d} = V_{max-g} - V_{ld}. \tag{4.3}$$

From ANSI C84.1 [137], V_{max-g} = 1.05 p.u. Therefore, the V_{max-d} is chosen from 1.0 p.u. to 1.05 p.u. as given follows:

$$1 \text{ p.u.} \leq V_{max-d} \leq 1.05 \text{ p.u.} \tag{4.4}$$

Minimum voltage limit of the day

The minimum voltage limit of the day is the voltage value below which the LV ac bus voltage is changed to mitigate the voltage drop in the distribution system. Therefore, it is considered as the sum of the minimum voltage limit specified by the grid and the limit difference.

$$V_{min-d} = V_{min-g} + V_{ld}. \tag{4.5}$$

From ANSI C84.1 [137], V_{min-g} = 0.95 p.u. Therefore, the V_{min-d} is chosen from 0.95 p.u. to 1.0 p.u. as given follows.

$$0.95 \text{ p.u.} \leq V_{min-d} \leq 1 \text{ p.u.} \tag{4.6}$$

The limit difference is varied from 0 p.u. to 0.05 p.u. in order to choose the V_{max-d} and V_{min-d} as per (4.4) and (4.6).

Voltage set point 1

The voltage set point 1 is the LV ac bus voltage to be maintained during the voltage rise mitigation mode. Therefore, it is chosen as a control variable which varies between the minimum voltage limit given by grid code and 1.0 p.u. as given follows.

$$0.95 \text{ p.u.} \leq V_{sp1} \leq 1 \text{ p.u} \tag{4.7}$$

Voltage set point 2

The voltage set point 2 is the LV ac bus voltage to be maintained during the voltage drop mitigation mode. Therefore, it is chosen as a control variable which varies between 1.0

p.u. and the maximum voltage limit given by grid code as given follows.

$$1 \text{ p.u.} \leq V_{sp2} \leq 1.05 \text{ p.u.}. \tag{4.8}$$

Now, the determination of LV ac bus voltage using the rules of proposed voltage control method is explained in following section.

4.4 DETERMINATION OF THE LV AC BUS VOLTAGES USING THE RULES OF VOLTAGE CONTROL METHOD

In literature, it is shown that the SBTSPBOC is a better voltage control method out of various set points based voltage control methods. In order to compare the proposed method with respect to SBTSPBOC, in this section the rules of SBTSPBOC voltage control method as well as the proposed method are discussed.

4.4.1 Switching Between Two Set Points Based on Current

In this method, depending on the LV ac bus current direction, the LV ac bus voltage is decided. The current direction at the LV ac bus is indicated by its corresponding direct axis current ($I_{d-lv}(t)$) direction. Thus $I_{d-lv}(t)$ is used to decide the required LV ac bus voltage. The negative $I_{d-lv}(t)$ indicates that the total load is less as compared to the RESs present in the distribution network which might lead to voltage rise violations. Therefore, if $I_{d-lv}(t)$ is negative, the $V_{lv}(t)$ is set to V_{sp1} to avoid any voltage rise violations. Similarly, the positive $I_{d-lv}(t)$ indicates that the total load is more as compared to the RESs present in the distribution network which might lead to voltage drop violations. Therefore, if $I_{d-lv}(t)$ is positive, the $V_{lv}(t)$ is set to V_{sp2} to avoid any voltage drop violations. It means that there are two rules in this method as given follows.

1. **Rule 1:** If the direct axis current of LV ac bus is negative, $V_{lv}(t)$ is set to V_{sp1} i.e., $V_{lv}(t) = V_{sp1}$.
2. **Rule 2:** If the direct axis current of LV ac bus is positive, $V_{lv}(t)$ is set to V_{sp2} i.e., $V_{lv}(t) = V_{sp2}$.

This rule-based voltage control method of SBTSPBOC is shown in Fig. 4.4.

4.4.2 Proposed Method of Voltage Control

In this method, depending on the maximum and minimum load bus voltages ($V_{max}(t)$ and $V_{min}(t)$), the LV ac bus voltage is decided. The maximum load bus voltage is the maximum of all the load bus voltages at each time. The minimum load bus voltage is the minimum of all the load bus voltages at each time. If maximum load bus voltage is more than the maximum voltage limit of the day, the LV ac bus voltage is set to voltage set points 1 to avoid voltage rise violations. Similarly, if minimum load bus voltage is less than the minimum voltage limit of the day, the LV ac bus voltage is set to voltage set point 2 to avoid voltage drop violations. If the maximum and minimum bus voltages are within their corresponding limits of the day, the LV ac bus voltage is not changed. Therefore, there are three rules as per this method. These are given as

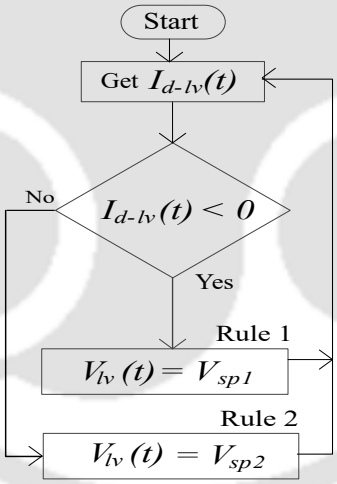

Fig. 4.4 Rule-based voltage control method of SBTSPBOC.

1. **Rule 1:** In voltage rise mitigation mode i.e., if maximum bus voltage is more than the maximum voltage limit of the day, $V_{lv}(t) = V_{sp1}$.
2. **Rule 2:** In voltage drop mitigation mode i.e., if minimum bus voltage is less than the minimum voltage limit of the day, $V_{lv}(t) = V_{sp2}$.
3. **Rule 3:** If the maximum and minimum bus voltages are within their respective limits, $V_{lv}(t)$ is not changed.

This proposed rule-based voltage control method is shown in Fig. 4.5. Now, the de-

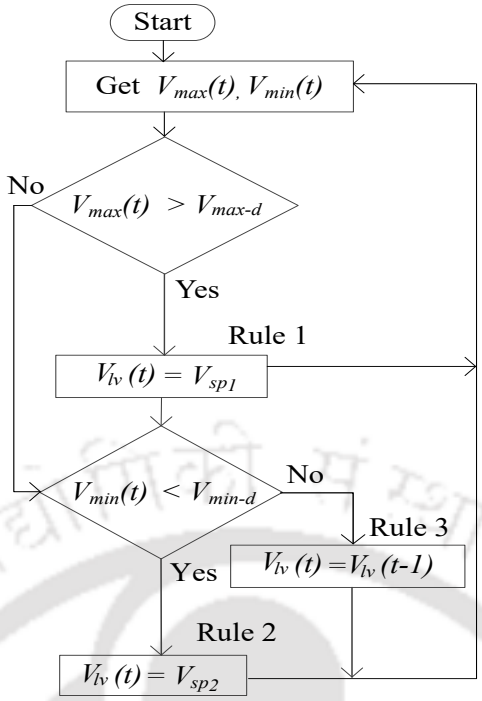

Fig. 4.5 Proposed rule-based voltage control method.

termination of optimal control inputs for optimizing the proposed rule-based voltage control method is discussed.

4.5 DETERMINATION OF OPTIMAL CONTROL INPUTS

The optimization problem formulation for determining the optimal control inputs and its solution method are discussed in this section.

4.5.1 Optimization Problem Formulation

The considered objective function and constraints are given as follows:

$$\text{minimize } f = \sum_{t=1}^{T} \sum_{i=1}^{N_b} (V_l^i(t) - V_{ref})^2. \tag{4.9}$$

subjected to

1. Power balance constraint

$$P_{lv}(t) = \sum_{i=1}^{n_l} P_l^i(t) + P_{loss}(t) - \sum_{j=1}^{n_r} P_{rc}^j(t). \tag{4.10}$$

2. Voltage magnitudes constraint

$$V_{min-g} < V_l^i((t) < V_{max-g} \tag{4.11}$$

Equation (4.9) indicates that the objective is to minimize the sum of all the residential load bus voltage deviations from V_{ref} for all the times of the day. Equation (4.10) shows the power balance constraint at LV ac bus by neglecting the power converters loss. Equation (4.11) indicates the constraints of load bus voltage magnitudes.

4.5.2 Solving the Optimization Problem

The considered problem is an optimal power flow problem. The backward forward sweep method is used for obtaining power flow solution. The considered objective function is a nonlinear function. Therefore, the proposed optimal control problem is solved using GA with ga solver in MATLAB. The method of solving the optimization problem using GA is explained in detail in Section 2.5 of Chapter 2. The default values are chosen for various parameters of GA, except for population size. The population size is an important parameter to choose. Because if it is small, the convergence might not be achieved. Therefore, population size is chosen based on the number of control variables. In case of proposed voltage control method, there are three control variables i.e., voltage set point 1, 2, and voltage limit difference (in case of voltage control method of SBTSPBOC, there are two control variables i.e., voltage set point 1 and 2). Further, in GA it is possible for different runs to provide different optimal values. Therefore, to avoid any sub-optimal solutions and guarantee global optimum solution, the population size is tuned such that multiple simulation runs converge precisely to the same value. Accordingly the population size is chosen as 30 in proposed voltage control method and chosen as 20 in voltage control method of SBTSPBOC. The control inputs corresponding to the optimal decision variables i.e., V^o_{max-d},V^o_{min-d}, V^o_{sp1}, and V^o_{sp2} are the optimal control inputs of the day for the proposed rule-based voltage control method.

4.6 PERFORMANCE INDICATORS

Performance indicators such as voltage rise margin (V_{rm}), voltage drop margin (V_{dm}), and average voltage deviation (V_{avg-d}) are developed to know the impact of voltage control methods. These are explained in this section.

Voltage Rise Margin

It is defined as the difference between the maximum voltage limit specified by the grid code (V_{max-g}) and worst maximum bus voltage in the distribution network. This is given as

$$V_{rm} = (V_{max-g} - V_{wmax}). \tag{4.12}$$

From (4.12), V_{rm} can be positive or negative depending on V_{wmax}. The more positive V_{rm} indicates a better system voltage profile (worst maximum bus voltage is close to 1.0 p.u.) and a higher possibility of increasing the PV penetration level. The negative V_{rm} indicates the voltage rise violation. Therefore, for effective voltage control method, the value of V_{rm} should be greater than or equal to zero ($V_{rm} \geq 0$).

Voltage Drop Margin

It is defined as the difference between the worst minimum bus voltage in the distribution network and minimum voltage limit specified by the grid code (V_{min-g}). This is given by

$$V_{dm} = (V_{wmin} - V_{min-g}). \tag{4.13}$$

From (4.13), V_{dm} can be positive or negative depending on V_{wmin}. The more positive V_{dm} indicates a better system voltage profile (worst minimum bus voltage is close to 1.0 p.u.) and a higher possibility of increasing the loading level. The negative V_{dm} indicates the voltage drop violation. Therefore, for effective voltage control method, the value of V_{dm} should be greater than or equal to zero ($V_{dm} \geq 0$).

Therefore, both V_{rm} and V_{dm} should be positive for no voltage violations in the network.

Average Voltage Deviation

It is important to maintain the voltages at all buses close to reference voltage (V_{ref}) of 1.0 p.u. for all the time. A performance indicator known as average voltage deviation is considered which is defined as the average of residential bus voltage deviations from

1.0 p.u. over a day as given in (4.14).

$$V_{avg-d} = \frac{\sum_{t=1}^{T}\sum_{i=1}^{N_b}|V_i(t) - V_{ref}|}{T \times N_b}. \tag{4.14}$$

For effective voltage control method, the value of V_{avg-d} should be low. This indicates better system voltage profile (bus voltages are close to 1.0 p.u.).

Now, the simulation results of the proposed optimal rule-based voltage control method are discussed in following section.

4.7 SIMULATION RESULTS

The voltage control methods are tested on the considered case study in MATLAB on a 64-bit operating system PC with a processor of Intel(R) Core(TM) i5-6500 CPU @ 3.2 GHz.

It is known that there exist both voltage rise and voltage drop issues in distribution systems. Therefore, the proposed method is validated for following cases which cause both voltage rise and voltage drop issues.

Case 1: During less load demand and less PV energy availability

Case 2: During more load demand and less PV energy availability

Case 3: During less load demand and more PV energy availability

Case 4: During more load demand and more PV energy availability

The loads are considered to be operating at a lagging power factor of 0.85 at all the times of the day. The simulation results obtained for these cases are discussed as follows:

4.7.1 Case 1

In this case, the peak load power is considered as 0.2 times the rated peak load power and peak PV power is considered as 0.2 times the installed PV power.

Without voltage control

In this case, the LV ac bus voltage is always maintained at 1.0 p.u. as shown in Fig. 4.6(a). For this LV ac bus voltage, the resulting load bus voltage profiles over a day are shown in Fig. 4.6(b). The V_{rm}, V_{dm} and V_{avg-d} are determined as 0.046 p.u., 0.033 p.u., and 0.005 p.u., respectively. The positive values of V_{rm} and V_{dm} indicate that there are no voltage rise and voltage drop violations in the distribution network. This is because in this case there is less demand and less PV power over a day.

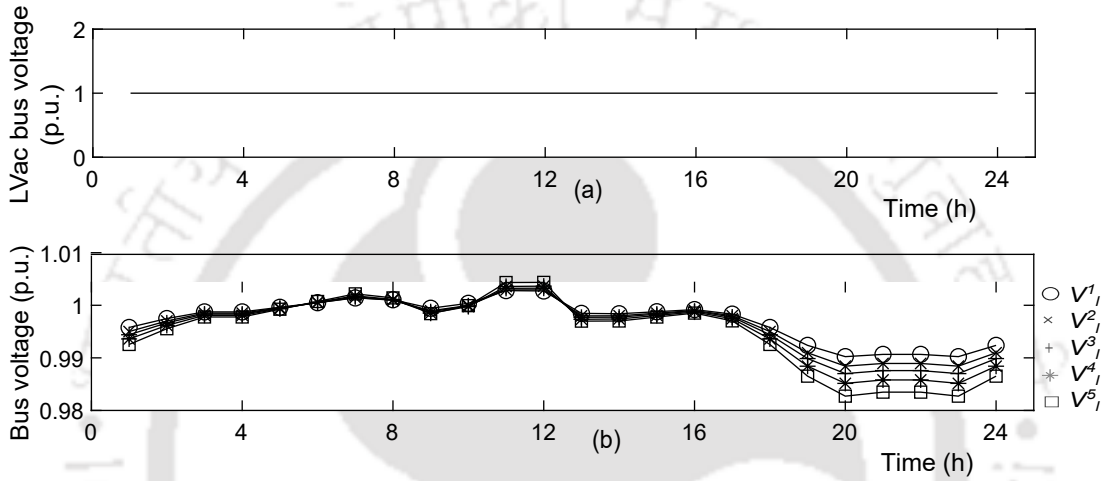

Fig. 4.6 Case 1 without voltage control. (a) LV ac bus voltage. (b) Load bus voltages.

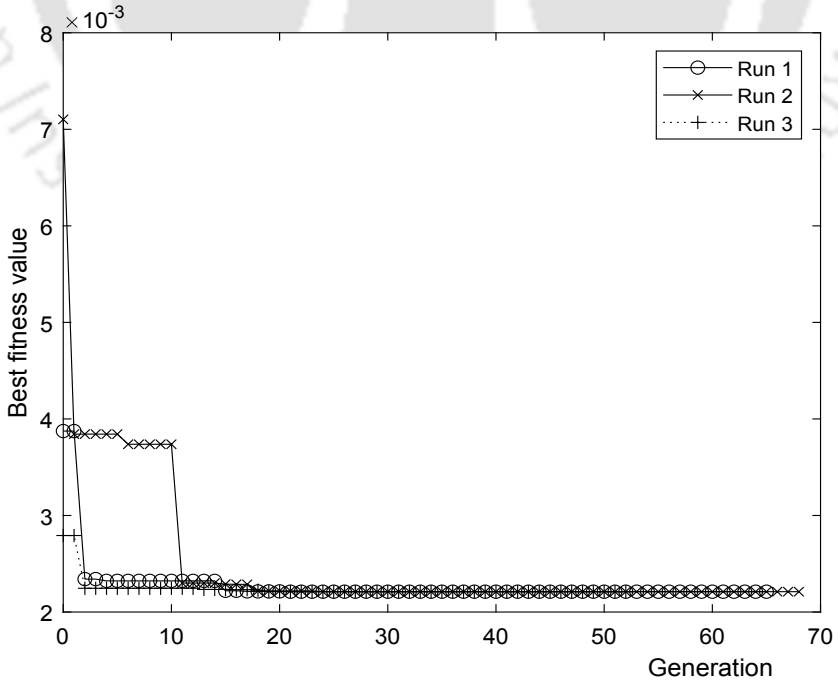

Fig. 4.7 Best fitness values obtained using GA in Case 1 with SBTSPBOC.

Switching between two set points based on current

For this method, the optimal voltage set points 1 and 2 are determined using GA. The best fitness values plot of GA is shown in Fig. 4.7. The optimization is terminated when the average change in the fitness value become less than function tolerance of 10^{-6}. It indicates that the best fitness value is 0.002 p.u. The corresponding voltage set points are optimal voltage set points 1 and 2 which are determined as 0.99 p.u. and 1.006 p.u. respectively. As per the voltage control method, the LV ac bus voltage is chosen as one of these set points as shown in Fig. 4.8(a). For this LV ac bus voltage, the resulting load bus voltage profiles over a day are shown in Fig. 4.8(b). The V_{rm}, V_{dm} and V_{avg-d} are determined as 0.04 p.u., 0.04 p.u., and 0.0035 p.u., respectively. The positive values of V_{rm} and V_{dm} indicate that there are no voltage rise and voltage drop violations in the distribution network. The V_{rm} and V_{dm} values are more as compared to the case of without voltage control. Moreover, the V_{avg-d} is less as compared to the case of without voltage control. These indicate the improved voltage profile with the voltage control method as compared to the case of without voltage control.

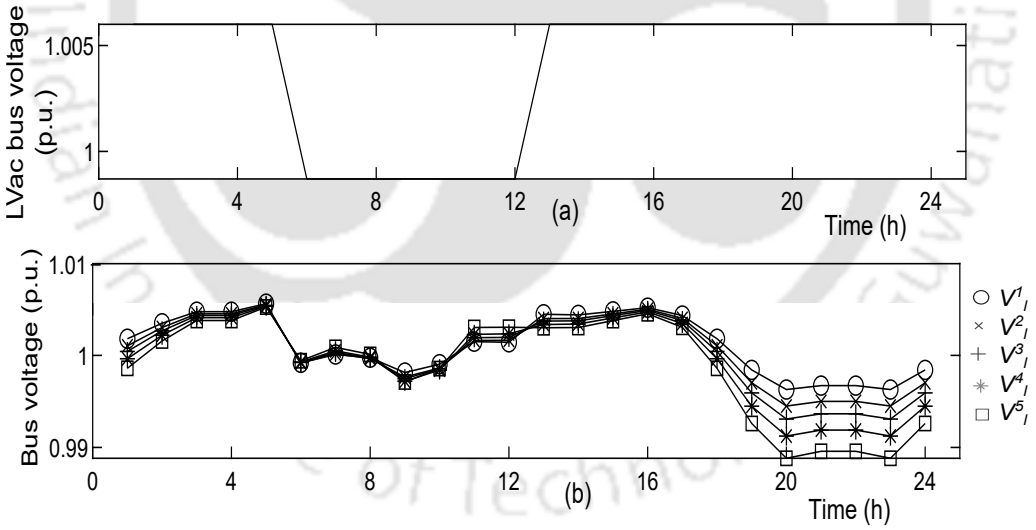

Fig. 4.8 Case 1 with SBTSPBOC. (a) LV ac bus voltage. (b) Load bus voltages.

Proposed method

For this method, the optimal voltage set points 1, 2 and voltage limit difference are determined using GA. The best fitness values plot of GA is shown in Fig. 4.9. The optimization is terminated when the average change in the fitness value become less than function tolerance of 10^{-6}. It indicates that the best fitness value is 0.0009 p.u.

The corresponding voltage set points and voltage limit difference are optimal voltage set points 1, 2 and optimal voltage limit difference which are determined as 0.97 p.u., 1.012 p.u. and 0.04 p.u., respectively. The optimal maximum and minimum voltage limits of the day corresponding to the optimal limit difference are 1.009 p.u. and 0.99 p.u., respectively. Using these control inputs i.e., maximum/minimum voltage limits of the day and set points, the LV ac bus voltage is maintained as per the voltage control method as shown in Fig. 4.10(a). For this LV ac bus voltage, the resulting load bus voltage profiles over a day are shown in Fig. 4.10(b). The V_{rm}, V_{dm} and V_{avg-d} are determined as 0.045 p.u., 0.043 p.u., and 0.002 p.u., respectively. The positive values of V_{rm} and V_{dm} indicate that there are no voltage rise and voltage drop violations in the distribution network. The V_{rm} and V_{dm} values are more as compared to the case of without voltage control and voltage control method of SBTSBOC. Moreover, V_{avg-d} is less as compared to the case of without voltage control and SBTSPBOC methods. These performance indicators show the improved voltage profile with this voltage control method as compared to the case of without voltage control and SBTSPBOC methods.

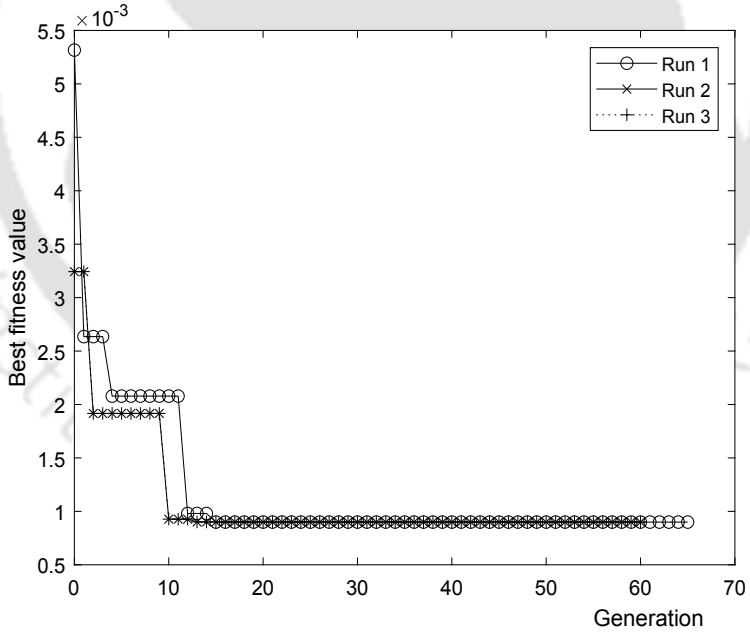

Fig. 4.9 Best fitness values obtained using GA in Case 1 with proposed method.

The above discussed performance indicators for the case of without voltage control, SBTSPBOC, and proposed methods are given in Table 4.1.

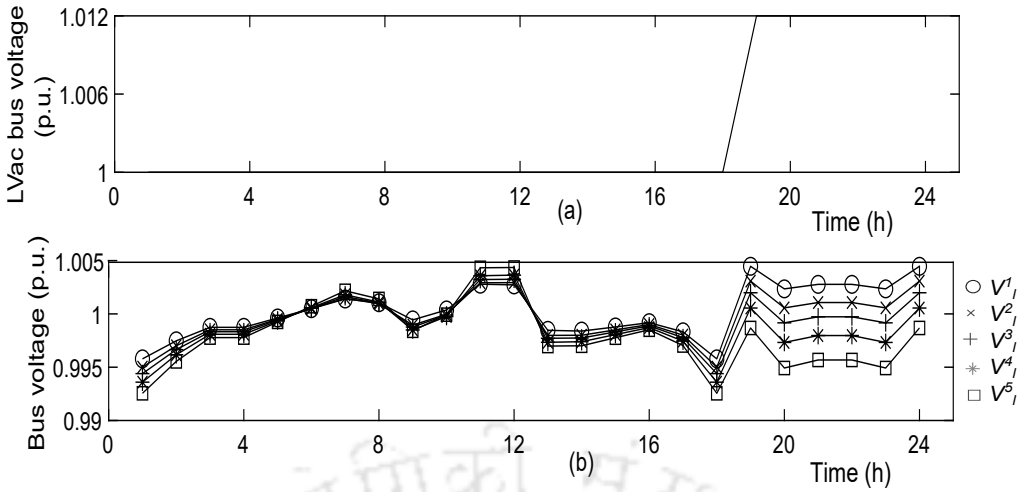

Fig. 4.10 Case 1 with proposed method. (a) LV ac bus voltage. (b) Load bus voltages.

Table 4.1 Performance Indicators for Case 1 in p.u.

Performance indicator	Without voltage control	SBTSPBOC [87]	Proposed
V_{rm}	0.046	0.044	0.045
V_{dm}	0.033	0.04	0.043
V_{avg-d}	0.005	0.0035	0.0022

4.7.2 Case 2

In this case, the peak load power is considered as the rated peak load power and peak PV power is considered as 0.2 times the installed PV power.

Without voltage control

In this case, the LV ac bus voltage is always maintained at 1.0 p.u. as shown in Fig. 4.11(a). For this LV ac bus voltage, the resulting load bus voltage profiles over a day are shown in Fig. 4.11(b). The V_{rm}, V_{dm} and V_{avg-d} are determined as 0.05 p.u., -0.04 and 0.03 p.u., respectively. The positive values of V_{rm} and V_{dm} indicate that there are no voltage rise and voltage drop violations in the distribution network. This is because in this case there is increased load demand as compared to Case 1.

Switching between two set points based on current

For this method, the best fitness value using GA is determined as 0.073 p.u. The corresponding voltage set points are optimal voltage set points 1 and 2 which are determined

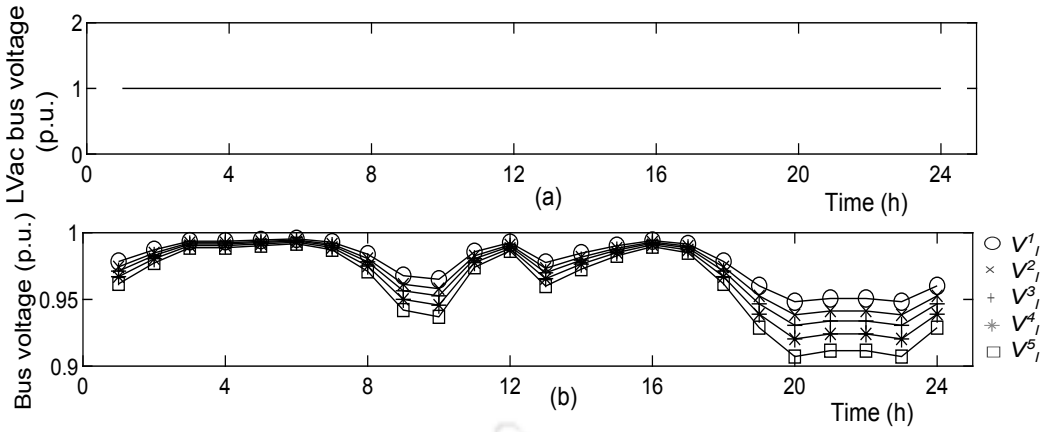

Fig. 4.11 Case 2 without voltage control. (a) LV ac bus voltage. (b) Load bus voltages.

as 0.97 p.u. and 1.04 p.u., respectively. As per the voltage control method, the LV ac bus voltage is chosen as one of these set points as shown in Fig. 4.12(a). For this LV ac bus voltage, the resulting load bus voltage profiles over a day are shown in Fig. 4.12(b). The V_{rm}, V_{dm} and V_{avg-d} are determined as 0.016 p.u., 0.00005 p.u., and 0.02 p.u., respectively. The positive values of V_{rm} and V_{dm} indicate that there are no voltage rise and voltage drop violations in the distribution network. The V_{rm} and V_{dm} values are more as compared to the case of without voltage control. Moreover, the V_{avg-d} is less as compared to the case of without voltage control. These indicate the improved voltage profile with the voltage control method as compared to the case of without voltage control.

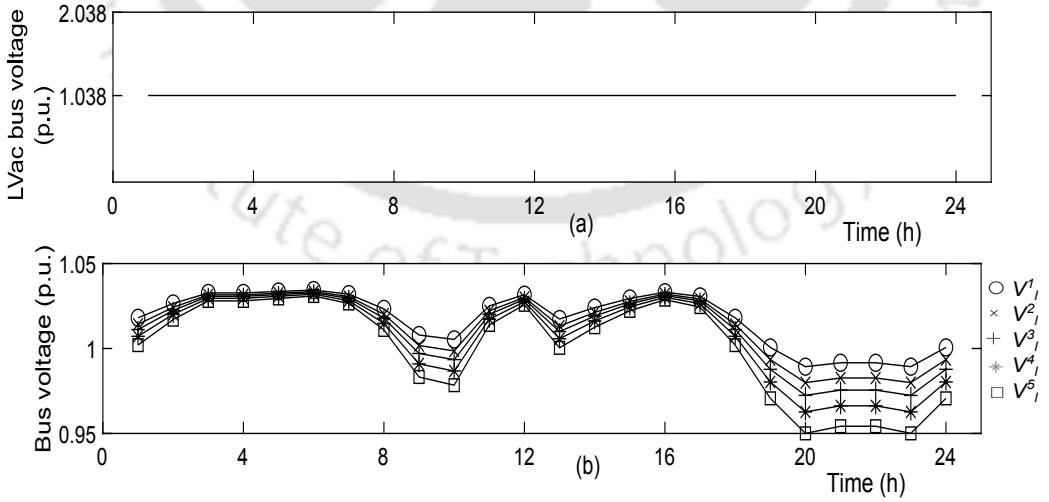

Fig. 4.12 Case 2 with SBTSPBOC. (a) LV ac bus voltage. (b) Load bus voltages.

Proposed method

For this method, the optimal voltage set points 1, 2 and voltage limit difference are determined using GA. The best fitness value is determined as 0.038 p.u. The corresponding voltage set points and voltage limit difference are optimal voltage set points 1, 2 and optimal voltage limit difference which are determined as 1.0 p.u., 1.049 p.u., and 0.021 p.u., respectively. The optimal maximum and minimum voltage limits of the day corresponding to the optimal limit difference are 1.03 p.u. and 0.97 p.u., respectively. Using these control inputs i.e., maximum/minimum voltage limits of the day and set points, the LV ac bus voltage is maintained as per the voltage control method as shown in Fig. 4.13(a). For this LV ac bus voltage, the resulting load bus voltage profiles over a day are shown in Fig. 4.13(b). The V_{rm}, V_{dm} and V_{avg-d} are determined as 0.02 p.u., 0.011 p.u., and 0.014 p.u., respectively. The positive values of V_{rm} and V_{dm} indicate that there are no voltage rise and voltage drop violations in the distribution network. The V_{rm} and V_{dm} values are more as compared to the case of without voltage control and voltage control method of SBTSBOC. Moreover, the V_{avg-d} is less as compared to the case of without voltage control and SBTSPBOC methods. These performance indicators show the improved voltage profile with this voltage control method as compared to the case of without voltage control and SBTSPBOC methods.

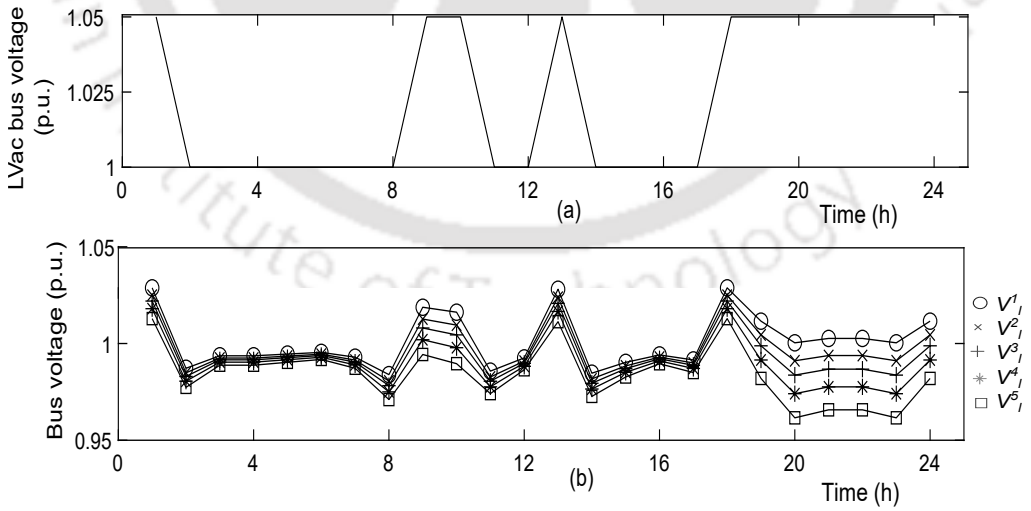

Fig. 4.13 Case 2 with proposed method. (a) LV ac bus voltage. (b) Load bus voltages.

The above discussed performance indicators for the case of without voltage control, SBTSPBOC, and proposed methods are given in Table 4.2.

Table 4.2 Performance Indicators for Case 2 in p.u.

Performance indicator	Without voltage control	SBTSPBOC [87]	Proposed
V_{rm}	0.055	0.016	0.02
V_{dm}	-0.043	0.00005	0.01
V_{avg-d}	0.03	0.02	0.014

4.7.3 Case 3

In this case, the peak load power is considered as 0.2 times the rated peak load power and peak PV power is considered as the installed PV power.

Without voltage control

In this case, the LV ac bus voltage is always maintained at 1.0 p.u. as shown in Fig. 4.14(a). For this LV ac bus voltage, the resulting load bus voltage profiles over a day are shown in Fig. 4.14(b). The V_{rm}, V_{dm} and V_{avg-d} are determined as -0.006 p.u., 0.033 p.u., and 0.027 p.u., respectively. The negative value of V_{rm} indicates that there are voltage rise violations in the distribution network. However, the positive value of V_{dm} indicates that there are no voltage drop violations in the distribution network. This is because in this case there is increased PV power available as compared to Case 1.

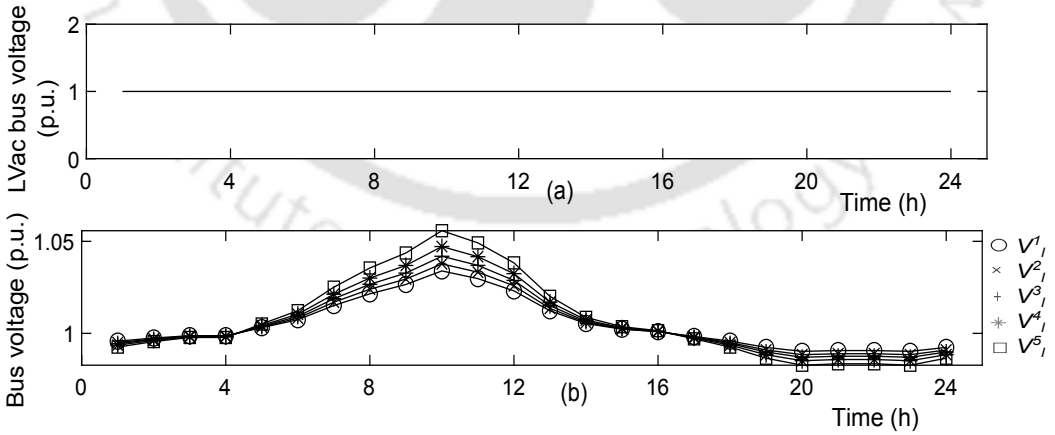

Fig. 4.14 Case 3 without voltage control. (a) LV ac bus voltage. (b) Load bus voltages.

Switching between two set points based on current

For this method, the best fitness value using GA is determined as 0.015 p.u. The corresponding voltage set points are optimal voltage set points 1 and 2 which are determined

as 0.98 p.u., and 1.008 p.u., respectively. As per the voltage control method, the LV ac bus voltage is chosen as one of these set points as shown in Fig. 4.15(a). For this LV ac bus voltage, the resulting load bus voltage profiles over a day are shown in Fig. 4.15(b). The V_{rm}, V_{dm} and V_{avg-d} are determined as 0.0127 p.u., 0.03 p.u., and 0.009 p.u., respectively. The positive values of V_{rm} and V_{dm} indicate that there are no voltage rise and voltage drop violations in the distribution network. The V_{rm} and V_{dm} values are more as compared to the case of without voltage control. Moreover, the V_{avg-d} is less as compared to the case of without voltage control. These indicate the improved voltage profile with the voltage control method as compared to the case of without voltage control.

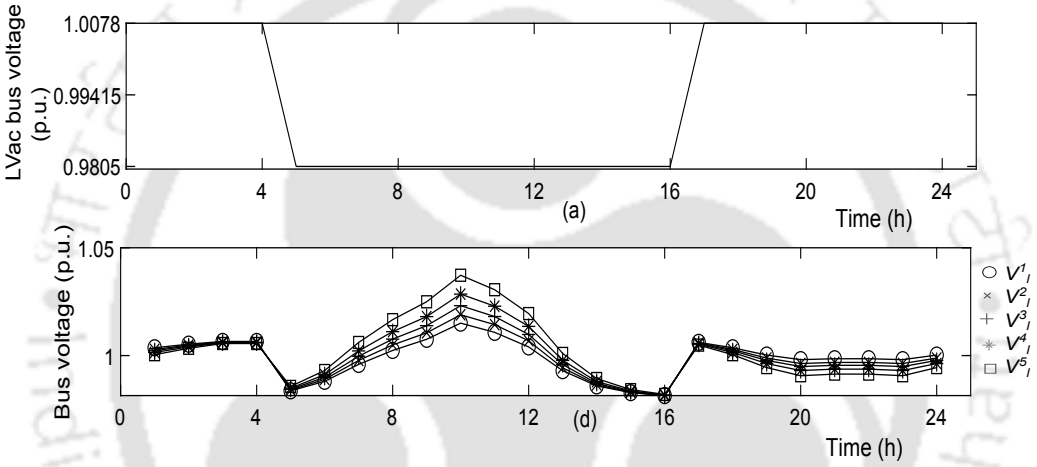

Fig. 4.15 Case 3 with SBTSPBOC. (a) LV ac bus voltage. (b) Load bus voltages.

Proposed method

For this method, the optimal voltage set points 1, 2 and voltage limit difference are determined using GA. The best fitness value is determined as 0.0078 p.u. The corresponding voltage set points and voltage limit difference are optimal voltage set points 1, 2 and optimal voltage limit difference which are determined as 0.97 p.u., 1.006 p.u. and 0.032 p.u., respectively. The optimal maximum and minimum voltage limits of the day corresponding to the optimal limit difference are 1.02 p.u. and 0.98 p.u., respectively. Using these control inputs i.e., maximum/minimum voltage limits of the day and set points, the LV ac bus voltage is maintained as per the voltage control method as shown in Fig. 4.16(a). For this LV ac bus voltage, the resulting load bus voltage profiles over a day are shown in Fig. 4.16(b). The V_{rm}, V_{dm} and V_{avg-d} are determined as 0.023 p.u.,

0.03 p.u., and 0.006 p.u., respectively. The positive values of V_{rm} and V_{dm} indicate that there are no voltage rise and voltage drop violations in the distribution network. The V_{rm} and V_{dm} values are more as compared to the case of without voltage control and voltage control method of SBTSBOC. Moreover, the V_{avg-d} is less as compared to the case of without voltage control and SBTSPBOC methods. These performance indicators show the improved voltage profile with this voltage control method as compared to the case of without voltage control and SBTSPBOC methods.

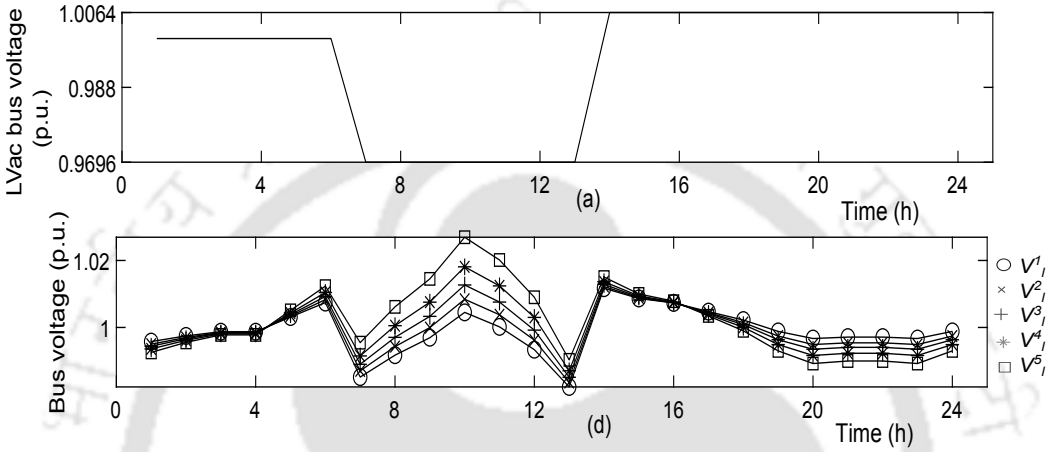

Fig. 4.16 Case 3 with proposed method. (a) LV ac bus voltage. (b) Load bus voltages.

The above discussed performance indicators for the case of without voltage control, SBTSPBOC, and proposed methods are given in Table 4.3.

Table 4.3 Performance Indicators for Case 3 in p.u.

Performance indicator	Without voltage control	SBTSPBOC [87]	Proposed
V_{rm}	-0.006	0.013	0.023
V_{dm}	0.033	0.03	0.03
V_{avg-d}	0.027	0.009	0.006

4.7.4 Case 4

In this case, the peak load power is considered as the rated peak load power and peak PV power is considered as the installed PV power.

Without voltage control

In this case, the LV ac bus voltage is always maintained at 1.0 p.u. as shown in Fig. 4.17(a). For this LV ac bus voltage, the resulting load bus voltage profiles over a day are shown in Fig. 4.17(b).

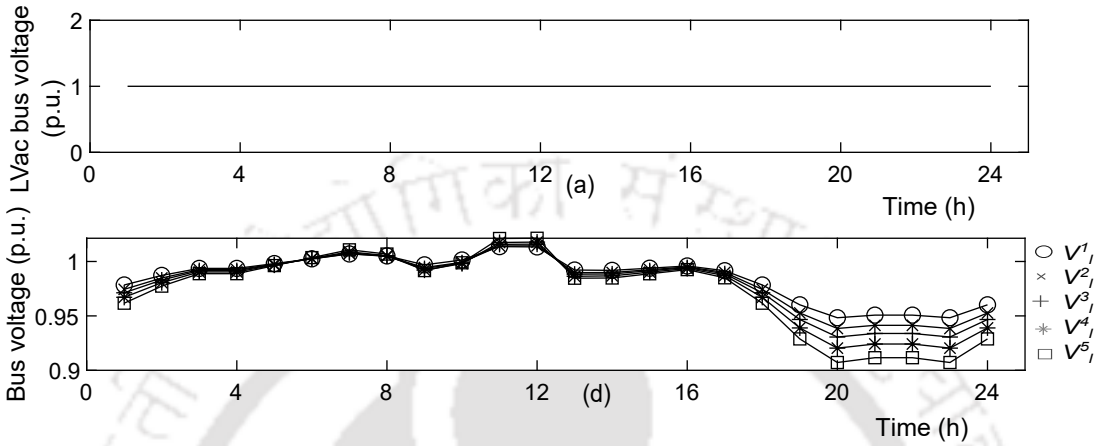

Fig. 4.17 Case 4 without voltage control. (a) LV ac bus voltage. (b) Load bus voltages.

The V_{rm}, V_{dm} and V_{avg-d} are determined as 0.029 p.u., -0.043 p.u., and 0.025 p.u., respectively. The positive value of V_{rm} indicates that there are no voltage rise violations in the distribution network. This is because in this case the more PV power is compensated with the more load power. However, the negative value of V_{dm} indicates that there are voltage drop violations in the distribution network. This is because during the peak load hours there is no PV power available for compensation.

Switching between two set points based on current

For this method, the best fitness value using GA is determined as 0.065 p.u. The corresponding voltage set points are optimal voltage set points 1 and 2 which are determined as 0.99 p.u. and 1.04 p.u. respectively. As per the voltage control method, the LV ac bus voltage is chosen as one of these set points as shown in Fig. 4.18(a). For this LV ac bus voltage, the resulting load bus voltage profiles over a day are shown in Fig. 4.18(b). The V_{rm}, V_{dm} and V_{avg-d} are determined as 0.013 p.u., 0.00005 p.u., and 0.02 p.u., respectively. The positive values of V_{rm} and V_{dm} indicate that there are no voltage rise and voltage drop violations in the distribution network. The V_{rm} and V_{dm} values are more as compared to the case of without voltage control. Moreover, the V_{avg-d} is less as compared to the case of without voltage control. These indicate the improved volt-

age profile with the voltage control method as compared to the case of without voltage control.

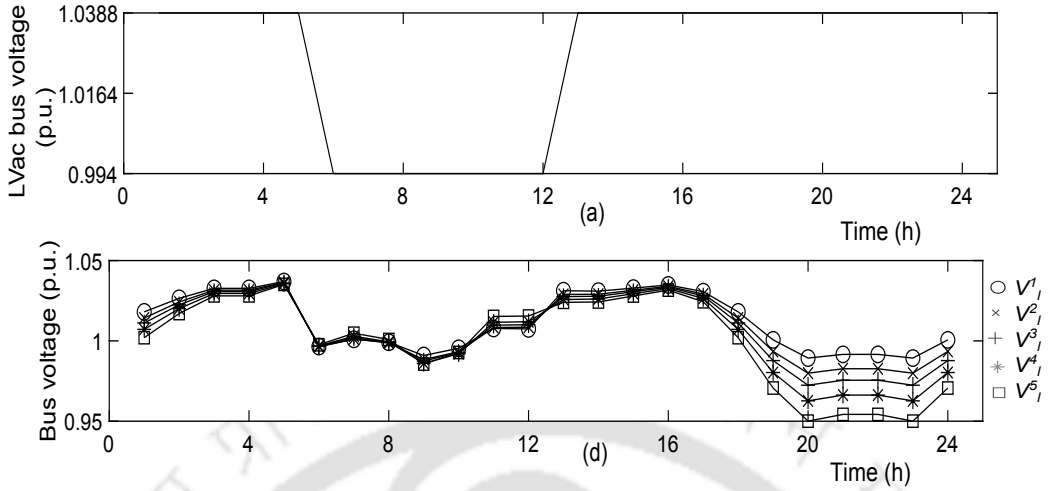

Fig. 4.18 Case 4 with SBTSPBOC. (a) LV ac bus voltage. (b) Load bus voltages.

Proposed method

For this method, the optimal voltage set points 1, 2 and voltage limit difference are determined using GA. The best fitness value is determined as 0.03 p.u. The corresponding voltage set points and voltage limit difference are optimal voltage set points 1, 2 and optimal voltage limit difference which are determined as 0.99 p.u., 1.05 p.u., and 0.008 p.u., respectively. The optimal maximum and minimum voltage limits of the day corresponding to the optimal limit difference are 1.042p.u. and 0.96 p.u., respectively. Using these control inputs i.e., maximum/minimum voltage limits of the day and set points, the LV ac bus voltage is maintained as per the voltage control method as shown in Fig. 4.19(a). For this LV ac bus voltage, the resulting load bus voltage profiles over a day are shown in Fig. 4.19(b). The V_{rm}, V_{dm} and V_{avg-d} are determined as 0.03 p.u., 0.012 p.u., and 0.012 p.u., respectively. The positive values of V_{rm} and V_{dm} indicate that there are no voltage rise and voltage drop violations in the distribution network. The V_{rm} and V_{dm} values are more as compared to the case of without voltage control and voltage control method of SBTSBOC. Moreover, the V_{avg-d} is less as compared to the case of without voltage control and SBTSPBOC methods. These performance indicators show the improved voltage profile with this voltage control method as compared to the case of without voltage control and SBTSPBOC methods. The above discussed performance indicators for the case of without voltage control, SBTSPBOC, and proposed methods

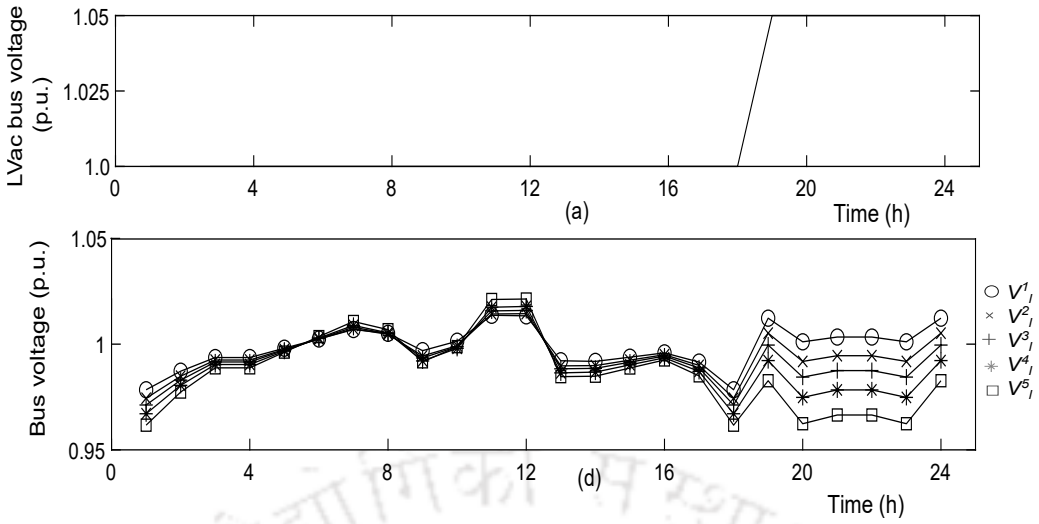

Fig. 4.19 Case 4 with proposed method. (a) LV ac bus voltage. (b) Load bus voltages.

are given in Table 4.4.

Table 4.4 Performance Indicators for Case 4 in p.u.

Performance indicator	Without voltage control	SBTSPBOC [87]	Proposed
V_{rm}	0.03	0.013	0.03
V_{dm}	-0.04	0.00005	0.01
V_{avg-d}	0.025	0.02	0.012

4.8 CONCLUSIONS

In this chapter, an optimal rule-based voltage control method is proposed considering maximum and minimum voltages limits of the day. The proposed method is tested for different possible cases of load and PV power profiles. The proposed method is compared with the method of switching between two set points based on current. The obtained results have shown that the voltage rise and voltage drop margins are more with proposed method as compared to switching between two set points based on current in all the cases. This indicates that the PV penetration and loading levels in distribution network can be increased to a higher level with proposed method as compared to switching between two set points based on current. Further, it is observed that the average voltage deviation reduction in the range of 20.33%-67.78% is achieved using the switching between two set points based on current with respect to the case of no voltage control. However, the average voltage deviation reduction in the range of

51.63%-75.56% is achieved using the proposed method with respect to the case of no voltage control. This indicates that the voltage profile is significantly improved with the proposed method as compared to switching between two set points based on current.

CHAPTER 5

OPTIMAL RULE-BASED PEAK SHAVING ALONG WITH VOLTAGE CONTROL AND ITS IMPACT ON ISOLATED DG-BESS-PV-WIND DISTRIBUTION SYSTEM

In Chapter 2, the optimal rule-based peak shaving method is proposed considering the day-ahead load and PV power profiles as inputs. The grid peak power over a day is minimized while optimally controlling BESS irrespective of the energy price profiles i.e., the energy price is not considered as input while controlling the BESS. In Chapter 3, the optimal rule-based DR method is proposed considering the day-ahead energy price (both buying and selling energy price) profiles along with load and PV power profiles as inputs. The energy consumption cost over a day is minimized while controlling the BESS. In both the Chapters 2 and 3, the LV ac bus voltage is maintained at 1.0 p.u. irrespective of the load and RES power variation over a day. To show the impact of optimal control of LV ac bus voltage, an optimal rule-based voltage control method is proposed in Chapter 4 considering the day-ahead load and PV power profiles as inputs. The voltage deviation over a day is minimized while controlling LV ac bus voltage using a back-to-back converter as smart power converter. In Chapters 2-4, the possibility of reactive power control in LV distribution systems is not discussed. Moreover, the energy management control methods are proposed and tested on grid-connected systems.

In this chapter, to show the impact of optimal control of the BESS along with the optimal control of LV ac bus voltage, and reactive power control of RES converters, an isolated distribution system is considered. The isolated MGs are important to support the loads which are not connected to utility grid supply [167]. The isolated MGs depend on DGs for power supply due to their low installation cost, simple and reliable operation. However, the high operating cost is the main disadvantage of DGs which depends on its fuel consumption. The use of RESs and BESSs is encouraged to avoid high operating cost of DGs [168]. In DG based systems, it is not sufficient to reduce the power

requirement of the system in order to reduce the fuel consumption of DG. Because the fuel consumption depends on the rating of DG along with the power requirement [16]. The rating of DG can be reduced by the peak shaving method. Therefore, it is possible to reduce the fuel consumption of DG using proposed peak shaving method. However, there are certain limitations in the proposed rule-based peak shaving method which is discussed in Chapter 2 as given follows.

1. The battery charge/discharge efficiencies and its power limits are not considered while determining the control inputs and formulating the rules of the proposed control method.
2. The load and RES powers are used as different inputs for deciding the charge and discharge modes of the battery. Accordingly, the control inputs are determined and the rules of the peak shaving method are formulated. These are not applicable when there is only one input power such as net load power at a bus is available (e.g. DG supplying the LV ac bus power requirement).

Consideration of charge/discharge efficiencies, power limits of the battery, and availability of one input power requires modifications to the rule-based peak shaving method as discussed in Chapter 2. Accordingly, in this chapter the modified rule-based peak shaving method is discussed i.e., the charge/discharge modes of the battery, the control inputs and the rules of the peak shaving method are modified. Further, the impact of the peak shaving method in a DG supplied MG is not discussed in the existing literature. To fill this research gap, the impact of the proposed peak shaving method on DG rating, fuel consumption of DG, and self consumption rate of the system is presented in this chapter. In summary, the contributions of this chapter are as follows:

1. To propose an optimal rule-based peak shaving method using BESS while minimizing the LV ac bus power using smart power converters.
2. To know the impact of the proposed optimal rule-based peak shaving method on the DG rating, fuel consumption of DG over a day and self consumption rate of the system.

The remainder of the chapter is organized as follows: The chosen system is described in Section 5.1. Then, the overview of the proposed control is presented in Section 5.2.

Later, the slave level optimization for minimizing LV ac bus demand is explained in Section 5.3. The determination of operating modes of the battery and control inputs of the rule-based peak shaving method is discussed in Section 5.4. Further, the determination of battery schedules and optimal control inputs is explained in Section 5.5 and 5.6, respectively. The results and conclusions are presented in Section 5.7 and 5.8, respectively.

5.1 SYSTEM DESCRIPTION

The chosen isolated DG supplied MG system is shown in Fig 5.1. The MG represents the modified CIGRE residential distribution system [169], [157]. The resistance and reactance of lines are chosen as per [157]. The different components of the system are discussed as follows:

1. **Loads:** There are different residential loads L1-L5 connected at bus 7, 8, 9, 10 and 11, respectively. The constant power loads are considered with an operating power factor of 0.85 lagging.
2. **Renewable energy sources**: Wind power sources Wind 1, Wind 2 and Wind 3 are present at bus 8, 9 and 11, respectively. The PV source is connected at bus 10. These RESs are connected through power converters to the load terminals. The dc/ac power converters which are used to connect RESs to the LV ac system i.e., WC1, WC2, PVC and WC3 are considered as RES converters. The RES converters are operated in grid-following mode to maintain the required active/reactive powers. The active power of the RES converters i.e., P_{rc}^{j} is considered the same as the maximum power point (MPP) power available from the RESs. The Q_{rc}^{j} is chosen optimally which will be discussed in following sections. The power balance equation at the LV ac bus with load and RES converters powers is given in (5.1).

$$P_{lv}(t) = \sum_{i=1}^{n_l} P_l^i(t) + P_{loss}(t) - \sum_{j=1}^{n_r} P_{rc}^j(t) \tag{5.1}$$

where t represents the time interval $[(t-1)\times T_c, t\times T_c]$ with T_c = 1 hour. The P_{lv} is used for obtaining LV ac bus power demand and injecting powers.

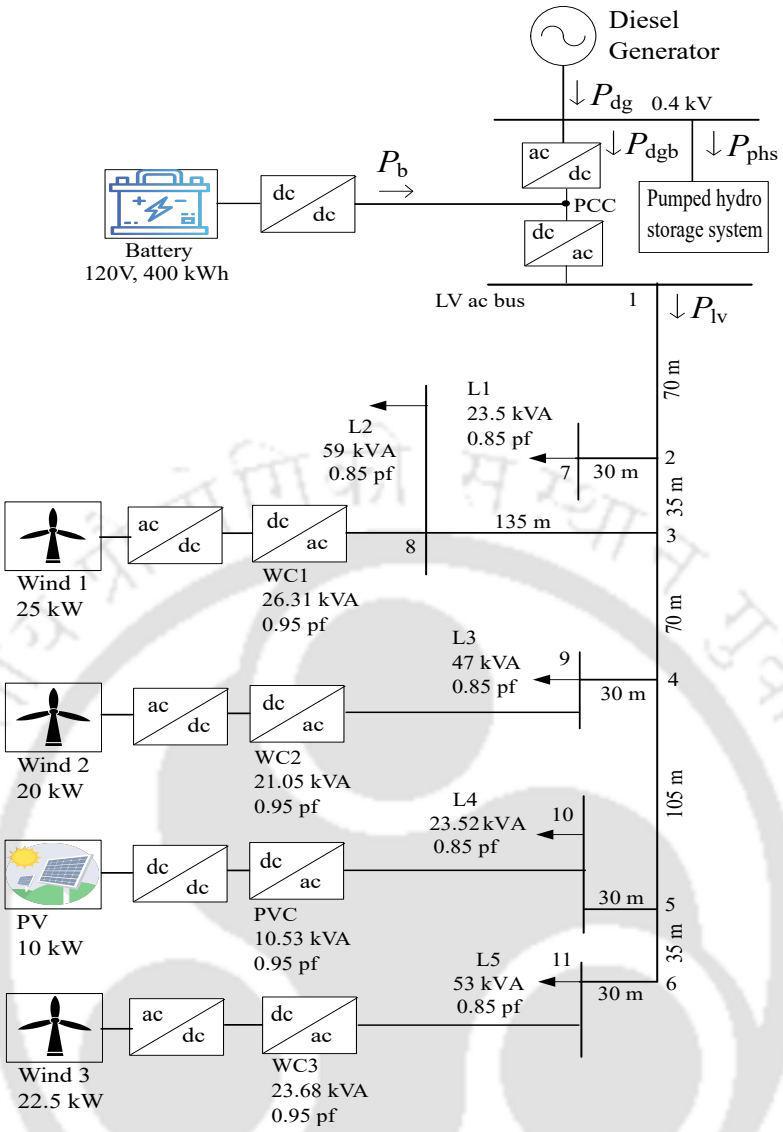

Fig. 5.1 Isolated DG supplied MG system .

The P_{lvd} is given in (5.2),

$$\begin{aligned} P_{lvd}(t) &= P_{lv}(t),\ P_{lv} > 0 \\ &= 0,\ \text{otherwise.} \end{aligned} \tag{5.2}$$

The P_{lvi} is given in (5.3),

$$\begin{aligned} P_{lvi}(t) &= -P_{lv}(t),\ P_{lv} \leq 0 \\ &= 0,\ \text{otherwise.} \end{aligned} \tag{5.3}$$

3. **Back-to-back converter:** The back-to-back converter operating in grid forming mode is used to maintain the voltage and frequency at the LV ac bus as per the requirement. In this chapter, the LV ac bus voltage is optimally controlled. This

will be discussed in following sections.

4. **Battery energy storage system**: The battery is connected at the PCC i.e., dc bus of the back-to-back converter through a dc-dc converter. This converter is considered to be operating in grid following mode to maintain its power as per the required charge/discharge schedules. The P_b is given as follows:

$$\begin{aligned} P_b(t) &= -P_{b-c}(t)/e_c,\ \forall t \in t_c \\ &= P_{b-d}(t) \times e_d,\ \forall t \in t_d. \end{aligned} \tag{5.4}$$

The charge/discharge schedules of the battery are obtained optimally using the proposed optimal rule-based peak shaving method.

5. **Diesel generator**: The DG is used for balancing the deficit demand of the distribution system. It is connected to ac/dc converter of the back-to-back converter. The bus to which DG is connected is called as DG bus. The DG bus power i.e., $P_{dgb}(t)$ is determined by

$$P_{dgb}(t) = P_{lv}(t) - P_b(t). \tag{5.5}$$

The P_{dg} is calculated using P_{dgb} as follows:

$$\begin{aligned} P_{dg}(t) &= P_{dgb}(t),\ P_{dgb} > 0 \\ &= 0,\ \text{otherwise}. \end{aligned} \tag{5.6}$$

The fuel consumption of DG is given as

$$FC_{dg}(t) = (a \times P_{dg}(t)) + (b \times P_{dg-r}) \tag{5.7}$$

where a and b are chosen as 0.246 L/kWh and 0.08415 L/kWh, respectively [113].

6. **Pumped hydro storage**: If there is injected power available at DG bus, it can not be taken by the DG. In general, the excess power available in the system is sent to either a dump load or any storage device if available in isolated MGs. Since the dump load is a combination of resistors, its usage leads to the wastage of excess power. To avoid this, it is assumed that PHS is available to take care of the excess power [170]. The PHS is charged with the excess power available in the system after the optimal utilization of the battery. The PHS power depends on DG bus

power (difference between distribution system power requirement and the battery power) as given in (5.8),

$$\begin{aligned} P_{phs}(t) &= -P_{dgb}(t),\ P_{dgb} \leq 0 \\ &= 0,\ \text{otherwise.} \end{aligned} \tag{5.8}$$

The detailed operation and discharging phenomenon of PHS is not the scope of this work.

Now, the overview of the proposed peak shaving method in the chosen islanding DG supplied residential distribution system is discussed as follows:

5.2 OVERVIEW OF THE PROPOSED PEAK SHAVING METHOD

The overview of the proposed control is shown in Fig. 5.2. It includes various steps to realize the minimization of peak DG power which are discussed as follows:

1. The first step is the day-ahead forecasting of load and RES powers. The day-ahead forecasts of load and RES powers are required to determine the optimal LV ac bus powers. In recent years, several studies have been conducted for forecasting load and RESs power [142]. Data driven approaches for forecasting the RES and load power values have gained popularity due to the increased availability of monitoring data [143]. This monitoring data mainly includes weather forecast and historical energy usage data. Therefore, using the data driven approaches such as statistical and machine learning methods, the required day-ahead load and RESs power can be forecasted [144]. In this work, it is assumed that these forecasts are available. All the powers defined in this work are obtained using these day-ahead forecasts which are further used to determine the day-ahead schedules of the battery.
2. The second step is the slave level optimization. It is used to minimize the LV ac bus power while controlling the LV ac bus voltage and reactive power of RES converters at each time of the forecast horizon i.e., one day (T = 24 h). This is performed for the whole day in order to obtain the LV ac bus power curve over the day. The constraints of the optimization problem are load bus voltage

magnitudes and RES converter ratings. Therefore, the slave level optimization helps in maintaining the load bus voltages within the grid code limits at all the times of the day. Moreover, the minimization of LV ac bus power through slave level optimization leads to the reduction of the power drawn from the DG which helps in the reduction of peak DG power.

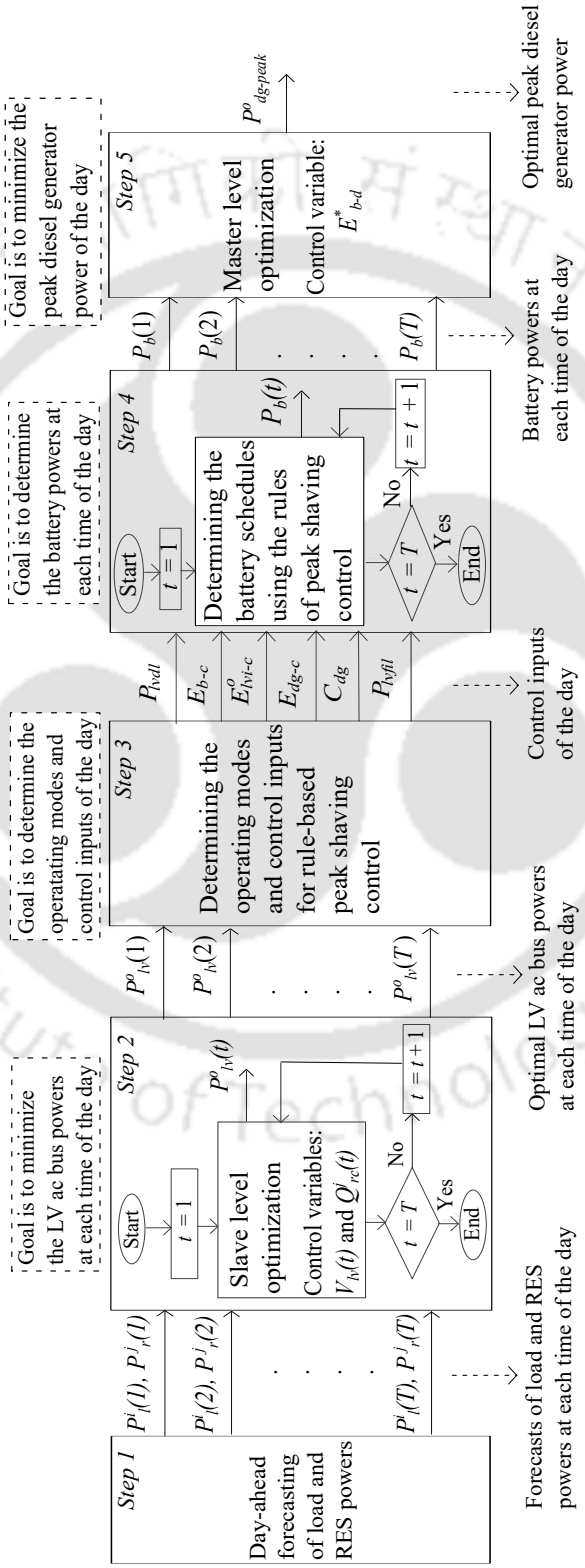

Fig. 5.2 Overview of the proposed peak shaving method.

3. The third step is the determination of the operating modes of the battery and control inputs for rule-based peak shaving method. These are determined using the LV ac bus power curve of the day which is obtained through slave level optimization. The operating modes of the battery are chosen such that peak DG power is limited to the LV ac bus demand limit. The LV ac bus demand limit is defined as the optimal LV ac bus demand above which DG is not used to supply power to the system.

   The control inputs for rule-based peak shaving are determined such that they depend on a control variable known as the dischargeable energy of the battery. The dischargeable energy of the battery is defined as the amount of energy that can be discharged from the battery over the forecast horizon without violating its power and SoC constraints. In this scenario, there exists a dischargeable energy of the battery which results in minimum peak power over a day. It means that the control inputs of rule-based peak shaving method are same for the whole day corresponding to the dischargeable energy of the battery of that particular day. This indicates that the control inputs have to be determined only once per day.

4. The fourth step is the determination of the battery schedules using the rules of peak shaving method. The rules are formulated based on the control inputs which are obtained in Step 3 to decide the charge/discharge schedules of the battery over a day.

5. The fifth step is the master level optimization. It minimizes the peak DG power while controlling the dischargeable energy of the battery. The control inputs corresponding to the optimal dischargeable energy of the battery are considered as the optimal control inputs for rule-based peak shaving method.

From the aforementioned Steps 1-5, it can be seen that the master level optimization has to be done only once per day whereas the slave level optimization is performed twenty four times per day (for hourly dispatch of the battery). Also, it is not possible to solve master level optimization problem without the knowledge of the slave level optimization results of whole day. Therefore, the master and slave level problems cannot be formulated as a single optimization problem as they are two separate problems which do not involve any decomposition.

These steps of the proposed method are discussed in detail in following sections.

5.3 SLAVE LEVEL OPTIMIZATION

In this level, the LV ac bus voltage and RES converters are optimally controlled to minimize the power requirement of the LV ac bus for each time of the day. The objective function is given in (5.9) and constraints are given from (5.10)-(5.13).

$$\text{minimize } f = \sum_{i=1}^{n_l} P_l^i(t) + P_{loss}(t) - \sum_{j=1}^{n_r} P_{rc}^j(t). \tag{5.9}$$

subjected to

1. Power balance constraint

$$P_{lv}(t) = \sum_{i=1}^{n_l} P_l^i(t) + P_{loss}(t) - \sum_{j=1}^{n_r} P_{rc}^j(t). \tag{5.10}$$

2. Bus voltages constraint

$$V_{min} \leq V_l^i(t) \leq V_{max}. \tag{5.11}$$

3. RES converters constraints

$$pf_{rc-min} \leq pf_{rc}^j(t) \leq 1. \tag{5.12}$$

$$\sqrt{(P_{rc}^j(t))^2 + (Q_{rc}^j(t))^2} \leq S_{rc-r}^j. \tag{5.13}$$

The objective function is chosen as to minimize the power drawn from the LV ac bus as given in (5.9). Equation (5.10) shows the power balance constraint at the LV ac bus neglecting power converters losses. Equation (5.11) indicates the load bus voltage magnitude constraint. The V_{min} and V_{max} are chosen as 0.95 p.u. and 1.05 p.u., respectively. The constraints of power factor and kVA rating of RES converters are presented in (5.12) and (5.13), respectively. The pf_{rc-min} is chosen as 0.8. Note that the line thermal limits are not incorporated in optimization problem. They are assumed to be satisfied since the normal operation of the system is considered in this work without any contingencies.

The considered objective function is a nonlinear function. Therefore, the proposed optimal control problem is solved using GA with ga solver in MATLAB. The method

of solving the optimization problem using GA is explained in detail in Section 2.5 of Chapter 2. The default values are chosen for various parameters of GA, except for population size. The population size is an important parameter to choose. Because if it is small, the convergence might not be achieved. Therefore, population size is chosen based on the number of control variables. There are five control variables in this optimization i.e., the LV ac bus voltage and reactive power of RES converters. Further, in GA it is possible for different runs to provide different optimal values. Therefore, to avoid any sub-optimal solutions and guarantee global optimum solution the population size is tuned such that multiple simulation runs converge precisely to the same value and chosen as 50.

The control variable V_{lv} is chosen as follows:

$$0.95 \leq V_{lv}(t) \leq 1.05. \tag{5.14}$$

The control variables Q_{rc}^{j} are chosen as

$$0 \leq Q_{rc}^{j} \leq (tan(cos^{-1}(pf_{rc-min})) \times S_{rc-r}^{j}). \tag{5.15}$$

The GA provides the optimal control variables and thereby optimal LV ac bus power values as output. These optimal LV ac bus power values obtained over a day are used to determine the operating modes of the battery and control inputs of the proposed rule-based peak shaving method as discussed in following section.

5.4 DETERMINATION OF OPERATING MODES OF THE BATTERY AND CONTROL INPUTS

The method of determination of operating modes of the battery and control inputs for rule-based peak shaving method are discussed in this section.

5.4.1 Operating Modes

There are two operating modes as discussed follows:

1. **Discharging Mode:** In order to limit DG power to LV ac bus demand limit, the battery should be discharged whenever the optimal LV ac bus demand is more than the LV ac bus demand limit. Therefore, the discharging mode is during the time t_d when $P^o_{lvd}(t) > P_{lvdl}$.

2. **Charging Mode:** It is possible to charge the battery whenever the optimal LV ac bus demand is less than the LV ac bus demand limit. Therefore, charging mode is during the time t_c when $P^o_{lvd}(t) \leq P_{lvdl}$.

Now, the determination of control inputs of the rule-based peak shaving method based on the operating modes of the battery is discussed as follows:

5.4.2 Control Inputs

The required control inputs for the proposed rule-based peak shaving method are determined using the optimal LV ac bus power values obtained from the slave level optimization. The sequential order of determining these control inputs is shown in Fig. 5.3. The determination process of these control inputs is discussed as follows:

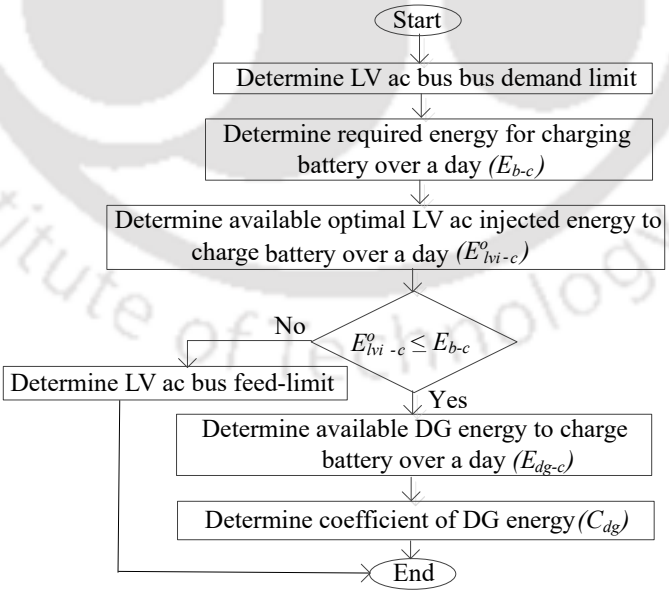

Fig. 5.3 The sequential process of determination of control inputs.

LV ac bus demand limit

In order to limit $P_{dg}(t)$ to P_{lvdl}, the battery has to supply the required power of $(P^{o}_{lvd}(t) - P_{lvdl})$ during discharging mode. However, considering discharging power limit, battery discharge power is given as

$$\begin{aligned} P_{b-d}(t) &= (P^{o}_{lvd}(t) - P_{lvdl})/e_d, (P^{o}_{lvd}(t) - P_{lvdl}) \leq P_{b-dl} \\ &= P_{b-dl}, (P^{o}_{lvd}(t) - P_{lvdl}) > P_{b-dl} \end{aligned} \tag{5.16}$$

Then, required energy to be discharged by the battery is determined as

$$E_{b-d} = \sum_{t=1}^{T} P_{b-d}(t) \times T_c. \tag{5.17}$$

Now, the LV ac bus demand limit is determined such that the energy to be discharged by the battery is equal to the dischargeable energy of the battery i.e.,

$$E_{b-d} = E^{*}_{b-d}. \tag{5.18}$$

Here, the dischargeable energy of the battery is considered as a control variable which varies between 0 kWh and E_{b-r}.

$$0 \leq E^{*}_{b-d} \leq E_{b-r}. \tag{5.19}$$

From this range, E^{*}_{b-d} is chosen optimally through the master level optimization which will be discussed in following section. Substituting (5.17) in (5.18) gives

$$\sum_{t=1}^{T} P_{b-d}(t) \times T_c - E^{*}_{b-d} = 0. \tag{5.20}$$

Equation (5.20) is in the form of $f(P_{lvdl}) = 0$, with P_{lvdl} as independent variable. It means that the problem of finding the LV ac bus demand limit becomes a root finding problem. In order to solve this, regula falsi method is used. The applied regula falsi method to determine P_{dl} is shown as a flowchart in Fig. 5.4.

According to the regula falsi method, the initial LV ac demand limits P_{lvdl1}, P_{lvdl2} are chosen such that $f(P_{lvdl1})$ is positive and $f(P_{lvdl2})$ is negative. Then, P_{lvdl0} is deter-

mined as follows:

$$P_{lvdl0} = \frac{1}{m}(0 - f(P_{lvdl1})) + P_{lvdl1}, \text{ where}$$
$$m = \frac{f(P_{lvdl2}) - f(P_{lvdl1})}{(P_{lvdl2} - P_{lvdl1})}. \tag{5.21}$$

Then, $f(P_{lvdl0})$ is determined. When $|f(P_{lvdl0})| < e$, P_{lvdl0} is considered as P_{lvdl}. When $|f(P_{lvdl0}| > e$, either P_{lvdl1} is replaced by P_{lvdl0} (if $f(P_{lvdl0}) > 0$) or P_{lvdl2} is replaced by P_{lvdl0} (if $f(P_{lvdl0}) < 0$). Then, the above process is continued till P_{lvdl0} becomes P_{lvdl}.

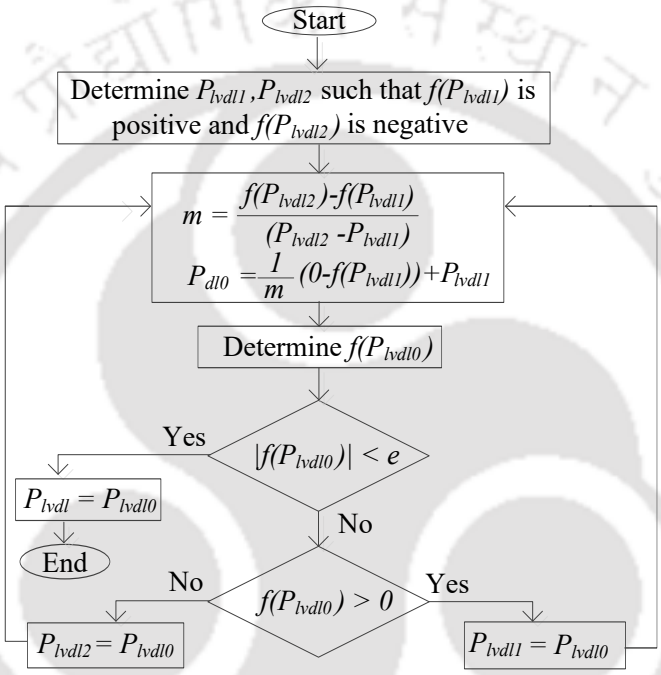

Fig. 5.4 Determination of the LV ac bus demand limit using regula falsi method.

Required energy for charging the battery over a day

For flexible day-to-day management of the battery, it has to be charged with same energy that is to be discharged by the battery. Therefore, required energy for charging the battery is equal to energy to be discharged by the battery over a day as given follows:

$$E_{b-c} = E_{b-d} = E^*_{b-d}. \tag{5.22}$$

Available optimal LV ac bus injected energy to charge the battery over a day

The required energy for charging the battery has to come either from the LV ac bus or DG. Firstly, available optimal LV ac bus injected energy to charge the battery is calculated. If it is not sufficient, then only available DG energy to charge the battery is determined and used for charging the battery. During t_c, the complete P^o_{lvi} is available for charging the battery as the optimal LV ac bus demand is less than the LV ac bus demand limit. However, considering the charging power limit, the available optimal LV ac bus injected power to charge the battery is given in (5.23),

$$\begin{aligned} P^o_{lvi-c}(t) &= P^o_{lvi}(t), P^o_{lvi}(t) \leq P_{b-cl} \\ &= P^l_{b-c}, P^o_{lvi}(t) > P_{b-cl}. \end{aligned} \tag{5.23}$$

Then, available optimal LV ac bus injected energy to charge the battery is determined as given in (5.24),

$$E^o_{lvi-c} = \sum_{t=1}^{T} P^o_{lvi-c}(t) \times T_c \tag{5.24}$$

Available DG energy to charge the battery over a day

When $E^o_{lvi-c} < E_{b-c}$, the deficit energy required for completely charging the battery is supplied by DG. Since DG power has to be limited to the LV ac bus demand limit, the available DG power to charge the battery is equal to P_{lvdl} subtracted by $P^o_{lvd}(t)$ which is given as

$$\begin{aligned} P_{dg-c}(t) &= P_{lvdl} - P^o_{lvd}(t), \forall t \in t_c \\ &= 0, \text{ otherwise.} \end{aligned} \tag{5.25}$$

Then, available DG energy to charge the battery is determined using

$$E_{dg-c} = \sum_{t=1}^{T} P_{dg-c}(t) \times T_c. \tag{5.26}$$

Coefficient of DG energy to charge the battery

When $E^o_{lvi-c} < E_{b-c}$, the DG has to supply only the deficit energy of $E^o_{lvi-c} - E_{b-c}$ over a day to the battery for flexible day-to-day management. It means that the total available DG energy for charging the battery is not required to be supplied to the battery. In this case, a coefficient known as coefficient of DG energy to charge the battery (C_{dg}) is considered which is determined as follows:

$$\begin{aligned} C_{dg}E_{dg-c} &= E_{b-c} - E^o_{lvi-c} \\ C_{dg} &= \frac{E_{b-c} - E^o_{lvi-c}}{E_{dg-c}}. \end{aligned} \tag{5.27}$$

LV ac bus feed-in limit

When $E^o_{lvi-c} \geq E_{b-c}$, the complete available optimal LV ac bus injected energy is not required to be used for charging the battery. In this case, an LV ac bus feed-in limit is considered. This LV ac bus feed-in limit is the available optimal LV ac bus injected power to charge the battery below which the battery charging is not done. It means that the available optimal LV ac bus injected power is not used to charge the battery whenever $P^o_{lvi-c}(t) \leq P_{lvfil}$. Therefore, the battery is charged with $P^o_{lvi-c}(t) - P_{lvfil}$ whenever $P^o_{lvi-c}(t) > P_{lvfil}$ during t_c i.e.,

$$\sum (P^o_{lvi-c}(t) - P_{lvfil}) \times T_c = E_{b-c}, \forall t \in t_c \&\& t_{lvimf} \tag{5.28}$$

where symbol '&&' indicates logical AND operator. Then,

$$\sum (P^o_{lvi-c}(t) - P_{lvfil}) \times T_c - E_{b-c} = 0, \forall t \in t_c \&\& t_{lvimf}. \tag{5.29}$$

Equation (5.29) is in form of $f(P_{lvfil}) = 0$, where

$$f(P_{lvfil}) = \sum (P^o_{lvi-c}(t) - P_{lvfil}) \times T_c - E_{b-c}, \forall t \in t_c \&\& t_{lvimf}. \tag{5.30}$$

In (5.29), P_{lvfil} is an independent variable. It is solved using the root finding algorithm of the regula falsi method which is similar to the determination of LV ac demand limit. This is shown in Fig. 5.5

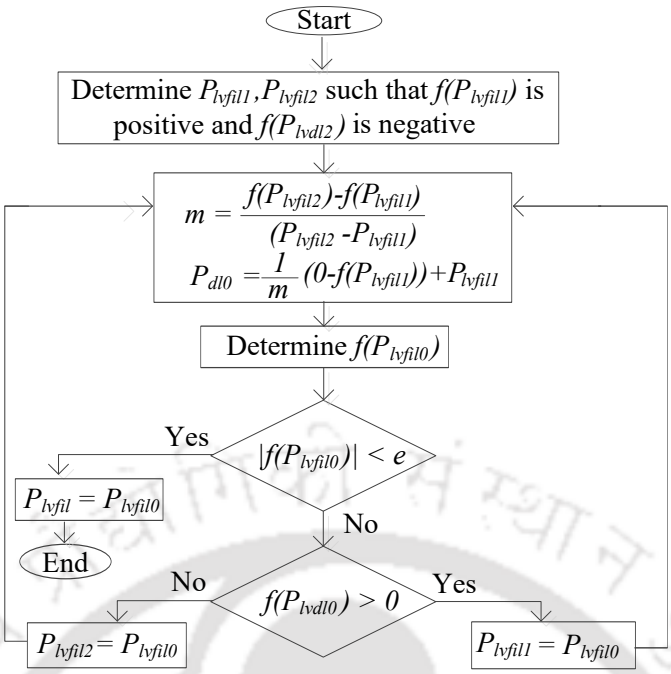

Fig. 5.5 Determination of the LV ac bus feed-in limit using regula falsi method.

Firstly, initial LV ac bus feed-in limits P_{lvfil1}, P_{lvfil2} are chosen such that $f(P_{lvfil1})$ is positive and $f(P_{lvfil2})$ is negative. Then, P_{lvfil0} is determined as follows:

$$\begin{aligned} P_{lvfil0} &= \frac{1}{m}(0 - f(P_{lvfil1})) + P_{lvfil1}, \text{ where} \\ m &= \frac{f(P_{lvfil2}) - f(P_{lvfil1})}{(P_{lvfil2} - P_{lvfil1})}. \end{aligned} \tag{5.31}$$

Then, $f(P_{lvfil0})$ is determined. When $|f(P_{lvfil0})| < e$, P_{lvfil0} is considered as P_{lvfil}. When $|f(P_{lvfil0}| > e$, either P_{lvfil1} is replaced by P_{lvfil0} (if $f(P_{lvfil0}) > 0$) or P_{lvfil2} is replaced by P_{lvfil0} (if $f(P_{lvfil0}) < 0$). Then, the above process is continued till P_{lvfil0} becomes P_{lvfil}.

Now, the determination of battery schedules using the rules of proposed peak shaving method is explained in following section.

5.5 DETERMINATION OF THE BATTERY SCHEDULES USING THE RULES OF PEAK SHAVING METHOD

The rules to determine the charge/discharge schedules of the battery are formulated to limit DG power and pumped hydro storage power to the corresponding LV ac bus demand and feed-in limits, respectively. The formulated rules are shown as flowchart

in Fig. 5.6. These rules are discussed as follows:

Rule 1: During t_d, the battery discharges by the amount $P_{b-d}(t)$ as per (5.16) to limit P_{dg} to P_{lvdl}.

Rule 2: During t_c, if $E^o_{lvi-c} \leq E_{b-c}$ both the optimal LV ac bus injected power and DG power are used to charge the battery i.e., $P_{b-c}(t) = P^o_{lvi-c-b}(t) + P_{dg-c-b}(t)$. Here $P^o_{lvi-c-b}(t) = P^o_{lvi-c}(t)$ and $P_{dg-c-b}(t) = C_{dg}P_{dg-c}(t)$ as per (5.23) and (5.27).

Rule 3: During t_c, if $E^o_{lvi-c} > E_{b-c} \&\& P^o_{lvi-c}(t) > P_{lvfil}$, only the optimal LV ac bus injected power is used to charge the battery i.e., $P_{b-c}(t) = P^o_{lvi-c-b}(t)$. Here $P^o_{lvi-c-b}(t) = P^o_{lvi-c}(t) - P_{lvfil}$ as per (5.23) and definition of the LV ac bus feed-in limit.

Rule 4: During t_c, if $E^o_{lvi-c} > E_{b-c} \&\& P^o_{lvi-c}(t) \leq P_{lvfil}$, the battery is not charged by either the optimal LV ac bus injected power or DG power i.e., $P_{b-c}(t) = 0$ as per the definition of the LV ac bus feed-in limit.

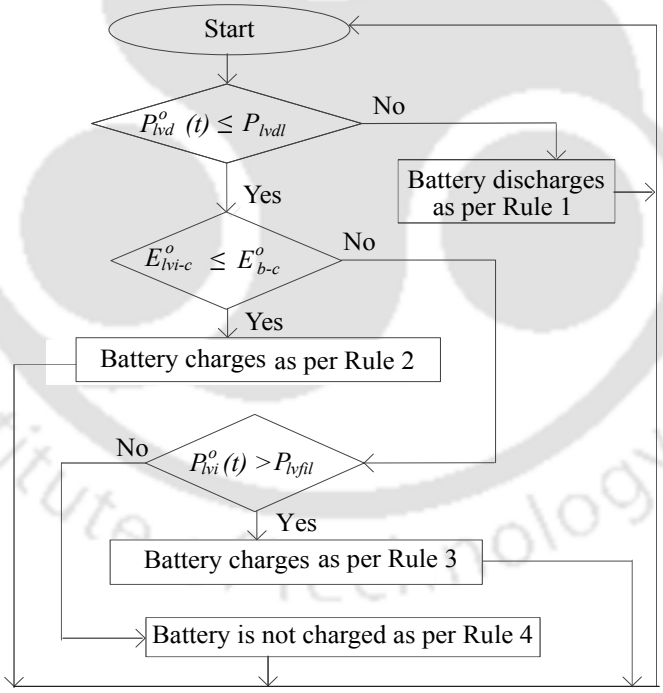

Fig. 5.6 Determination of the battery charge/discharge schedules using the proposed rule-based peak shaving method.

The SoC of the battery during discharging and charging modes is calculated using coulomb-counting method [146].

Now, the master level optimization which is used for determining the optimal control inputs for the rule-based peak shaving method is discussed as follows:

5.6 MASTER LEVEL OPTIMIZATION

In this level, the optimal control inputs are determined to minimize the peak power of DG. The objective function is given in (5.32) and constraints are given from (5.33)-(5.37),

$$\text{minimize} \;\; f = P_{dg-peak} = \; \text{maximum}(P_{dg}(t)). \tag{5.32}$$

subjected to

1. Power balance constraint

$$P_{dgb}(t) + P_b(t) = P_{lv}(t). \tag{5.33}$$

2. Battery SoC Constraints

$$SoC_l \leq SoC(t) \leq SoC_u, SoC_f = SoC_i. \tag{5.34}$$

3. Battery charge/discharge power constraints

$$P_{b-c}(t) \leq P_{b-cl}, P_{b-d}(t) \leq P^l_{b-d}. \tag{5.35}$$

4. Battery energy capacity constraint

$$E^*_{b-d} \leq E_{b-r}. \tag{5.36}$$

5. Constraint of available energy to charge the battery

$$E_{dg-c} + E^o_{lvi-c} \geq E_{b-c}. \tag{5.37}$$

Equation (5.33) gives the power balance constraint. Equation (5.34) indicates the constraints of SoC limits of the battery and the flexible day-to-day operation of the battery. The SoC of the battery is calculated using coulomb counting method [147], [148]. Equation (5.35) indicates the constraints of charge/discharge powers of the battery, respectively. Equation (5.36) indicates that dischargeable energy of battery should be less than the battery energy capacity. Equation (5.37) shows that the sum of the available grid and PV energies to charge the battery should be more than or equal to the required energy for charging the battery.

The E^*_{b-d} is considered as a control variable, since the control inputs of the peak shaving method depend on E^*_{b-d}. Note that determination of fitness function requires the DG

powers over a day, which are determined using (5.6) and (5.33). For obtaining the battery schedules the proposed rules are used. The considered fitness function is non linear. Therefore, GA is used to solve the optimization problem as discussed earlier. The population size is tuned such that multiple simulation runs converge precisely to the same value and chosen as 20. This population size is less as there is only one control variable in this optimization problem. The solution of this optimization problem provides optimal dischargeable energy of the battery and thus optimal control inputs of the peak shaving method.

Now, the simulation results of the proposed optimal rule-based peak shaving method are discussed in following section.

5.7 SIMULATION RESULTS

The simulation results are obtained using MATLAB on a 64-bit operating system PC with a processor of Intel(R) Core(TM) i5-6500 CPU @ 3.2 GHz. The fuel consumption of DG depends on DG rating. Therefore, the rating of DG is determined by testing the proposed peak shaving method in worst case scenario as discussed follows.

5.7.1 Diesel Generator Rating

In general the rating of a device is chosen based on the worst operating conditions. In the proposed control, the DG is used to balance the deficit load demand (load demand that is not supplied by the RESs). The BESS is employed for peak shaving purpose while supplying the deficit load demand along with DG. Moreover, BESS involves energy capacity rating. In this scenario, the worst operating conditions occur when the daily deficit load demand is maximum, and individual load demands are such that their peak power values coincide over the day. In order to reflect this scenario, it is considered that RES converters does not supply any power over the entire day. Further, load profiles are considered such that all the loads are operating at its peak during 9:00 and 12:00 hours over a day [141]. In this case the total load power is shown in Fig. 5.7(a). The total energy of load demand over the day is 2010 kWh. Note that the DG rating is determined without considering any contingencies. The obtained results during

this scenario are discussed as follows:

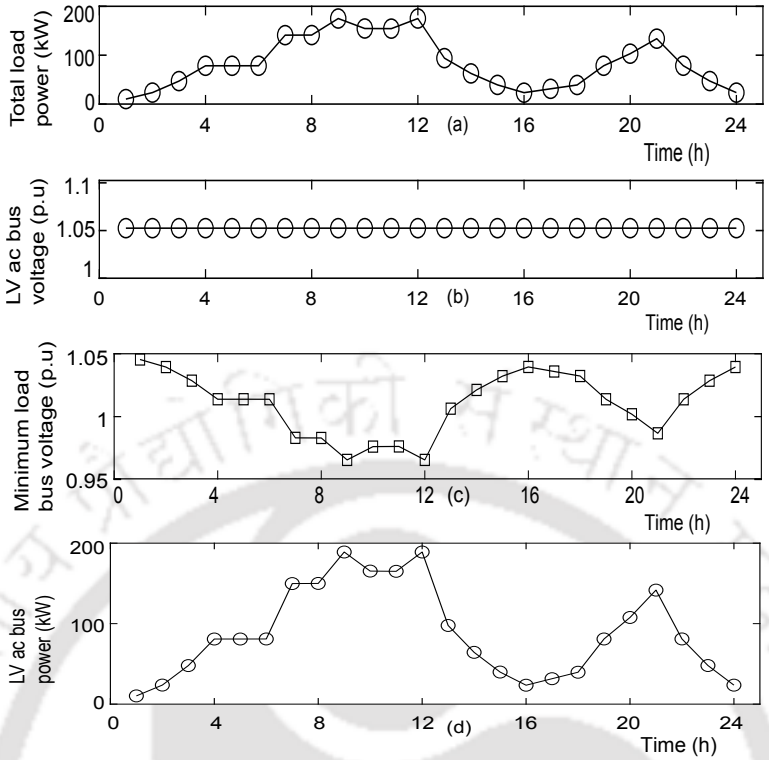

Fig. 5.7 Slave level optimization while determining the rating of DG. (a) Total load power . (b) LV ac bus voltage. (c) Minimum load bus voltage. (d) Optimal LV ac bus power.

Optimal LV ac bus powers over the day

In this level the optimal LV ac bus power values over a day are determined. The determined optimal LV ac bus voltage (V_{lv}^{o}) is 1.05 p.u. for all the times as shown in Fig. 5.7(b). This is because there is no RES converters power in this case. In this situation there will be only voltage drop scenario. Therefore, the minimum load bus voltage profile which is occurring at L5 is shown in Fig. 5.7(c). The load bus voltages are above 0.95 p.u. which indicates that there are no voltage drop violations. The resulting optimal LV ac bus power values are shown in Fig. 5.7(d). It indicates that the peak optimal LV ac bus power is 189.02 kW.

Optimal control inputs of the rule-based peak shaving method

The optimal LV ac bus power values obtained from the slave level optimization are used as inputs to the rule-based peak shaving method. Using these LV ac bus power values,

Table 5.1 Battery Parameters

Parameter	Value	Parameter	Value
e_c	0.95	SoC_l/SoC_u	0.2/0.9
e_d	0.95	SoC_i	0.5
E_{b-r}	400 kWh	P_{b-cl}	100 kW
V_{b-r}	120 V	P^l_{b-d}	100 kW

the optimal control inputs are obtained with the help of master level optimization. The best fitness values are obtained for multiple runs of GA as shown in Fig. 5.8. It shows that the minimum value for all the runs is equal to 137.82 kW which is the optimal peak DG power ($P^o_{dg-peak}$). The optimal dischargeable energy of the battery is found to be 194.84 kWh. The corresponding control inputs i.e., optimal LV ac bus demand limit, energy required for charging battery, available LV ac bus injected energy to charge battery, available DG energy to charge battery, and coefficient of DG energy to charge battery (P^o_{lvdl}, E^o_{b-c}, E^o_{lvi-c}, E^o_{dg-c}, and C^o_{dg}) are calculated as 137.82 kW, 194.84 kWh, 0 kWh, 1380.6 kWh and 0.14, respectively. The feed-in limit (P^o_{lvfil}) is not applicable in this case as there is no injected LV ac bus power available.

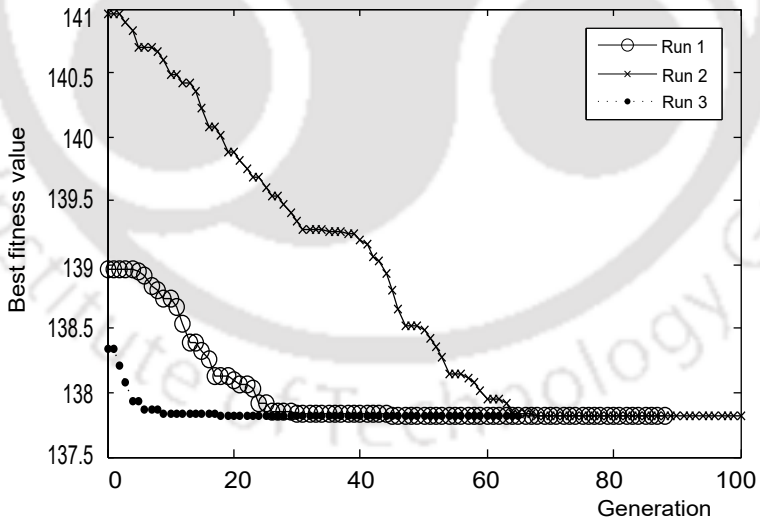

Fig. 5.8 Best fitness values obtained using GA with master level optimization while determining the rating of DG.

Battery schedules and diesel generator powers over the day

The optimal LV ac bus powers are shown in Fig. 5.9(a). The resulting charge/discharge schedules of the battery corresponding to the LV ac bus powers along with its SoC are

shown in Fig. 5.9(b). This shows that the battery power and SoC are maintained within their limits. Moreover, SoC at the end of the day is maintained equal to the SoC of start of the day to ensure flexible day to day management of the battery. The resulting DG

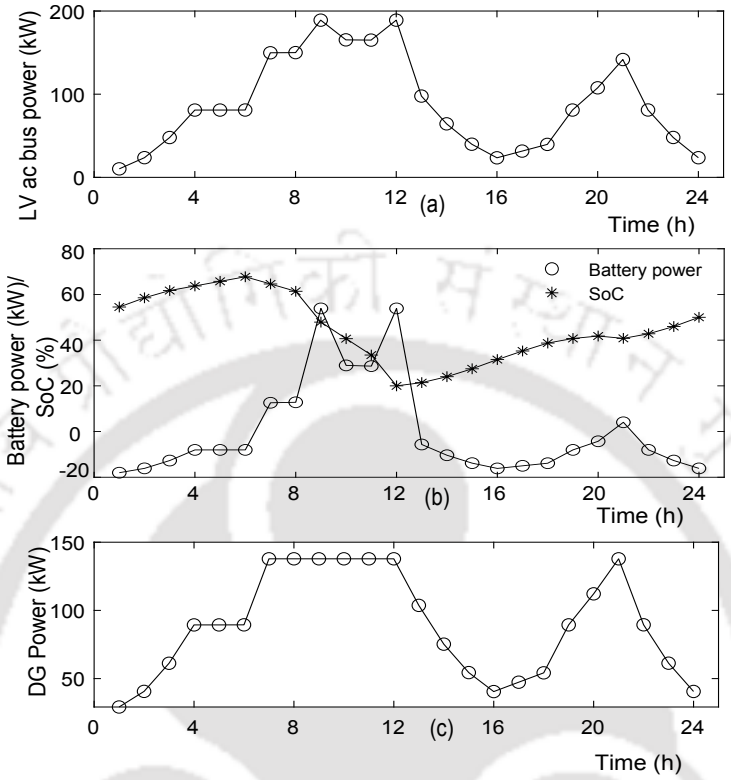

Fig. 5.9 Master level optimization while determining the rating of DG. (a) LV ac bus power. (b) Charge/discharge powers and SoC of the battery. (c) DG power.

power is shown in Fig 5.9(c). This shows that the DG power is limited to P^{o}_{lvdl} of 137.82 kW which justifies the proposed peak shaving method. This peak DG power which is obtained in worst operating conditions is considered as the DG rating.

The rule-based methods discussed in literature [42], [100], [127], [128], [133] have validated their algorithms for various possible scenarios as per their proposed method. As per the proposed peak shaving method in this chapter, two different possible cases exist considering the RESs characteristics. The first case is when the available optimal LV ac bus injected energy to charge the battery is less than or equal to required energy to charge the battery over a day. The second case is when the available optimal LV ac bus injected energy to charge the battery is more than the required energy to charge the battery over a day. The results of the optimal rule-based control for the first possible case are verified while determining the rating of DG. In order to verify the second case and show the impact of the proposed peak shaving method on fuel consumption of DG and self consumption rate of the system a case study is considered as given follows.

5.7.2 Case Study

The performance of the proposed method is tested in this case considering the day-ahead forecasts of load and RES powers as inputs. The day-ahead load powers are considered such that they are operating at half of their peak loads during 9:00 and 12:00 hours of the day. The total energy of the load demand over the day is 1005 kWh. The day-ahead RES powers are considered such that they are operating at their installed capacities during their maximum power generation hours. The total energy of the RESs over the day is 1165.5 kWh . The total load power and RESs power profiles are shown in Fig. 5.10(a) [141], [166]. The obtained results are discussed as follows:

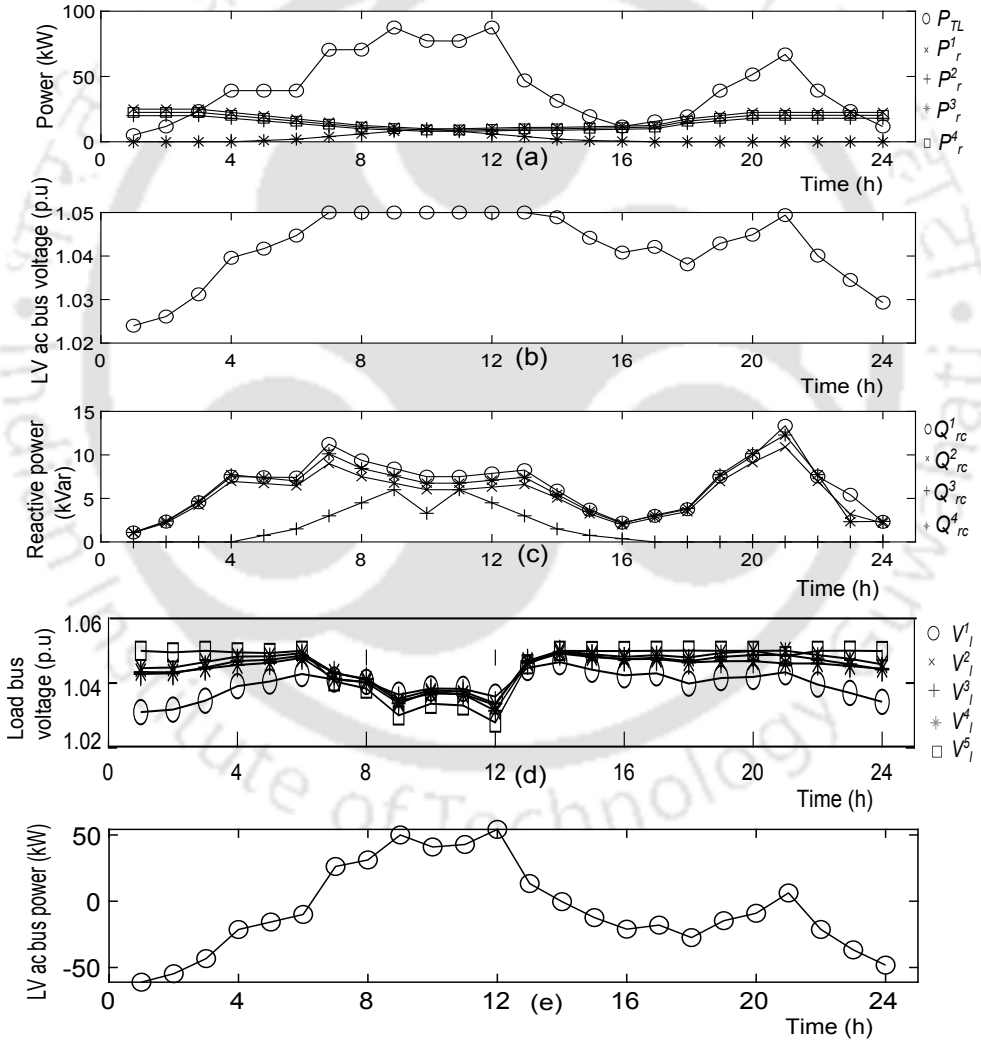

Fig. 5.10 Slave level optimization during case study analysis. (a) Total load and RES powers . (b) LV ac bus voltage. (c) Reactive power of RES converters. (d) Load bus voltages. (e) Optimal LV ac bus power.

Optimal LV ac bus powers over the day

The determined optimal LV ac bus voltage and reactive powers of RES converters (V_{lv}^{o} and Q_{rc}^{oj}) are shown in the Fig. 5.10(b) and (c) , respectively. These indicate that the voltage at the LV ac bus and reactive power supplied by RES converters are controlled as per the variation of load and RESs power. For this case there will be both voltage rise and voltage drop conditions due to the presence of RESs power. Therefore, all the load bus voltage profiles are shown in Fig. 5.10(d). This indicates that there are no voltage drop and voltage rise violations as load bus voltages are within 0.95 p.u. and 1.05 p.u. at all the hours of the day. The resulting optimal LV ac bus power values over a day are shown in Fig. 5.10(e). It indicates that the peak optimal LV ac bus power is 54.19 kW.

Optimal control inputs of the rule-based peak shaving method

Using this optimal LV ac bus power profile, the determined optimal control inputs i.e., optimal LV ac bus demand limit, energy required for charging battery, available LV ac bus injected energy to charge battery, and LV ac bus feed-in limit (P_{lvdl}^{o}, E_{b-c}^{o}, E_{lvi-c}^{o} and P_{lvfil}^{o}) are 0.19 kW, 277.11 kWh, 415.45 kWh and 9.20 kW, respectively. In this case E_{lvi-c}^{o} is more than E_{b-c}^{o}. Therefore, available DG energy to charge battery and coefficient of DG energy to charge battery (E_{dg-c}^{o} and C_{g-c}^{o}) are not applicable.

Battery schedules and diesel generator powers over the day

The optimal LV ac bus powers are shown in Fig. 5.11(a). The resulting charge/discharge schedules of the battery corresponding to the LV ac bus powers along with its SoC are shown in Fig. 5.11(b). This shows that the battery power and SoC are maintained within their limits. Moreover, SoC at the end of the day is maintained equal to the SoC of start of the day to ensure flexible day to day management of the battery. The resulting DG power is shown in Fig 5.11(c). This shows that the DG power is limited to P_{lvdl}^{o} of 0.19 kW. The resulting PHS power is shown in Fig. 5.11(d). This shows that the PHS power is limited to P_{lvfil}^{o} of 9.21 kW. This justifies the proposed peak shaving method.

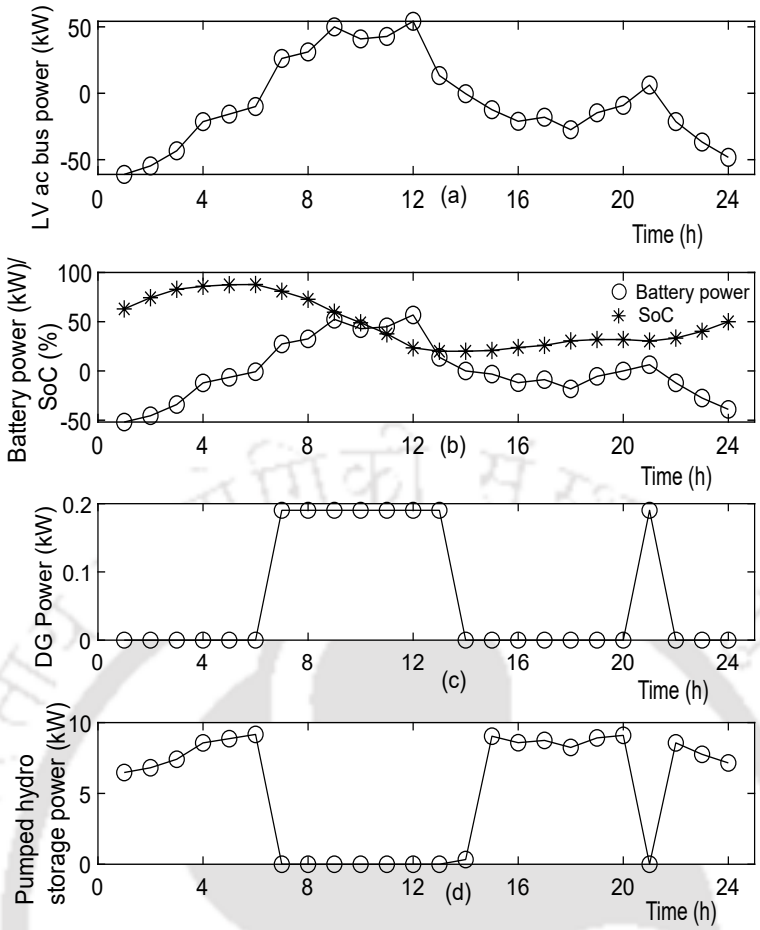

Fig. 5.11 Master level optimization during the case study analysis. (a) LV ac bus power. (b) Charge/discharge powers and SoC of the battery. (c) DG power. (d) PHS power.

5.7.3 Performance Indicators

The performance indicators of DG rating, fuel consumption of DG over the day, and self consumption rate of the system are considered as discussed follows.

Diesel generator rating

The comparison of the DG rating with respect to base case (when there is no minimization of the LV ac bus power and no peak shaving method) and with respect to the case when there is only LV ac bus power minimization without peak shaving method [91]–[94] is given in Table 5.2. It shows that the DG rating is 190.7 kW for base case and 189.02 kW with only LV ac bus power minimization without peak shaving method. This indicates that the DG power rating is reduced by 27.09% with the proposed peak shaving method as compared to the case when there is only LV ac bus power minimization.

Table 5.2 Diesel Generator Rating

Method	P_{dg-r} (kW)
Base case	190.7
Minimization of LV ac bus power without the peak shaving [91]–[94]	189.02
Minimization of LV ac bus power along with the proposed peak shaving	137.82

Fuel consumption of diesel generator over the day

The total fuel consumption of DG over a day is calculated as follows:

$$TFC_{dg} = \sum_{t=1}^{T} [(a \times P_{dg}(t)) + (b \times P_{dg-r})]. \tag{5.38}$$

The quantitative comparison considering TFC_{dg} is shown in Table 5.3. It shows that the TFC_{dg} without the minimization of LV ac bus power and without the peak shaving method is 451.5 L. The TFC_{dg} with only LV ac bus power minimization without the peak shaving method is 446.88 L. However, with LV ac bus power minimization and the proposed peak shaving method TFC_{dg} is calculated as 278.72 L. This indicates that the fuel consumption is reduced by 37.63% with the proposed peak shaving method as compared to the case when there is only LV ac bus power minimization.

Self consumption rate

Self consumption rate is defined as the ratio of self consumed RESs energy and total generated RESs energy [171] i.e.,

$$SCR = \frac{E_r - E_{phs}}{E_r}. \tag{5.39}$$

The quantitative comparison considering *SCR* is shown in Table 5.3. It shows that the *SCR* without minimization of LV ac bus power and without the peak shaving method is calculated as 0.6453. The *SCR* with only LV ac bus power minimization without the peak shaving method is 0.6436. However, with LV ac bus power minimization

and the proposed peak shaving method *SCR* is calculated as 0.9. This indicates that the fuel consumption is reduced by 38.88% with the proposed peak shaving method as compared to the case when there is only LV ac bus power minimization.

Table 5.3 Fuel Consumption and Self Consumption Rate for Case Study

Method	TFC_{dg} (L)	*SCR*
Base case	451.5	64.53%
Minimization of LV ac bus powers without the peak shaving [91]–[94]	446.88	64.36%
Minimization of LV ac bus powers along with the proposed peak shaving	278.72	90%

5.8 CONCLUSIONS

In this chapter, peak shaving is achieved using optimal control of battery energy storage in diesel generator supplied isolated microgrid. The low voltage ac bus power requirement is minimized through a slave level optimization and the rule-based control is optimized through a master level optimization. It is observed that the diesel generator rating is reduced by 27.09% with the proposed peak shaving method as compared to the case when there is only low voltage ac bus demand minimization. Further, it is observed that the fuel consumption of diesel generator is reduced by 37.63% and self consumption rate is increased by 38.88% with the proposed peak shaving method as compared to the case when there is only low voltage ac bus power minimization.

CHAPTER 6

CONCLUSIONS

6.1 SUMMARY OF THE THESIS WORK

The integration of distributed energy resources causes new challenges such as increased customer expectations and requirements for supporting bi-directional energy flow. The energy management and voltage control play an important role in dealing with these challenges of modern power systems. The battery energy storage and smart power converters are widely used to implement the energy management and voltage control applications. Therefore, this thesis is dedicated to the development of optimal rule-based methods for peak shaving, demand response, and voltage control applications using the battery energy storage systems and smart power converters. The proposed methods are tested in MATLAB for different possible cases and their impact is analyzed through various performance indicators of the system. The contributions of the thesis work are summarized as given in Table 6.1 and discussed as follows. It shows that the proposed peak shaving and DR methods are implemented using the battery charge/discharge power control capability whereas the proposed voltage control is implemented using the LV ac bus voltage control capability. Further, the proposed peak shaving is modified while minimizing the LV ac bus power using the battery charge/discharge power, LV ac bus voltage, and reactive power of RES converters control capabilities.

These contributions and their major findings are explained as follows.

- A novel optimal rule-based peak shaving method is proposed considering both demand and feed-in limits together to minimize the peak grid power over a day. The proposed method is tested on the considered PV-BESS system and validated in MATLAB. It is observed that the grid demand and feed-in powers are limited to the corresponding optimal demand and feed-in limits of the day, respectively while maintaining the flexible day-to-day management of the battery. The peak grid power reduction in the range of 28.67-55.66% is achieved through the proposed method with respect to the case when there is no PV-BESS.

Table 6.1 Contributions of the Thesis.

S.No	Considered system	Proposed method	Control application		
			BESS charge/ discharge control	LV ac bus voltage control	RES converters reactive power control
1	Grid-connected PV-BESS system	Peak shaving	Yes	No	No
2	Grid-connected PV-BESS system	Demand response	Yes	No	No
3	Grid-connected LV ac distribution system with PV sources	Voltage control	No	Yes	No
4	Isolated LV ac distribution system with DG, BESS, wind, and PV sources	Peak shaving while LV ac bus energy demand is minimized	Yes	Yes	Yes

- A novel optimal rule-based demand response method is proposed considering both buying and selling price profiles together to minimize the energy consumption cost over a day. The proposed method is tested on the considered PV-BESS system and validated in MATLAB. It is observed that the energy buying and selling prices are limited to the corresponding optimal energy buying and selling price limits of the day, respectively while maintaining the flexible day-to-day management of the battery. The energy consumption cost reduction in the range of 5.4-34.09% is achieved through the proposed method with respect to the case when there is no PV-BESS.

- A novel optimal rule-based voltage control method is proposed using the maximum and minimum load bus voltages to minimize the voltage deviation of the low voltage ac distribution system over a day. The proposed optimal rule-based voltage control method is tested on the considered distribution system with high penetration of photovoltaic sources and validated in MATLAB. It is observed that the voltage profile is improved with the proposed voltage control method. In case if the control inputs are chosen based on direct axis low voltage ac bus current, the average voltage deviation reduction in the range of 20.33%-67.78% is achieved with respect to the case when there is no voltage control. In case if the control inputs are chosen as per the proposed method, the average voltage deviation reduction in the range of 51.63%-75.56% is achieved with respect to the case when there is no voltage control.

- The proposed optimal rule-based peak shaving method is modified to apply in a diesel generator supplied isolated low voltage ac distribution system and its impact is presented. This modified optimal rule-based peak shaving method is tested on the considered isolated distribution system and validated in MATLAB. It is observed that the diesel generator rating can be reduced by 27.09% with the proposed peak shaving method as compared to the case when there is no peak shaving control. Further, it is observed that the fuel consumption of diesel generator is reduced by 37.63% and self consumption rate is increased by 38.88% with the proposed peak shaving method as compared to the case when there is no peak shaving control.

- All these proposed optimal rule-based energy management and voltage control

methods are simple and easy to implement in real-time. Because, the implementation of these methods does not require the optimization problem to be solved at each time of the day. The rule-based methods are optimized by determining the control inputs optimally before the start of a day using the knowledge of day-ahead forecasts of that particular day. These optimal control inputs are determined only once per day which are same for the whole day. During the real-time operation, the required output (e.g. battery charge/discharge power, low voltage ac bus voltage and reactive power references of renewable energy source converters) over a day corresponding to the base inputs (e.g. load, PV power, and energy price) is obtained automatically using the optimal control inputs and rules of the proposed method.

6.2 FUTURE SCOPE OF THE WORK

The performance of the proposed optimal rule-based energy management and voltage control methods depends on the accuracy of the day ahead forecasts. In this thesis, it is assumed that the available day ahead forecasts are perfect. It means that the forecast errors in the load, renewable energy source powers, and energy prices are not considered. In case if the actual load, RES powers and energy prices are different from the day-ahead forecasts due to forecast errors, desired performance of the proposed methods may not be achieved (e.g. in case of peak shaving, the peak power may not be limited to the optimal demand limit and flexible day-to-day management of the battery may not be maintained). Further, the cost-benefit analysis of implementing proposed methods in real-time with the installations of battery energy storage systems and smart power converters has to be performed. This cost benefit analysis requires the detailed modelling of the systems components as well as the detailed analysis of the benefits associated with the proposed rule-base methods.

Therefore, to know the impact of forecast errors on the performance of the proposed optimal rule-based methods, developing the real-time implementation strategies to avoid the impacts of forecast errors, and the cost benefit analysis of real-time implementation of the proposed methods are the future scope of this work.

APPENDIX A

LINE DATA OF CIGRE RESIDENTIAL DISTRIBUTION NETWORK

The line data i.e., the resistance and reactance values of the lines of the CIGRE residential distribution network is given in Table A.1 [172].

Table A.1 Line Data of CIGRE Residential Distribution Network .

From line-to line	R (ohm/km)	X (ohm/km)
1-2	0.284	0.083
2-3	0.284	0.083
3-4	0.284	0.083
4-5	0.284	0.083
5-6	0.284	0.083
2-7	3.69	0.094
3-8	0.497	0.086
4-9	0.871	0.081
5-10	0.871	0.081
6-11	0.38	0.082

This line data is used for obtaining power flow solution which is required for determining the bus voltages, power losses, and power flows of lines.

APPENDIX B

PERFORMANCE OF PROPOSED ENERGY MANAGEMENT APPLICATIONS FOR DIFFERENT CONTROL HORIZON

In the chapters discussed in the thesis, the control horizon is considered as 1 hour. In order to show the impact of changing control horizon on performance of proposed rule-based methods, a control horizon of 15 minutes is considered. The obtained results for the modified control horizon are presented for rue-based peak shaving and demand response methods which are discussed in Chapter 2 and 3, respectively.

B.1 Performance of Proposed Peak Shaving Method

To show the impact of changing control horizon, the Case 1 i.e., winter load profile with more PV energy availability is considered as discussed in Chapter 2. The optimal dischargeable energy of the battery is found to be 5.54 kWh. The optimal control inputs i.e., optimal demand limit, energy required for charging battery, available PV energy to charge battery, and feed-in limit are 1.73 kW, 5.54 kWh, 5.7 kWh and 0.035 kW, respectively. The optimal control inputs for different T_c values are shown in Table B.1. It is observed that the optimal control inputs are not significantly changed as compared to the case of control horizon of 1 hour which are discussed in Section 2.6.1 of chapter 2. This is due to the fact that the objective function of peak grid power involves only grid power. Therefore, the change in optimal control input values is not significant. The load power, PV power, battery power, SoC of battery, and grid power profiles are shown in Fig. B.1(a)-(d) for the control horizon of 15 minutes. It is observed that the grid powers are limited to the optimal demand and feed-in limits of the day while maintaining the flexible day-to-day management of the battery. This validates the proposed peak shaving method.

Table B.1 Optimal Control Inputs

Input parameter	T_c=1 hour	T_c=15 minutes
P^o_{dl} (kW)	1.72	1.73
E^o_{b-c} (kWh)	5.46	5.54
E^o_{pv-c} (kWh)	5.69	5.7
E^o_{g-c} (kWh)	NA	NA
C^o_g	NA	NA
P^o_{fil} (kW)	0.05	0.035

B.2 Performance of Proposed Demand Response Method

To show the impact of changing control horizon, the Case 1 i.e., more PV energy availability over a day is considered as discussed in Chapter 3. The optimal buying price limit is found to be 8.30 INR. The corresponding optimal control inputs i.e., optimal energy required for charging battery, available PV energy to charge battery, and energy selling price limit are 8.80 kWh, 23.87 kWh and 6.74 INR, respectively. The optimal control inputs for different T_c values are shown in Table B.2. It is observed that the optimal control inputs are slightly different as compared to the case of control horizon of 1 hour which are discussed in Section 3.6.1 of chapter 3. This is because here in this case the energy buying and selling price are also considered as input along with the load and PV powers. Moreover, the objective function i.e., the energy consumption cost involves the terms of energy buying price, energy selling price, grid demand and injection power. Due to the presence of more number of variables in objective function, the change in optimal control input values is significant. The energy buying and selling price, load power, PV power, battery power, SoC of battery, and grid power profiles are shown in Fig. B.2(a)-(e) for the control horizon of 15 minutes. From the grid power, it is observed that the energy buying and selling prices are limited to their corresponding optimal limits of the day with flexible day-to-day management of the battery. This validates the proposed DR method.

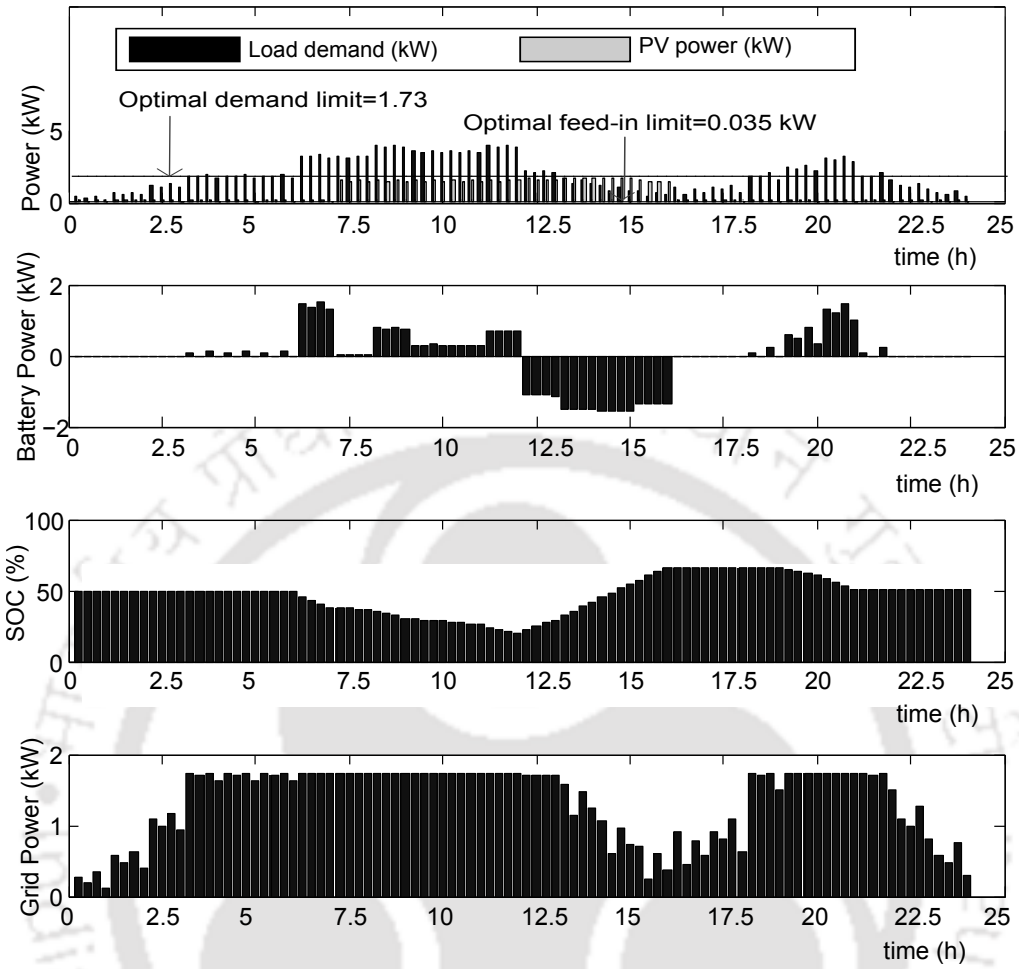

Fig. B.1 Case 1 for T_c= 15 minutes. (a) Load and PV power profiles. (b) Charge/discharge schedules of the battery. (c) SoC of the battery. (d) Grid power.

Table B.2 Optimal Control Inputs

Input parameter	T_c=1 hour	T_c=15 minutes
EP^o_{bl} (INR)	8.23	8.30
E^o_{b-c} (kWh)	7.13	8.8
E^o_{pv-c} (kWh)	27.6	23.87
E^o_{g-c} (kWh)	NA	NA
EP^o_{sbl} (INR)	NA	NA
EP^o_{sl} (INR)	6.43	6.74

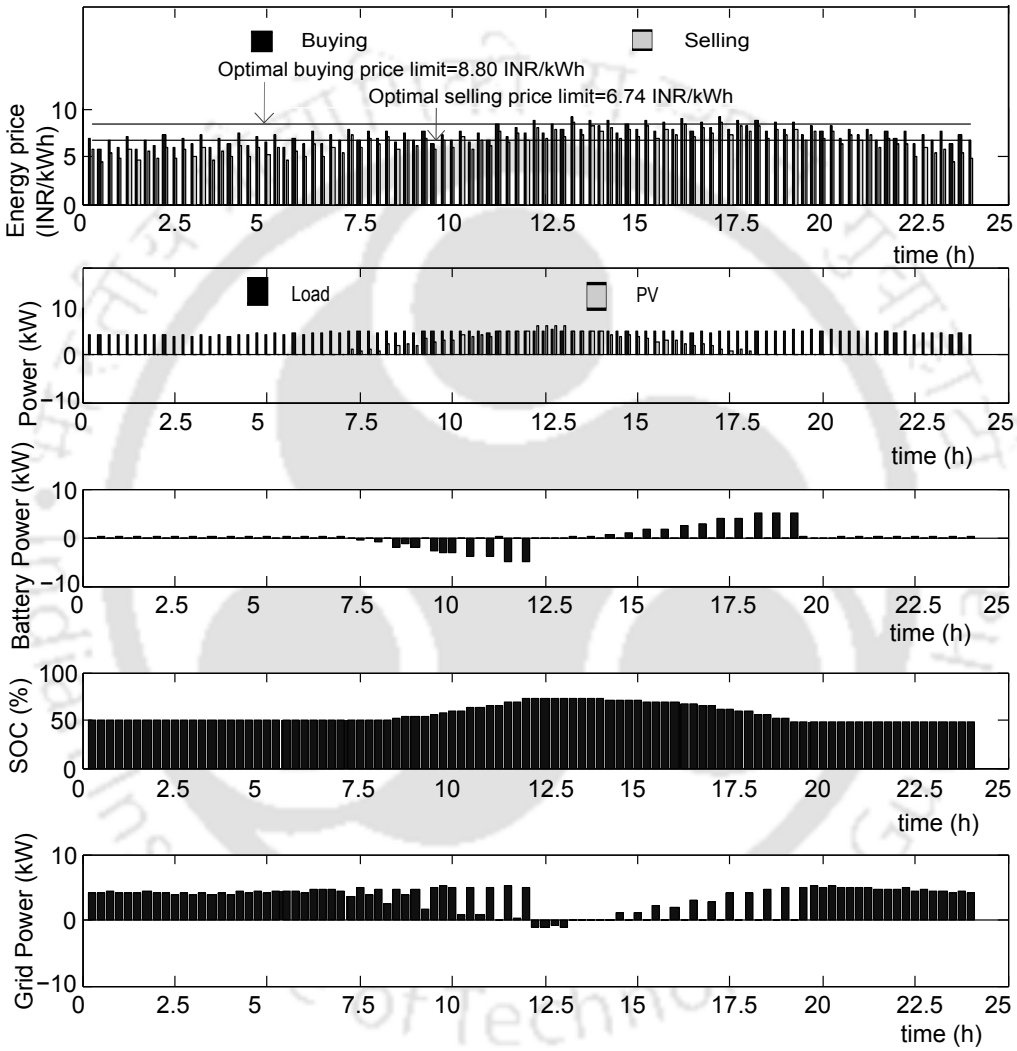

Fig. B.2 Case 1 for T_c=15 minutes. (a) Energy price . (b) Load and PV power profiles . (c) Charge/discharge schedules of the battery. (d) SoC of the battery. (e) Grid power.

REFERENCES

[1] C. Zou, Q. Zhao, G. Zhang, and B. Xiong, "Energy revolution: From a fossil energy era to a new energy era," *Natural Gas Industry B*, vol. 3, no. 1, pp. 1–11, 2016.

[2] A. Muhtadi, D. Pandit, N. Nguyen, and J. Mitra, "Distributed energy resources based microgrid: Review of architecture, control, and reliability," *IEEE Transactions on Industry Applications*, vol. 57, no. 3, pp. 2223–2235, 2021.

[3] A. J. D. Rathnayaka, V. M. Potdar, T. S. Dillon, O. K. Hussain, and E. Chang, "A methodology to find influential prosumers in prosumer community groups," *IEEE Transactions on Industrial Informatics*, vol. 10, no. 1, pp. 706–713, 2014.

[4] R. Mieth, S. Acharya, A. Hassan, and Y. Dvorkin, "Learning-enabled residential demand response: Automation and security of cyberphysical demand response systems," *IEEE Electrification Magazine*, vol. 9, no. 1, pp. 36–44, 2021.

[5] A. Zahedi, "A review of drivers, benefits, and challenges in integrating renewable energy sources into electricity grid," *Renewable and Sustainable Energy Reviews*, vol. 15, no. 9, pp. 4775–4779, 2011.

[6] "Ministry of new and renewable energy, government of india, annual report 2020-21." [Online]. Available: https://mnre.gov.in/img/documents/uploads/file_f-1618564141288.pdf

[7] "Central electricity authority, ministry of power, government of india, installed capacity report 2020-21." [Online]. Available: https://cea.nic.in/installed-capacity-report/?lang=en

[8] P. Gajewski and K. Pieńkowski, "Control of the hybrid renewable energy system with wind turbine, photovoltaic panels and battery energy storage," *Energies*, vol. 14, no. 6, 2021.

[9] S. Impram, S. Varbak Nese, and B. Oral, "Challenges of renewable energy penetration on power system flexibility: A survey," *Energy Strategy Reviews*, vol. 31, p. 100539, 2020.

[10] C. Kumar, R. Zhu, G. Buticchi, and M. Liserre, "Sizing and soc management of a smart-transformer-based energy storage system," *IEEE Transactions on Industrial Electronics*, vol. 65, no. 8, pp. 6709–6718, 2018.

[11] Y. E. García Vera, R. Dufo-López, and J. L. Bernal-Agustín, "Energy management in microgrids with renewable energy sources: A literature review," *Applied Sciences*, vol. 9, no. 18, 2019.

[12] H. Shayeghi and M. Alilou, "3 - distributed generation and microgrids," in *Hybrid Renewable Energy Systems and Microgrids*, E. Kabalci, Ed. Academic Press, 2021, pp. 73–102.

[13] A. Purwadi, Y. Haroen, M. Zamroni, N. Heryana, and A. Saryanto, "Study of hybrid pv-diesel power generation system at sebira island-kepulauan seribu," in *2012 International Conference on Power Engineering and Renewable Energy (ICPERE)*, 2012, pp. 1–7.

[14] G. P. Holdmann, R. W. Wies, and J. B. Vandermeer, "Renewable energy integration in alaska's remote islanded microgrids: Economic drivers, technical strategies, technological niche development, and policy implications," *Proceedings of the IEEE*, vol. 107, no. 9, pp. 1820–1837, 2019.

[15] G. Velasco, F. Casellas, F. Guinjoan, H. Martínez, and R. Piqué, "Grid-pv-diesel hybrid system management application to med-solar project scenarios," in *2015 IEEE 15th International Conference on Environment and Electrical Engineering (EEEIC)*, 2015, pp. 713–718.

[16] L. Bhamidi and S. Sivasubramani, "Optimal planning and operational strategy of a residential microgrid with demand side management," *IEEE Systems Journal*, vol. 14, no. 2, pp. 2624–2632, 2020.

[17] T. H. Kiang, C. H. Koon, T. S. Peng, L. J. Rong, and T. P. Jin, "Application of hybrid generator system in smart grid," *Energy Procedia*, vol. 143, pp. 686–692, 2017, leveraging Energy Technologies and Policy Options for Low Carbon Cities.

[18] H. Alharbi and K. Bhattacharya, "Stochastic optimal planning of battery energy storage systems for isolated microgrids," *IEEE Transactions on Sustainable Energy*, vol. 9, no. 1, pp. 211–227, 2018.

[19] S. Ganesan, S. Padmanaban, R. Varadarajan, U. Subramaniam, and L. Mihet-Popa, "Study and analysis of an intelligent microgrid energy management solution with distributed energy sources," *Energies*, vol. 10, no. 9, 2017.

[20] A. Noori, Y. Zhang, N. Nouri, and M. Hajivand, "Multi-objective optimal placement and sizing of distribution static compensator in radial distribution networks with variable residential, commercial and industrial demands considering reliability," *IEEE Access*, vol. 9, pp. 46 911–46 926, 2021.

[21] N. Qachchachi, H. Mahmoudi, and A. E. Hasnaoui, "Optimal power flow for a hybrid ac/dc microgrid," in *2014 International Renewable and Sustainable Energy Conference (IRSEC)*, Oct 2014, pp. 559–564.

[22] W.-M. Lin, C.-S. Tu, and M.-T. Tsai, "Energy management strategy for microgrids by using enhanced bee colony optimization," *Energies*, vol. 9, no. 1, 2016.

[23] Y. Zheng, B. M. Jenkins, K. Kornbluth, and C. Træholt, "Optimization under uncertainty of a biomass-integrated renewable energy microgrid with energy storage," *Renewable Energy*, vol. 123, pp. 204–217, 2018.

[24] M. R. Sandgani and S. Sirouspour, "Priority-based microgrid energy management in a network environment," *IEEE Transactions on Sustainable Energy*, vol. 9, no. 2, pp. 980–990, 2018.

[25] A. Elmouatamid, R. Ouladsine, M. Bakhouya, N. El Kamoun, M. Khaidar, and K. Zine-Dine, "Review of control and energy management approaches in micro-grid systems," *Energies*, vol. 14, no. 1, 2021.

[26] T. Thien, H. Axelsen, M. Merten, and D. U. Sauer, "Energy management of stationary hybrid battery energy storage systems using the example of a real-world 5 mw hybrid battery storage project in germany," *Journal of Energy Storage*, vol. 51, p. 104257, 2022.

[27] "Hornsdale power reserve." [Online]. Available: https://hornsdalepowerreserve.com.au/our-vision/

[28] "Green mountain power battery storage portfolio." [Online]. Available: https://encorerenewableenergy.com/project/green-mountain-power-battery-storage-portfolio/

[29] "Grid scale battery energy storage systems: Will they meet expectations?" [Online]. Available: https://www.orfonline.org/expert-speak/grid-scale-battery-energy-storage-systems/

[30] "Front matter," in *Large-Scale Wind Power Grid Integration*, N. Wang, C. Kang, and D. Ren, Eds. Oxford: Academic Press, 2016, p. iii.

[31] A. Aoun, M. Ghandour, A. Ilinca, and H. Ibrahim, "13 - demand-side management," in *Hybrid Renewable Energy Systems and Microgrids*, E. Kabalci, Ed. Academic Press, 2021, pp. 463–490.

[32] Y. Liu, W. Du, L. Xiao, H. Wang, S. Bu, and J. Cao, "Sizing a hybrid energy storage system for maintaining power balance of an isolated system with high penetration of wind generation," *IEEE Transactions on Power Systems*, vol. 31, no. 4, pp. 3267–3275, 2016.

[33] S. Obukhov, A. Ibrahim, M. A. Tolba, and A. M. El-Rifaie, "Power balance management of an autonomous hybrid energy system based on the dual-energy storage," *Energies*, vol. 12, no. 24, 2019.

[34] X. Wang, J. Xie, D. Yue, J. Zhao, Y. Xiao, and C. Cao, "Power balance control of energy storage unit in micro grid based on distributed gradient algorithm," in *2016 35th Chinese Control Conference (CCC)*, 2016, pp. 9924–9929.

[35] W. Zheng, K. Ma, and X. Wang, "Hybrid energy storage with supercapacitor for cost-efficient data center power shaving and capping," *IEEE Transactions on Parallel and Distributed Systems*, vol. 28, no. 4, pp. 1105–1118, 2017.

[36] B. Aksanli, "Data center peak power management with energy storage devices," *IEEE Internet Computing*, vol. 21, no. 4, pp. 26–33, 2017.

[37] M. Dabbagh, B. Hamdaoui, and A. Rayes, "Peak power shaving for reduced electricity costs in cloud data centers: Opportunities and challenges," *IEEE Network*, vol. 34, no. 3, pp. 148–153, 2020.

[38] X. Li, X. Cao, C. Li, B. Yang, M. Cong, and D. Chen, "A coordinated peak shaving strategy using neural network for discretely adjustable energy-intensive load and battery energy storage," *IEEE Access*, vol. 8, pp. 5331–5338, 2020.

[39] V. Kalkhambkar, R. Kumar, and R. Bhakar, "Energy loss minimization through peak shaving using energy storage," *Perspectives in Science*, vol. 8, pp. 162 – 165, 2016, recent Trends in Engineering and Material Sciences.

[40] N. Chakraborty, A. Mondal, and S. Mondal, "Efficient Scheduling of Nonpreemptive Appliances for Peak Load Optimization in Smart Grid," *IEEE Transactions on Industrial Informatics*, vol. 14, no. 8, pp. 3447–3458, 2018.

[41] S. Zhao, X. Lin, and M. Chen, "Robust Online Algorithms for Peak-Minimizing EV Charging Under Multistage Uncertainty," *IEEE Transactions on Automatic Control*, vol. 62, no. 11, pp. 5739–5754, 2017.

[42] W. Wu, Y. Lin, R. Liu, Y. Li, Y. Zhang, and C. Ma, "Online EV Charge Scheduling Based on Time-of-Use Pricing and Peak Load Minimization: Properties and Efficient Algorithms," *IEEE Transactions on Intelligent Transportation Systems*, vol. 23, no. 1, pp. 572–586, 2022.

[43] Y. Mo, Q. Lin, M. Chen, and S. J. Qin, "Optimal Peak-Minimizing Online Algorithms for Large-Load Users with Energy Storage," in *IEEE INFOCOM 2021 -IEEE International Conference on Computer Communications Workshops (INFOCOM WKSHPS)*, 2021, pp. 1–2.

[44] Y. Riffonneau, S. Bacha, F. Barruel, and S. Ploix, "Optimal power flow management for grid connected pv systems with batteries," *IEEE Transactions on Sustainable Energy*, vol. 2, no. 3, pp. 309–320, 2011.

[45] W. Munawar and J.-J. Chen, "Peak power demand analysis and reduction by using battery buffers for monotonic controllers," in *2013 23rd International Workshop on Power and Timing Modeling, Optimization and Simulation (PATMOS)*, 2013, pp. 255–258.

[46] D. Kucevic, L. Semmelmann, N. Collath, A. Jossen, and H. Hesse, "Peak shaving with battery energy storage systems in distribution grids: A novel approach to reduce local and global peak loads," *Electricity*, vol. 2, no. 4, pp. 573–589, 2021.

[47] J. Leadbetter and L. Swan, "Battery storage system for residential electricity peak demand shaving," *Energy and Buildings*, vol. 55, pp. 685–692, 2012, cool Roofs, Cool Pavements, Cool Cities, and Cool World.

[48] K. Mahmud, M. J. Hossain, and G. E. Town, "Peak-load reduction by coordinated response of photovoltaics, battery storage, and electric vehicles," *IEEE Access*, vol. 6, pp. 29 353–29 365, 2018.

[49] D. T. Vedullapalli, R. Hadidi, and B. Schroeder, "Combined hvac and battery scheduling for demand response in a building," *IEEE Transactions on Industry Applications*, vol. 55, no. 6, pp. 7008–7014, 2019.

[50] D. M. Greenwood, N. S. Wade, P. C. Taylor, P. Papadopoulos, and N. Heyward, "A probabilistic method combining electrical energy storage and real-time thermal ratings to defer network reinforcement," *IEEE Transactions on Sustainable Energy*, vol. 8, no. 1, pp. 374–384, 2017.

[51] N. Ahmed, M. Levorato, and G. P. Li, "Residential consumer-centric demand side management," *IEEE Transactions on Smart Grid*, vol. 9, no. 5, pp. 4513–4524, 2018.

[52] Y. Guo, Q. Zhang, and Z. Wang, "Cooperative Peak Shaving and Voltage Regulation in Unbalanced Distribution Feeders," *IEEE Transactions on Power Systems*, vol. 36, no. 6, pp. 5235–5244, 2021.

[53] J. von Appen, T. Stetz, M. Braun, and A. Schmiegel, "Local voltage control strategies for pv storage systems in distribution grids," *IEEE Transactions on Smart Grid*, vol. 5, no. 2, pp. 1002–1009, 2014.

[54] G. Angenendt, S. Zurmühlen, R. Mir-Montazeri, D. Magnor, and D. U. Sauer, "Enhancing battery lifetime in pv battery home storage system using forecast based operating strategies," *Energy Procedia*, vol. 99, pp. 80–88, 2016, 10th International Renewable Energy Storage Conference, IRES 2016, 15-17 March 2016, Düsseldorf, Germany.

[55] P. Khajavi, H. Abniki, and A. B. Arani, "The role of incentive based demand response programs in smart grid," in *2011 10th International Conference on Environment and Electrical Engineering*, May 2011, pp. 1–4.

[56] B. Celik, R. Roche, S. Suryanarayanan, D. Bouquain, and A. Miraoui, "Electric energy management in residential areas through coordination of multiple smart homes," *Renewable and Sustainable Energy Reviews*, vol. 80, pp. 260 – 275, 2017.

[57] C. Keerthisinghe, A. C. Chapman, and G. Verbič, "Energy management of pv-storage systems: Policy approximations using machine learning," *IEEE Transactions on Industrial Informatics*, vol. 15, no. 1, pp. 257–265, 2019.

[58] C. Zhao, S. Dong, F. Li, and Y. Song, "Optimal home energy management system with mixed types of loads," *CSEE Journal of Power and Energy Systems*, vol. 1, no. 4, pp. 29–37, 2015.

[59] B. Jiang and Y. Fei, "Smart home in smart microgrid: A cost-effective energy ecosystem with intelligent hierarchical agents," *IEEE Transactions on Smart Grid*, vol. 6, no. 1, pp. 3–13, Jan 2015.

[60] Y. Xu and L. Tong, "Optimal Operation and Economic Value of Energy Storage at Consumer Locations," *IEEE Transactions on Automatic Control*, vol. 62, no. 2, pp. 792–807, 2017.

[61] J. Jin, Y. Xu, Y. Khalid, and N. Ul Hassan, "Optimal Operation of Energy Storage With Random Renewable Generation and AC/DC Loads," *IEEE Transactions on Smart Grid*, vol. 9, no. 3, pp. 2314–2326, 2018.

[62] N. Ahmed, M. Levorato, and G. P. Li, "Residential consumer-centric demand side management," *IEEE Transactions on Smart Grid*, vol. 9, no. 5, pp. 4513–4524, 2018.

[63] S. Althaher, P. Mancarella, and J. Mutale, "Automated demand response from home energy management system under dynamic pricing and power and comfort constraints," *IEEE Transactions on Smart Grid*, vol. 6, no. 4, pp. 1874–1883, 2015.

[64] K. S. Sedzro, A. J. Lamadrid, and M. C. Chuah, "Generalized minimax: A self-enforcing pricing scheme for load aggregators," *IEEE Transactions on Smart Grid*, vol. 9, no. 3, pp. 1953–1963, 2018.

[65] S. Shafiee, H. Zareipour, and A. M. Knight, "Developing Bidding and Offering Curves of a Price-Maker Energy Storage Facility Based on Robust Optimization," *IEEE Transactions on Smart Grid*, vol. 10, no. 1, pp. 650–660, 2019.

[66] J. Arteaga and H. Zareipour, "A Price-Maker/Price-Taker Model for the Operation of Battery Storage Systems in Electricity Markets," *IEEE Transactions on Smart Grid*, vol. 10, no. 6, pp. 6912–6920, 2019.

[67] R. Zhang, T. Jiang, G. Li, X. Li, and H. Chen, "Stochastic Optimal Energy Management and Pricing for Load Serving Entity With Aggregated TCLs of Smart Buildings: A Stackelberg Game Approach," *IEEE Transactions on Industrial Informatics*, vol. 17, no. 3, pp. 1821–1830, 2021.

[68] P. Yi, X. Dong, A. Iwayemi, C. Zhou, and S. Li, "Real-time opportunistic scheduling for residential demand response," *IEEE Transactions on Smart Grid*, vol. 4, no. 1, pp. 227–234, 2013.

[69] J. H. Yoon, R. Baldick, and A. Novoselac, "Dynamic demand response controller based on real-time retail price for residential buildings," *IEEE Transactions on Smart Grid*, vol. 5, no. 1, pp. 121–129, 2014.

[70] H. Lu, W. Jeon, T. Mount, and A. J. Lamadrid, "Can energy bids from aggregators manage deferrable demand efficiently?" in *2015 48th Hawaii International Conference on System Sciences*, pp. 2530–2539.

[71] P. D. Barta and D. Divényi, "Study about the price limit of res orders," in *2019 7th International Youth Conference on Energetics (IYCE)*, pp. 1–5.

[72] J. von Appen and M. Braun, "Sizing and improved grid integration of residential pv systems with heat pumps and battery storage systems," *IEEE Transactions on Energy Conversion*, vol. 34, no. 1, pp. 562–571, 2019.

[73] S. L. Arun and M. P. Selvan, "Intelligent residential energy management system for dynamic demand response in smart buildings," *IEEE Systems Journal*, vol. 12, no. 2, pp. 1329–1340, 2018.

[74] F. Hafiz, D. Lubkeman, I. Husain, and P. Fajri, "Energy storage management strategy based on dynamic programming and optimal sizing of pv panel-storage capacity for a residential system," in *2018 IEEE/PES Transmission and Distribution Conference and Exposition (T D)*, 2018, pp. 1–9.

[75] L. N. An and T. Q. Tuan, "Dynamic programming for optimal energy management of hybrid wind–pv–diesel–battery," *Energies*, vol. 11, no. 11, 2018.

[76] R. D. Trevizan, A. Stanley, J. H. Alexander, G. Robert, and G. Imre, "Integration of energy storage with diesel generation in remote communities," *MRS Energy Sustainability*, vol. 8, pp. 57–74, 2021.

[77] Y. Yoldas, S. Goren, and A. Onen, "Optimal control of microgrids with multi-stage mixed-integer nonlinear programming guided *Q*-learning algorithm," *Journal of Modern Power Systems and Clean Energy*, vol. 8, no. 6, pp. 1151–1159, 2020.

[78] H. V. M., D. Das, C. Kumar, H. B. Gooi, M. Saad, and X. Guo, "Increasing voltage support using smart power converter based energy storage system and load control," *IEEE Transactions on Industrial Electronics*, vol. 68, no. 12, pp. 12 364–12 374, 2020.

[79] R. Rosso, X. Wang, M. Liserre, X. Lu, and S. Engelken, "Grid-forming converters: Control approaches, grid-synchronization, and future trends–a review," *IEEE Open Journal of Industrial Applications*, vol. 2, pp. 93–109, 2021.

[80] R. Tonkoski, L. A. C. Lopes, and T. H. M. El-Fouly, "Coordinated active power curtailment of grid connected pv inverters for overvoltage prevention," *IEEE Transactions on Sustainable Energy*, vol. 2, no. 2, pp. 139–147, Apr. 2011.

[81] S. Ghosh, S. Rahman, and M. Pipattanasomporn, "Distribution voltage regulation through active power curtailment with pv inverters and solar generation forecasts," *IEEE Transactions on Sustainable Energy*, vol. 8, no. 1, pp. 13–22, Jan. 2017.

[82] N. Wang, J. Li, W. Hu, B. Zhang, Q. Huang, and Z. Chen, "Optimal reactive power dispatch of a full-scale converter based wind farm considering loss minimization," *Renewable Energy*, vol. 139, pp. 292–301, 2019.

[83] V. Sarfi and H. Livani, "Optimal volt/var control in distribution systems with prosumer ders," *Electric Power Systems Research*, vol. 188, p. 106520, 2020.

[84] C. L. Masters, "Voltage rise: the big issue when connecting embedded generation to long 11 kv overhead lines," *Power Engineering Journal*, vol. 16, no. 1, pp. 5–12, Feb. 2002.

[85] F. Ding, Y. Zhang, J. Simpson, A. Bernstein, and S. Vadari, "Optimal energy dispatch of distributed pvs for the next generation of distribution management systems," *IEEE Open Access Journal of Power and Energy*, vol. 7, pp. 287–295, 2020.

[86] C. Kumar, R. Manojkumar, S. Ganguly, and M. Liserre, "Impact of optimal control of distributed generation converters in smart transformer based meshed hybrid distribution network," *IEEE Access*, vol. 9, pp. 140 268–140 280, 2021.

[87] J. D. Watson, N. R. Watson, and B. Das, "Effectiveness of power electronic voltage regulators in the distribution network," *IET Generation, Transmission Distribution*, vol. 10, no. 15, pp. 3816–3823, 2016.

[88] S. Jazebi, S. Hosseinian, and B. Vahidi, "Dstatcom allocation in distribution networks considering reconfiguration using differential evolution algorithm," *Energy Conversion and Management*, vol. 52, no. 7, pp. 2777 – 2783, 2011.

[89] S. Lakshmi and S. Ganguly, "An on-line operational optimization approach for open unified power quality conditioner for energy loss minimization of distribution networks," *IEEE Transactions on Power Systems*, vol. 34, no. 6, pp. 4784–4795, 2019.

[90] V. Calderaro, G. Conio, V. Galdi, G. Massa, and A. Piccolo, "Optimal decentralized voltage control for distribution systems with inverter-based distributed generators," *IEEE Transactions on Power Systems*, vol. 29, no. 1, pp. 230–241, 2014.

[91] R. R. Jha, A. Dubey, C.-C. Liu, and K. P. Schneider, "Bi-level volt-var optimization to coordinate smart inverters with voltage control devices," *IEEE Transactions on Power Systems*, vol. 34, no. 3, pp. 1801–1813, 2019.

[92] G. De Carne, G. Buticchi, M. Liserre, and C. Vournas, "Load control using sensitivity identification by means of smart transformer," *IEEE Transactions on Smart Grid*, vol. 9, no. 4, pp. 2606–2615, 2018.

[93] J. Chen, M. Liu, G. De Carne, R. Zhu, M. Liserre, F. Milano, and T. O'Donnell, "Impact of smart transformer voltage and frequency support in a high renewable penetration system," *Electric Power Systems Research*, vol. 190, p. 106836, 2021.

[94] R. Anilkumar, G. Devriese, and A. K. Srivastava, "Voltage and reactive power control to maximize the energy savings in power distribution system with wind energy," *IEEE Transactions on Industry Applications*, vol. 54, no. 1, pp. 656–664, 2018.

[95] W. Zhuo, "Microgrid energy management strategy with battery energy storage system and approximate dynamic programming," in *2018 37th Chinese Control Conference (CCC)*, 2018, pp. 7581–7587.

[96] S. A. Alavi, A. Ahmadian, and M. Aliakbar-Golkar, "Optimal probabilistic energy management in a typical micro-grid based-on robust optimization and point estimate method," *Energy Conversion and Management*, vol. 95, pp. 314–325, 2015.

[97] G. Aghajani, H. Shayanfar, and H. Shayeghi, "Presenting a multi-objective generation scheduling model for pricing demand response rate in micro-grid energy management," *Energy Conversion and Management*, vol. 106, pp. 308–321, 2015.

[98] C. Chen, S. Duan, T. Cai, B. Liu, and G. Hu, "Smart energy management system for optimal microgrid economic operation," *IET Renewable Power Generation*, vol. 5, pp. 258–267, 2011.

[99] G. Corso, M. L. Di Silvestre, M. G. Ippolito, E. Riva Sanseverino, and G. Zizzo, "Multi-objective long term optimal dispatch of distributed energy resources in micro-grids," in *45th International Universities Power Engineering Conference UPEC2010*, 2010, pp. 1–5.

[100] M. J. Sanjari, H. Karami, and H. B. Gooi, "Analytical rule-based approach to online optimal control of smart residential energy system," *IEEE Transactions on Industrial Informatics*, vol. 13, no. 4, pp. 1586–1597, 2017.

[101] B. Khan and P. Singh, "Selecting a meta-heuristic technique for smart microgrid optimization problem: A comprehensive analysis," *IEEE Access*, vol. 5, pp. 13 951–13 977, 2017.

[102] Y. A. Katsigiannis, P. S. Georgilakis, and E. S. Karapidakis, "Hybrid simulated annealing–tabu search method for optimal sizing of autonomous power systems with renewables," *IEEE Transactions on Sustainable Energy*, vol. 3, no. 3, pp. 330–338, 2012.

[103] A. Q. Mohammed, K. A. Al-Anbarri, and R. M. Hannun, "Optimal combination and sizing of a stand–alone hybrid energy system using a nomadic people optimizer," *IEEE Access*, vol. 8, pp. 200 518–200 540, 2020.

[104] M. L. Puterman, "Dynamic programming," in *Encyclopedia of Physical Science and Technology (Third Edition)*, third edition ed., R. A. Meyers, Ed. New York: Academic Press, 2003, pp. 673–696.

[105] D. Liu, Y. Xu, Q. Wei, and X. Liu, "Residential energy scheduling for variable weather solar energy based on adaptive dynamic programming," *IEEE/CAA Journal of Automatica Sinica*, vol. 5, no. 1, pp. 36–46, 2018.

[106] J. Shen and A. Khaligh, "A supervisory energy management control strategy in a battery/ultracapacitor hybrid energy storage system," *IEEE Transactions on Transportation Electrification*, vol. 1, no. 3, pp. 223–231, 2015.

[107] M. Laguna and R. Martí, "Heuristics," in *Encyclopedia of Operations Research and Management Science*, S. I. Gass and M. C. Fu, Eds. Springer US, 2013, pp. 695–703.

[108] L. P. Fávero and P. Belfiore, "Chapter 19 - integer programming," in *Data Science for Business and Decision Making*, L. P. Fávero and P. Belfiore, Eds. Academic Press, 2019, pp. 887–918.

[109] S. Muthuraman and V. P. Venkatesan, "A comprehensive study on hybrid metaheuristic approaches used for solving combinatorial optimization problems," in *2017 World Congress on Computing and Communication Technologies (WCCCT)*, 2017, pp. 185–190.

[110] G. Hao, R. Cong, and H. Zhou, "Pso applied to optimal operation of a micro-grid with wind power," in *2014 Sixth International Symposium on Parallel Architectures, Algorithms and Programming*, July 2014, pp. 46–51.

[111] J. Radosavljević, M. Jevtić, and D. Klimenta, "Energy and operation management of a microgrid using particle swarm optimization," *Engineering Optimization*, vol. 48, no. 5, pp. 811–830, 2016.

[112] M. Mohammadi, S. H. Hosseinian, and G. B. Gharehpetian, "Ga-based optimal sizing of microgrid and dg units under pool and hybrid electricity markets," *International Journal of Electrical Power & Energy Systems*, vol. 35, pp. 83–92, 2012.

[113] B. Zhao, X. Zhang, J. Chen, C. Wang, and L. Guo, "Operation optimization of standalone microgrids considering lifetime characteristics of battery energy storage system," *IEEE Transactions on Sustainable Energy*, vol. 4, no. 4, pp. 934–943, 2013.

[114] L. Lengyel, "Validating rule-based algorithms," *Journal of Applied Sciences*, vol. 12, no. 4, pp. 59–75, 2015.

[115] J. Peng, H. He, and R. Xiong, "Rule based energy management strategy for a series–parallel plug-in hybrid electric bus optimized by dynamic programming," *Applied Energy*, vol. 185, pp. 1633 – 1643, 2017.

[116] "Ieee standard for the specification of microgrid controllers," *IEEE Std 2030.7-2017*, pp. 1–43, 2018.

[117] J. Almada, R. Leão, R. Sampaio, and G. Barroso, "A centralized and heuristic approach for energy management of an ac microgrid," *Renewable and Sustainable Energy Reviews*, vol. 60, pp. 1396–1404, 2016.

[118] C. Sun, G. Joos, S. Q. Ali, J. N. Paquin, C. M. Rangel, F. A. Jajeh, I. Novickij, and F. Bouffard, "Design and real-time implementation of a centralized microgrid control system with rule-based dispatch and seamless transition function," *IEEE Transactions on Industry Applications*, vol. 56, no. 3, pp. 3168–3177, 2020.

[119] F. R. Salmasi, "Control strategies for hybrid electric vehicles: Evolution, classification, comparison, and future trends," *IEEE Transactions on Vehicular Technology*, vol. 56, no. 5, pp. 2393–2404, 2007.

[120] A. A. Hussein, N. Kutkut, Z. J. Shen, and I. Batarseh, "Distributed battery microstorage systems design and operation in a deregulated electricity market," *IEEE Transactions on Sustainable Energy*, vol. 3, no. 3, pp. 545–556, 2012.

[121] N. Jalil, N. Kheir, and M. Salman, "A rule-based energy management strategy for a series hybrid vehicle," in *Proceedings of the 1997 American Control Conference (Cat. No.97CH36041)*, vol. 1, 1997, pp. 689–693 vol.1.

[122] S. Teleke, M. E. Baran, S. Bhattacharya, and A. Q. Huang, "Rule-based control of battery energy storage for dispatching intermittent renewable sources," *IEEE Transactions on Sustainable Energy*, vol. 1, no. 3, pp. 117–124, Oct 2010.

[123] T. Zhu, A. Mishra, D. Irwin, N. Sharma, P. Shenoy, and D. Towsley, "The case for efficient renewable energy management in smart homes," in *Proceedings of the Third ACM Workshop on Embedded Sensing Systems for Energy-Efficiency in Buildings*, ser. BuildSys '11. New York, NY, USA: Association for Computing Machinery, 2011, pp. 67–72.

[124] A. K. Barnes, J. C. Balda, and A. Escobar-Mejía, "A semi-markov model for control of energy storage in utility grids and microgrids with pv generation," *IEEE Transactions on Sustainable Energy*, vol. 6, no. 2, pp. 546–556, 2015.

[125] S. B. Raha and D. Biswas, "Fuzzy controlled demand response energy management for economic microgrid planning," in *2020 IEEE International Conference on Power Electronics, Smart Grid and Renewable Energy (PESGRE2020)*, 2020, pp. 1–6.

[126] J. Zupančič, E. Lakić, T. Medved, and A. F. Gubina, "Advanced peak shaving control strategies for battery storage operation in low voltage distribution network," in *2017 IEEE Manchester PowerTech*, 2017, pp. 1–6.

[127] Y. Yang, H. Li, A. Aichhorn, J. Zheng, and M. Greenleaf, "Sizing strategy of distributed battery storage system with high penetration of photovoltaic for voltage regulation and peak load shaving," *IEEE Transactions on Smart Grid*, vol. 5, no. 2, pp. 982–991, 2014.

[128] M. J. E. Alam, K. M. Muttaqi, and D. Sutanto, "Mitigation of rooftop solar pv impacts and evening peak support by managing available capacity of distributed energy storage systems," *IEEE Transactions on Power Systems*, vol. 28, no. 4, pp. 3874–3884, 2013.

[129] U. Kumar Jha, N. Soren, and A. Sharma, "An efficient hems for demand response considering tou pricing scheme and incentives," in *2018 2nd International Conference on Power, Energy and Environment: Towards Smart Technology (ICEPE)*, 2018, pp. 1–6.

[130] S. Bruno, G. Giannoccaro, and M. La Scala, "A demand response implementation in tertiary buildings through model predictive control," *IEEE Transactions on Industrial Applications*, vol. 55, no. 6, pp. 7052–7061, 2019.

[131] J. Wang, J. Wang, Q. Wang, and X. Zeng, "Control rules extraction and parameters optimization of energy management for bus series-parallel amt hybrid powertrain," *Journal of The Franklin Institute*, vol. 355, no. 5, pp. 2283 – 2312, 2018.

[132] T. Mesbahi, N. Rizoug, P. Bartholomeüs, R. Sadoun, F. Khenfri, and P. Le Moigne, "Optimal energy management for a li-ion battery/supercapacitor hybrid energy storage system based on a particle swarm optimization incorporating nelder–mead simplex approach," *IEEE Transactions on Intelligent Vehicles*, vol. 2, no. 2, pp. 99–110, 2017.

[133] A. L. Bukar, C. W. Tan, L. K. Yiew, R. Ayop, and W.-S. Tan, "A rule-based energy management scheme for long-term optimal capacity planning of grid-independent microgrid optimized by multi-objective grasshopper optimization algorithm," *Energy Conversion and Management*, vol. 221, p. 113161, 2020.

[134] M. Fekri Moghadam, M. Metcalfe, W. G. Dunford, and E. Vaahedi, "Demand side storage to increase hydroelectric generation efficiency," *IEEE Transactions on Sustainable Energy*, vol. 6, no. 2, pp. 313–324, 2015.

[135] M. G. Damavandi, J. R. Martí, and V. Krishnamurthy, "A methodology for optimal distributed storage planning in smart distribution grids," *IEEE Transactions on Sustainable Energy*, vol. 9, no. 2, pp. 729–740, 2018.

[136] W. Chiu, J. Hsieh, and C. Chen, "Pareto optimal demand response based on energy costs and load factor in smart grid," *IEEE Transactions on Industrial Informatics*, vol. 16, no. 3, pp. 1811–1822, 2020.

[137] X. Liu, A. Aichhorn, L. Liu, and H. Li, "Coordinated control of distributed energy storage system with tap changer transformers for voltage rise mitigation under high photovoltaic penetration," *IEEE Transactions on Smart Grid*, vol. 3, no. 2, pp. 897–906, June 2012.

[138] W.-C. Chu, B.-K. Chen, and C.-H. Liao, "Allocating the costs of reactive power purchased in an ancillary service market by modified y-bus matrix method," *IEEE Transactions on Power Systems*, vol. 19, no. 1, pp. 174–179, 2004.

[139] K. R. Reddy and S. Meikandasivam, "Load flattening and voltage regulation using plug-in electric vehicle's storage capacity with vehicle prioritization using

anfis," *IEEE Transactions on Sustainable Energy*, vol. 11, no. 1, pp. 260–270, 2020.

[140] F. Hafiz, M. A. Awal, A. R. d. Queiroz, and I. Husain, "Real-time stochastic optimization of energy storage management using deep learning-based forecasts for residential pv applications," *IEEE Transactions on Industry Applications*, vol. 56, no. 3, pp. 2216–2226, 2020.

[141] K. Gaur, H. Kumar, R. P. K. Agarwal, K. V. S. Baba, and S. K. Soonee, "Analysing the electricity demand pattern," in *2016 National Power System Conference*, Dec. 2016, pp. 1–6.

[142] K. Y. Bae, H. S. Jang, and D. K. Sung, "Hourly Solar Irradiance Prediction Based on Support Vector Machine and Its Error Analysis," *IEEE Transactions on Power Systems*, vol. 32, no. 2, pp. 935–945, 2017.

[143] K. Amasyali and N. M. El-Gohary, "A review of data-driven building energy consumption prediction studies," *Renewable Sustainable Energy Reviews*, vol. 81, pp. 1192–1205, 2018.

[144] M. Xia, H. Shao, X. Ma, and C. W. de Silva, "A Stacked GRU-RNN-Based Approach for Predicting Renewable Energy and Electricity Load for Smart Grid Operation," *IEEE Transactions on Industrial Informat.*, vol. 17, no. 10, pp. 7050–7059, 2021.

[145] S. Chun and A. Kwasinski, "Analysis of classical root-finding methods applied to digital maximum power point tracking for sustainable photovoltaic energy generation," *IEEE Transactions on Power Electronics*, vol. 26, no. 12, pp. 3730–3743, Dec. 2011.

[146] M. Hosseinzadeh and F. R. Salmasi, "Robust optimal power management system for a hybrid ac/dc micro-grid," *IEEE Transactions on Sustainable Energy*, vol. 6, no. 3, pp. 675–687, 2015.

[147] J. Peng, H. Fan, H. He, and D. Pan, "A rule-based energy management strategy for a plug-in hybrid school bus based on a controller area network bus," *Energies*, vol. 8, no. 6, pp. 5122–5142, 2015.

[148] Q. Chen, N. Liu, C. Hu, L. Wang, and J. Zhang, "Autonomous Energy Management Strategy for Solid-State Transformer to Integrate PV-Assisted EV Charging Station Participating in Ancillary Service," *IEEE Transactions on Industrial Informatics*, vol. 13, no. 1, pp. 258–269, 2017.

[149] W. K. A. Najy, H. H. Zeineldin, and W. L. Woon, "Optimal protection coordination for microgrids with grid-connected and islanded capability," *IEEE Transactions on Industrial Electronics*, vol. 60, no. 4, pp. 1668–1677, 2013.

[150] V. Kumar, J. K. Chhabra, and D. Kumar, "Parameter adaptive harmony search algorithm for unimodal and multimodal optimization problems," *Journal of Computational Science*, vol. 5, no. 2, pp. 144–155, 2014.

[151] X.-S. Yang, "Chapter 6 - genetic algorithms," in *Nature-Inspired Optimization Algorithms (Second Edition)*, second edition ed., X.-S. Yang, Ed. Academic Press, 2021, pp. 91–100.

[152] O. Yeniay, "Penalty Function Methods for Constrained Optimization with Genetic Algorithms," *Mathematical Computational Applications*, vol. 10, no. 1, pp. 45–56, 2005.

[153] S. Das and S. Mukhopadhyay, "Sensing error minimization for cognitive radio in dynamic environment using death penalty differential evolution based threshold adaptation," in *2016 IEEE Annual India Conference (INDICON)*, 2016, pp. 1–6.

[154] E. D. Kostopoulos, G. C. Spyropoulos, and J. K. Kaldellis, "Real-world study for the optimal charging of electric vehicles," *Energy Reports*, vol. 6, pp. 418–426, 2020.

[155] Y.-Y. Hong and M.-Y. Wu, "Markov model-based energy storage system planning in power systems," *IEEE Systems Journal*, vol. 13, no. 4, pp. 4313–4323, 2019.

[156] Economics Division Central Electricity Regulatory Commission, "Report on short-term power market in india: 2018-19." [Online]. Available: https://cercind.gov.in/2019/market_monitoring/Annual%20Report%202018-19.pdf

[157] Cigre Task Force C6.04.02, "Benchmark systems for network integration of renewable and distributed energy resources," Apr. 2014.

[158] S. Ganguly, "Multi-objective planning for reactive power compensation of radial distribution networks with unified power quality conditioner allocation using particle swarm optimization," *IEEE Transactions on Power Systems*, vol. 29, no. 4, pp. 1801–1810, 2014.

[159] A. Radovanovic, T. Nesti, and B. Chen, "A Holistic Approach to Forecasting Wholesale Energy Market Prices," *IEEE Transactions on Power Systems*, vol. 34, no. 6, pp. 4317–4328, 2019.

[160] D. Q. Hung, N. Mithulananthan, and K. Y. Lee, "Determining pv penetration for distribution systems with time-varying load models," *IEEE Transactions on Power Systems*, vol. 29, no. 6, pp. 3048–3057, Nov 2014.

[161] A. Y. Elrayyah, M. Z. C. Wanik, and A. Bouselham, "Simplified approach to analyze voltage rise in lv systems with pv installations using equivalent power systems diagrams," *IEEE Transactions on Power Delivery*, vol. 32, no. 4, pp. 2140–2149, Aug 2017.

[162] Y. Zhou and Z. Wang, "A robust optimal trajectory tracking control for systems with an input delay," *Journal of the Franklin Institute*, vol. 353, no. 12, pp. 2627–2649, 2016.

[163] J. Zhang, Y. Lin, and P. Shi, "Output tracking control of networked control systems via delay compensation controllers," *Automatica*, vol. 57, pp. 85–92, 2015.

[164] R. Majumder, M. Dewadasa, A. Ghosh, G. Ledwich, and F. Zare, "Control and protection of a microgrid connected to utility through back-to-back converters," *Electric Power Systems Research*, vol. 81, no. 7, pp. 1424–1435, 2011.

[165] T. Aziz and N. Ketjoy, "Pv penetration limits in low voltage networks and voltage variations," *IEEE Access*, vol. 5, pp. 16 784–16 792, 2017.

[166] V. K. Agrawal, A. Khemka, K. Manoharan, D. Jain, and S. Mukhopadhyay, "Wind-solar hybrid system–an innovative and smart approach to augment renewable generation and moderate variability to the grid," in *2016 IEEE 7th Power India International Conference (PIICON)*, 2016, pp. 1–5.

[167] S. Mashayekh, M. Stadler, G. Cardoso, M. Heleno, S. C. Madathil, H. Nagarajan, R. Bent, M. Mueller-Stoffels, X. Lu, and J. Wang, "Security-constrained design of isolated multi-energy microgrids," *IEEE Transactions on Power Systems*, vol. 33, no. 3, pp. 2452–2462, 2018.

[168] H. V. M., A. K. Deka, and C. Kumar, "Capacity enhancement of a radial distribution grid using smart transformer," *IEEE Access*, vol. 8, pp. 72 411–72 423, 2020.

[169] K. Kant, C. Jain, and B. Singh, "A hybrid diesel-windpv-based energy generation system with brushless generators," *IEEE Transactions on Industrial Informatics*, vol. 13, no. 4, pp. 1714–1722, 2017.

[170] H. Mehrjerdi, R. Hemmati, M. Shafie-khah, and J. P. S. Catalao, "Zero energy building by multi-carrier energy systems including hydro, wind, solar and hydrogen," *IEEE Transactions on Industrial Informatics*, pp. 1–1, 2020.

[171] K. P. Satsangi, D. B. Das, G. S. Babu, and A. Saxena, "Real time performance of solar photovoltaic microgrid in india focusing on self-consumption in institutional buildings," *Energy for Sustainable Development*, vol. 52, pp. 40–51, 2019.

[172] S. A. Papathanassiou, N. D. Hatziargyriou, and K. Strunz, "A benchmark low voltage microgrid network," 2005.

LIST OF PAPERS BASED ON THESIS

PUBLICATIONS IN REFEREED JOURNALS

1. Rampelli Manojkumar, Chandan Kumar, Sanjib Ganguly, Hoay Beng Gooi, and Saad Mekhilef, "Voltage control using smart transformer via dynamic optimal set-points and limit tolerance in a residential distribution network with PV sources", *IET Generation, Transmission & Distribution*, 2020, 14, (22), p. 5143-5151.

2. Rampelli Manojkumar, Chandan Kumar, Sanjib Ganguly, and João P. S. Catalão, "Optimal Peak Shaving Control Using Dynamic Demand and Feed-In Limits for Grid-Connected PV Sources With Batteries", *IEEE Systems Journal*, vol. 15, no. 4, pp. 5560-5570, Dec. 2021.

3. Rampelli Manojkumar, Chandan Kumar, and Sanjib Ganguly, "Optimal Demand Response in a Residential PV Storage System Using Energy Pricing Limits", *IEEE Transactions on Industrial Informatics*, vol. 18, no. 4, pp. 2497-2507, April 2022.

4. Rampelli Manojkumar, Chandan Kumar, Sanjib Ganguly, Hoay Beng Gooi, Saad Mekhilef, and João P. S. Catalão, "Rule-Based Peak Shaving Using Master-Slave Level Optimization in a Diesel Generator Supplied Microgrid", *IEEE Transactions on Power Systems*, doi:10.1109/TPWRS.2022.318 7069.

PUBLICATIONS IN REFEREED CONFERENCES

1. Rampelli Manojkumar, Hrishikesan V M, Chandan Kumar, and Sanjib Ganguly, "Voltage Control Using Smart Transformer for Increasing Photovoltaic Penetration in a Distribution Grid", *20th International Conference on Intelligent System Application to Power Systems (ISAP)*, Delhi, India, 10-14 December, 2019, pp. 1-7.

2. Rampelli Manojkumar, Chandan Kumar, and Sanjib Ganguly, "Optimal Demand Response Using Dynamic Electricity Price Limit in a Hybrid AC/DC System", *21st National Power Systems Conference (NPSC)*, Gandhinagar, India, 17-19 December, 2020, pp. 1-6.